Technische Universität Kaiserslautern
Fachbereich Elektechnik und Informationstechnik
Lehrstuhl fur Integrierte Sensorsysteme
Prof. Dr.-Ing.Andreas König

Diplomarbeit

Large Area Tactile Sensors for

Smart Surfaces with

Low Power Consumption

Juan Miguel Andújar Morgado

Supervisor: Prof. Dr.-Ing. Andreas König

Begin: 1 March, 2011

End: 20 September, 2011

Erklärung

Hiermit erkläre ich, dass ich die vorliegende Diplomarbeit selbstständing verfasst habe. Bei der Erstellung wurden keine weiteren als die angegebenen Quellen und Hilfsmittel verwendet.

Kaiserslautern, den 20 September 2011

Juan Miguel Andújar Morgado

Contents

1 Introduction

1.1 Preface

The tactile sensors are able to detect the force applied by an object or person. Commonly, they are arrayed in matrix of force, where they act as variable resistance. The principal applications of tactile sensor are: robotic hands (to detect different slip, contact and texture), medical devices (to detect for instance breast cancer), artificial skin for robots (they can interact with the environment)

This report presents results from a selection of tactile sensors that have been designed and fabricated for a large area conception. The sensor is based on piezoresistivity of the material, where it only need a conductive material and electrodes to be able to detect contact. In this work, there have been presented the results from sensor made using printed circuit board. This report provides details regarding the design of the hardware, selecting the best shape of the electrode. Furthermore, we present a novel method to measure the tactel, this novel method is based on measuring the tactels independently, inspired in the common digital camera CMOS, where is shown that the new readout circuit works perfectly and the consumption is lower than other philosophies presented in this report.

1.2 Contributions

The main contributions in this report will be the following:

- The whole tactile sensor should be cheap.

- The power consumption should be as low as possible.

- The tactile sensor should be able to cover large area.

- The design electronic should be able to reduce errors and interferences caused by long wires, further, eliminate leak current paths when selecting a site.

2 Tactile sensor

The term **tactile sensor** includes all type of sensors which are able to detect contact. Tactile sensors are employed to detect force, force direction, thermal properties, texture, material stiffness, or simply to detect if the sensor has been touched or not. This means a tactile sensor can measure the stress, force, pressure, deformation, slip according to a distributed array of separate elements.

[1]*The development of humanoid robots has been very recently. Intelligent sensing capabilities of humanoid robots are critical for effective and safe interactions between robots and humans. Therefore, the research on artificial skins used for robotic applications has received significant attention. The primary purposes of artificial skins are to realize the information exchange between robot and human beings as well as environment and to serve as the sensing systems to avoid damages to humans or robots. The basic sensing capabilities of an artificial skin include the sense of touch, the sense of temperature, and so on. For a typical artificial skin, a large number of sensing elements, such as tactile sensors and temperature sensors, are required to be implemented on a flexible-sheet structure of about few hundred centimeters square area. Also, an artificial skin should have enough flexibility to cover a three-dimensional surface.*

There are many tactile sensor to be used, many of them are not able to measure with the same resolution and sensitivity as human skin, or if they are, they are too thick or inflexible.

The readout electronic is an important part of the tactile sensor, because they need to be able to measure a large amount of elements in a short time in order to reach an acceptable speed sample. The main categories of data which tactile sensors can transducer are:

- Simple contact: if the sensor detects or not contact.

- Magnitude of force: what amount of force is applied over the sensor.

- Three dimensional shape.

- Slip: the data which detect the relative movement of the sensor respect to a reference.

- Thermal properties.

The major transduction methods to develop tactile sensors are explained in next section.

---

[1]The italicized/emphasized text is a verbatim quotation from [15]

Tactile sensor based on Piezoresistivity [2]

The transduction method that has received the most attention in tactile sensor design is concerned with the change in resistance of a conductive material under applied pressure. Each resistor, whose value changes with the magnitude of the force, represents a resistive cell of the transducer. Different materials have been utilized to manufacture the basic cell. Conductive elastomers were among the first resistive materials used for the development of tactile sensors. They are insulating, natural or silicone-based rubbers made conductive by adding particles of conductive or semiconductive materials (e.g., silver or carbon). The changes in resistivity of the elastomers under pressure are produced basically by two different physical mechanisms. In the first approach, the change in resistivity of the elastomer under pressure is associated with deformation that alters the particle density within it. In the second approach, while the bulk resistance of the elastomer changes slightly when it is compressed, the design allows the increase of the area of contact between the elastomer and an electrode, and correspondingly a change in the contact resistance. The value of the resistance of a resistor with the the cross-section A and length l is:

$$R = \rho \frac{l}{A}$$

The changes in resistivity of the elastomers under pressure are produced basically by two different physical mechanisms. In the first approach, the change in resistivity of the elastomer under pressure is associated with deformation that alters the particle density within it. In the second approach, while the bulk resistance of the elastomer changes slightly when it is compressed, the design allows the increase of the area of contact between the elastomer and an electrode, and correspondingly a change in the contact resistance.

Tactile sensor based on the change of the capacitance

[3]*Tactile sensors within this category are concerned with measuring capacitance, with varies under applied load. The capacitance of a parallel-plate-capacitor depends on the separation of the plates and their areas. A sensor using an elastomeric separator between the plates provides compliance such that the capacitance will vary according to the applied normal load.* [3]*The capacitance between two parallel plates is given by*

$$C = \varepsilon \frac{A}{d}$$

where A is the plate area, d the distance between the plates, and ε the permittivity of the dielectric medium. A capacitive touch sensor relies on the applied force either changing the distance between the plates or the effective surface area of the capacitor. In such a sensor the two conductive plates of the sensor are separated by a dielectric medium, which is also used as the elastomer to give the sensor its force-to-capacitance characteristics.

---

[2]The italicized/emphasized text is a verbatim quotation from [1]
[3]The italicized/emphasized text is a verbatim quotation from [1]
[3]The italicized/emphasized text is a verbatim quotation from [3]

Tactile sensor based on Piezoelectricity

[4]*A material is called piezoelectric, if , when subjected to a stress or deformation, it produce electricity. Longitudinal piezoelectric effect occurs when the electricity in produced in the same direction or the stress. A transversal piezoelectric effect occurs when the electricity is produced in the direction perpendicular to the stress.*

[5]*Polymeric materials that exhibit piezoelectric properties are suitable for use as a touch or tactile sensors, while quartz and some ceramics have piezoelectric properties, polymers such as polyvinylidene fluoride (PVDF) are normally used in sensors.*

Tactile sensor based on magnetism[6]

There are two approaches to the design of touch or tactile sensors based on magnetic transduction. Firstly, the movement of a small magnet by an applied force will cause the flux density at the point of measurement to change. The flux measurement can be made by either a Hall effect or a magnetoresistive device. Second, the core of the transformer or inductor can be manufactured from a magnetoelastic material that will deform under pressure and cause the magnetic coupling between transformer windings, or a coil's inductance to change. A magnetoresistive or magnetoelastic material is a material whose magnetic characteristics are modified when the material is subjected to changes in externally applied physical forces. The magnetorestrictive or magnetoelastic sensor has a number of advantages that include high sensitivity and dynamic range, no measurable mechanical hysteresis, a linear response, and physical robustness.

If a very small permanent magnet is held above the detection device by a complaint medium, the change in flux caused by the magnet's movement due to an applied force can be detected and measured. The field intensity follows an inverse relationship, leading to a nonlinear response, which can be easily linearized by processing. A one-dimensional sensor where a row of twenty hall effect devices placed opposite a magnet has been constructed. A tactile sensor using magnetoelastic material has been developed, where the material was bonded to a substrate, and then used as a core for an inductor. As the core is stressed, the material's susceptibility changed, which is measured as a change in the coil's inductance.

Tactile sensor based on Optical[7]

Recent development in fiber optic technology and solid-state cameras have led to numerous novel tactile sensor design. Some of these designs employ flexible membranes incorporating a

---

[4]The italicized/emphasized text is a verbatim quotation from [1]

[5]The italicized/emphasized text is a verbatim quotation from [3]

[6] The italicized/emphasized text is a verbatim quotation from[3]

[7] The italicized/emphasized text is a verbatim quotation from [1]

reflecting surfaces. Light is introduced into the sensor via a fiber optic cable. A wide cone of light propagates out of the fiber, reflects back form the membrane, and is collected by a second fiber. When an external force is applied onto the elastomer. It shortens the distance between the reflective side of the membrane and the fibers.

Tactile sensor based on Optical fibre[8]

At the early, *optical fibres where used are solely for the transmission of light to and from the sensor, however tactile sensors can be constructed from the fibre itself. A number of tactile sensors have been developed using this approach. In the majority of cases either the sensor structure was too big to be attached to the fingers of robotic hand or the operation was too complex for use in the industrial environment. A suitable design can be based on internal-state microbending of optical fibres. Microbending is the process of light attenuation in the core of fibre when a mechanical bend or perturbation (of the order of few microns) is applied to the outer surface of the fibre. The degree of attenuation depends on the fibre parameter's as well as radius of curvature and spatial wavelength of the bend. Research has demonstrate the feasibility of effecting microbending on an optical fibre by the application of a force to a second orthogonal optical fibre.*

---

[8]The italicized/emphasized text is a verbatim quotation from [3]

3   Tactile Sensor for Large Areas

Many approaches have been used to create tactile sensors, many of them employ piezoresistivity or capacitivity, and others use optical or piezoelectrical technology. MEMS technologies on silicon or on polymers are used to manufacture these sensors, however, these technologies are not appropriate for large area sensors. It can cover circular surfaces. However, signal conditioning of is easier for piezoresisitive sensors rather than for capactive sensors. The piezoresistive tecnology allows sensors to have small electronic design and so it can be located to raw sensor. Most sensors reported to cover large areas are based on piezoresistive principles.

For instance, in [2] proposes the [9]*design and fabrication of the flexible sensor for large area sensing with higher resolution using screen printing technology. For optimal flexible structure characteristics, designed a bump protrusion on the membrane top is used to enhance the sensitivity response and a thixotropy material with higher viscosity is used to print the thick bump structures to reduce the diffusive effects and dimensional shrinkages after printing and curing.*
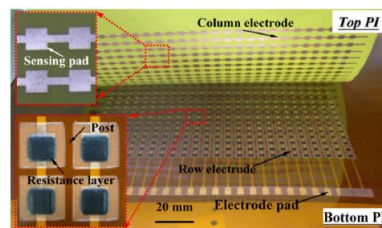

Fig. 3.1: *Flexible electronics sensor based on polyimide films for large area sensing.*[2].

In [4] shows[10]*the design of a tactile sensor intended to cover the forearm of the rescue robot ALACRAN. This robot is able to lift hundreds of kilograms so it has to be carefully designed because it will manipulate human beings that can be hurt. So it has to be aware of being in contact with a human being and how he or she is pressed. Not just a binary output is required because contact is often necessary, for instance when a human is held in the arms of the robot. For this sort of operations a kind of artificial skin must provide information about the contact between the robot and the human. This skin will cover the hands to carry out fine manipulation, but it will also cover large areas like forearms.*

---

[9]The italicized/emphasized text is a verbatim quotation from [2]

[10]The italicized/emphasized text is a verbatim quotation from [4]

Fig. 3.2: *shows the ALACRAN robot with the tactile sensor attached on the forearm.* [4].

In [5] develops[11]*a large-area sheet-type wireless power-transmission system on a plastic film by combining state-of-the-art printing and plastic microelectromechanicalsystem (MEMS) technologies. Complementary circuits integrating plastic MEMS switches and organic transistors allow us to realize large-area, flexible, high-power applications. When an electronic object that possesses a receiver coil at the bottom is approaching or placed on the sheet, the position of the object is contactlessly sensed by using electromagnetic coupling using a printed organictransistor active matrix. Subsequently, one of the elements of the two-dimensional array of sender coils is selected by a printed plastic MEMS switching matrix. In this way, power is selectively transmitted from one of the coils in the sender coil array to the receiver coil of the object by electromagnetic induction. As the device is manufactured using printing technologies, the large-area system is potentially inexpensive.*
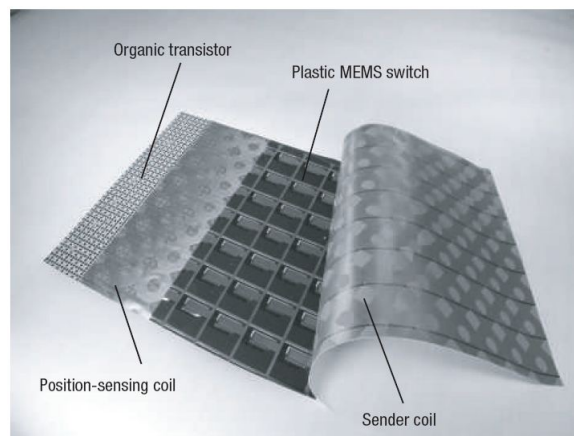

Fig. 3.3: *Photograph showing an exploded view of the wireless power-transmission sheet embedded in the floor and comprising a wireless power-transmission system and contactless position-sensing system. Part of the cover layer is peeling off. The size of all of the sheets is 21 x 21 cm^2 (64 power-transmission units and 64 position-sensing units).* [5].

---

[11]The italicized/emphasized text is a verbatim quotation from [5]

So, there have been shown different approach to accomplish tactile sensor for large areas. The two first use piezoresistive material where they have arrayed the elements in a big matrix. This type of the approach is the most common employed method when the tactile sensor uses piezoresistive material. But this kind of technology has the principal inconvenient which the consumption will be higher as the matrix has more elements. Because they usually use the "classic" methods to measure the drop of voltage on the elements, therefore, the consumption is high. However, the third approach presented, the consumption is very low because they use MEMS switches and organic transistor but the technology is very difficult to implement and accomplish.

In this report, there has been presented a novel method to measure the elements independently with low power consumption, ideal to be used in modules and the manufacturing is very simple because only is necessary a PCB which contents the electrodes and a conductive material.

4   Tactile sensor based on conductive foam

[12]*When elastomers show piezoresistance, it is called elastoresistance. Elastoresistance facilitates the construction of a simple, cheap, flexible and robust tactile sensor. It is a relatively old technology, governing some of the earliest tactile sensors to be built. It depends on the measurement of a resistance, which is just as easy for small or large elements, as long as the resistance does not become excessively large or small. This means that a spatial resolution of 1mm or below is straightforward to achieve, while more complex technologies, such as most optical sensors, are more difficult to miniaturise. Capacitive sensors, which have a similar simple structure, do not scale down as well because of the rapidly decreasing capacitance, which becomes more difficult to measure and more sensitive to noise. Elastoresistance also allows for both static measurements and very high frequencies.*

4.1   Working principle of the pressure conductive foam

Conductive elastomer[13]

The pressure conductive foam consist of a nonconductive matrix material with conductive particles or fibres. Electrically conductive polymer matrix composites have unique electrical and mechanical properties as well as many excellent properties of polymeric materials, such as light weight, low cost, ease of processing and corrosion resistance. The pressure conductive foam have been widely used in the areas of electromagnetic interference shielding, electrostatic discharge protection and conductive adhesives for die attachment in electronic packaging applications.

The most interesting composites have a nonconductive elastomer matrix. The most common particles are graphite, carbon black and small metal particles. Other semiconductive particles such as molybdenum, antimony, ferrous sulfide or carborundum are also used. Most, if not all, conductive rubbers show at least some elastoresistive behaviour.

Some of the conductive rubbers are sold as material in pressure sensitive switches and show a binary behaviour with a sudden change from a very high to a very low resistance. Others are produced with the purpose of electric connection between parts to prevent static electricity buildup, or as conformable electrodes in connection with the human body. This means most conductive rubbers are not designed to have the right properties for a proportional elastoresistive sensor, and a careful selection is necessary. To manufacture an adequate sensor material, an experimental, iterative process would be required, mixing different loadings of particles and measuring the properties. Moreover, mixing particles homogeneously through rubber can be difficult.

An exception is the CSA rubber produced by PCR Technical [24], which is specifically designed

---

[12]The italized/emphasized text is a verbatim quotation from [9]
[13]The italized/emphasized text is a verbatim quotation from [9]

to be used in sensors. The base material is polysiloxane (silicone rubber), and the electrically conductive particles are artificial graphite. The additives red ochre (Fe2O3) and amorphous silica (SiO2) are also present in a small amounts. The material is stabilised chemically, and contains neither the residual substances of antioxidants and plasticisers, nor curing agents. Moreover, volatile poly-siloxane components, which can cause poor contact with the electrodes, are carefully removed.

Phenomenon of the elastoresistance [14]

Both the bulk resistance of the rubber and the contact resistance between rubber and electrodes might change under the influence of pressure. The change in bulk resistance would be caused by the fact that the conductive particles come closer together, which results in more electric paths and thus a lower resistance (shown in paragraph about Percolation theory). The change in contact resistance is the result of a better contact. The change in contact resistance is the result of a better contact. The relative influence of both on the elastoresistive effect has long been uncertain.
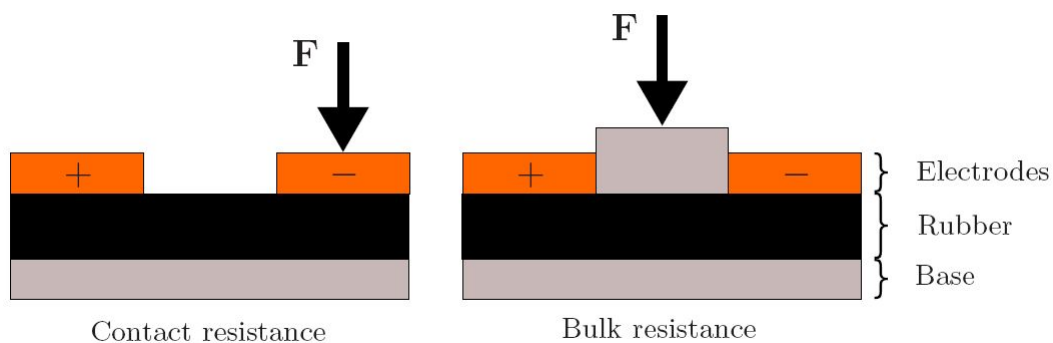

Fig. 4.1: Test setup to measure the respective influence of contact and bulk resistance[12].

The first experimental proof is acquired by gluing the sensor material to the electrodes with a conductive adhesive, which eliminates the contact resistance [14]. The measurement of the load-resistance curve of this situation reveals no dependency dependency between the load and the electrical resistance. This leads to the assumption that the contacting area is the important factor of the working principle.

In [12] are carried out several experiments to confirm this assumption, shown in Figure (4.1). *The picture on the left shows the first experiment, where the positive electrode is clamped firmly to establish good contact, while an external force is applied on the negative electrode to affect its contact resistance. On the right is shown the second experiment, both electrodes are clamped and a force is applied on the rubber directly that covers the entire surface between the electrodes. In this way, the contact resistance remains constant and any*

---

[14]The italized/emphasized text is a verbatim quotation from [9]

change is due to a change in bulk resistance. The results (Figure 4.2) show clearly that the influence of the bulk resistance is almost negligible compared to the contact resistance. In first picture is shown the variation of the contact resistance with applied force. The variation is large and the contact resistance clearly plays an important role. In second pictures is shown the variation of the bulk resistance with applied force. There is a light variation.
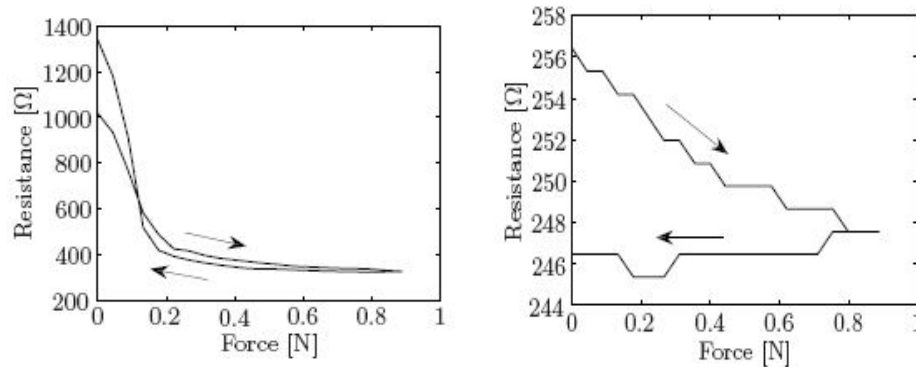
Fig. 4.2: Variation of the contact resistance and the bulk resistivity with applied force[12].

Percolation theory[15]

Percolation theory is relevant to the elastoresistive behaviour of conductive rubbers, as a certain percentage of the volume of these rubbers is conductive and the rest is not. A conductive rubber is in fact a resistance network, which changes under pressure (Figure (4.3)). Percolation theory describes which volume of particles is needed to have a conductivity path. This volume fraction is the percolation threshold. Below the threshold, there is no conductivity. Above the threshold, conductivity rises as the number of paths increases and the resistivity network becomes denser. In other words, the percolation effect can be explained as, the conductive foam behaves as isolated when no force is applied over it, that is to say the inside particles are uniformly distributed along the conductive foam without contacting each other. When one force is applied over conductive foam the inside carbon particles move together and its electrical resistance is reduced significantly, so that the resistance decreases as the applied pressure increases.

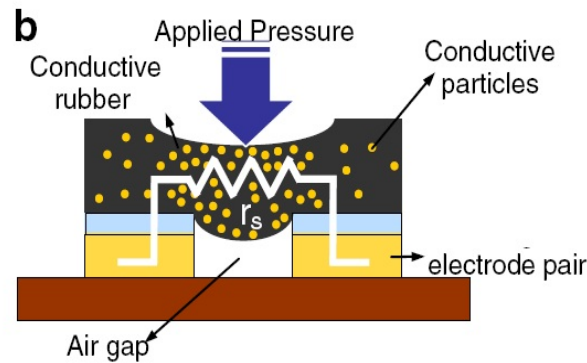[15]The italized/emphasized text is a verbatim quotation from [9]

Fig. 4.3: Schematic of a tactile sensing element under compression [15].

Elastoristance in a tactile sensor

[16] *Elastoresistance is well suited for pressure distribution sensors, because it allows a very simple and robust structure that is easy to miniaturise. The sensor itself only needs a thin sheet of conductive rubber and an array of electrodes. Since only a resistance has to be measured, the readout electronics can be simple as well. This measurement principle can thus offer low cost tactile sensors, which are thin, flexible, sensitive and robust. The main disadvantages originate from the elastomer and include relaxation, hysteresis, and nonlinear response. Due to this behaviour, elastoresistance cannot provide accurate absolute force measurements.*

All elastoresistive sensors require an interface between a conducting elastomer and electrodes. As mentioned before, material and surface quality of electrodes require some attention. In order to prevent oxidation, plating of the electrodes with gold is recommended.
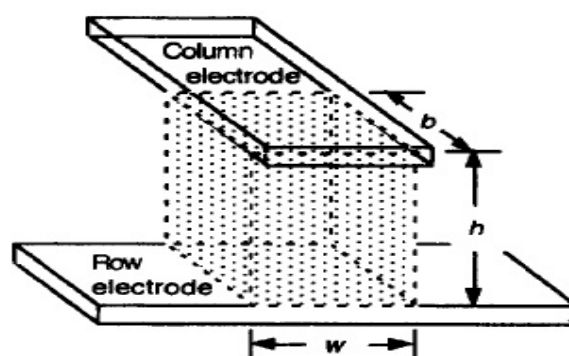

Fig. 4.4: A simple model of one sensor element mounted on two layer.

---

[16] The italized/emphasized text is a verbatim quotation from[9]

[17] *Commonly, the construction of the sensor cells is done by placing both electrodes on the back side of the sensor material, eliminating the fatigue problem. This arrangement presents an easy construction of tactile sensor matrices by adding horizontally and vertically aligned electrodes, getting a network of force sensitive resistor. There are others types of sensor cells, Figure (4.4), mounted on the facing sides of the sensor material [6][8], where the force is applied over upper electrodes directly. This contact can cause some problems, since the electrodes should be flexible, so the electrode is exposed to a bending stress reducing the life time of the sensor.*

[18]*According to the conductive chain barrier tunnelling effect, it can get the resistance of the complexes per unit area[10]:*

$$R = \frac{1}{p}\frac{k}{w}\frac{t^2 R_m}{m} \tag{4.1}$$

where m is carbon particle number of complexes per unit area, R is the resistance of conductive particles, k is the number of conductive chains per unit area, t is the number of carbon particles in each chain, p is the extrusion stress and k is Hooke coefficient. Let $q = K_t R_m/wm$ be the coefficient of resistance and pressure, so the resistance of the complex has a reciprocal relation with the extrusion stress, namely $R_{vol} = q/p$. As shown in Figure (4.5), R_{vol} is the volume of the resistance of the sensor material between the electrodes and the interface resistance are R_{inn} (interface resistance on inner electrode) and R_{outt} (interface resistance on the outer electrode).
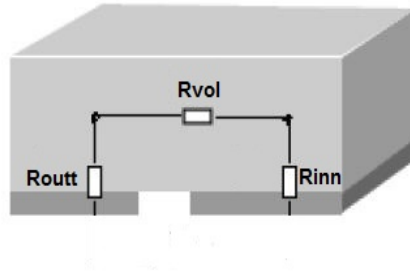

Fig. 4.5: Electrical circuit model between the electrodes of a tactel[21].

The electrodes working is based on the contact area. If a pressure is applied over the foam, the rough surface of the conductive material presses on the surface of the electrode. This pressure involves an increasing of the contact area, achieving so a change in the interface between the foam and the electrode, this carries a decreasing of the interface resistance. The contact resistance R_c can be described by [13]

$$R_c \propto \frac{\rho}{F} K \tag{4.2}$$

---

[17] The italized/emphasized text is a verbatim quotation from [14]
[18] The italized/emphasized text is a verbatim quotation from [10]

[19]*where ρ s the resistivity of the contacting interfacing, F is the normal force applied to the contact interfacing and K is a function of the roughness and elastic properties of the interfacing.* Thus, it is possible to get the relationship between the applied pressure and the interfacing resistance as a sum of its resistor[14]

$$R(F) = R_{inn} + R_{outt} + R_{vol} \tag{4.3}$$

---

[19]The italized/emphasized text is a verbatim quotation from [13]

There are many reports about tactile sensors based on conductive rubber. Below are shown the main works in this field, where it is explained the principle working of them.

4.1.1 Tactile sensing array using PI-copper films

In this work [15] is developed [20]*a flexible 32×32 temperature and tactile sensing array, which will serve as the artificial skin for robot applications. Pressure conductive rubber is employed as the tactile sensing material. In order to measure the pressure, small circular piece of pressure conductive rubber is placed on a electrode pair which predefined interdigical copper electrodes pairs, shown in Figure (4.6a). Note that to bond the rubber piece with the electrode pair, a Z-axis-conductive adhesive film is used. The mechanical and electrical properties of tactile sensing elements are measured. The flexible sensor arrays are bendable down to a 4 mm radius without any degradation in functionality, Figure (4.6b). They get measured different shape with different weights.*
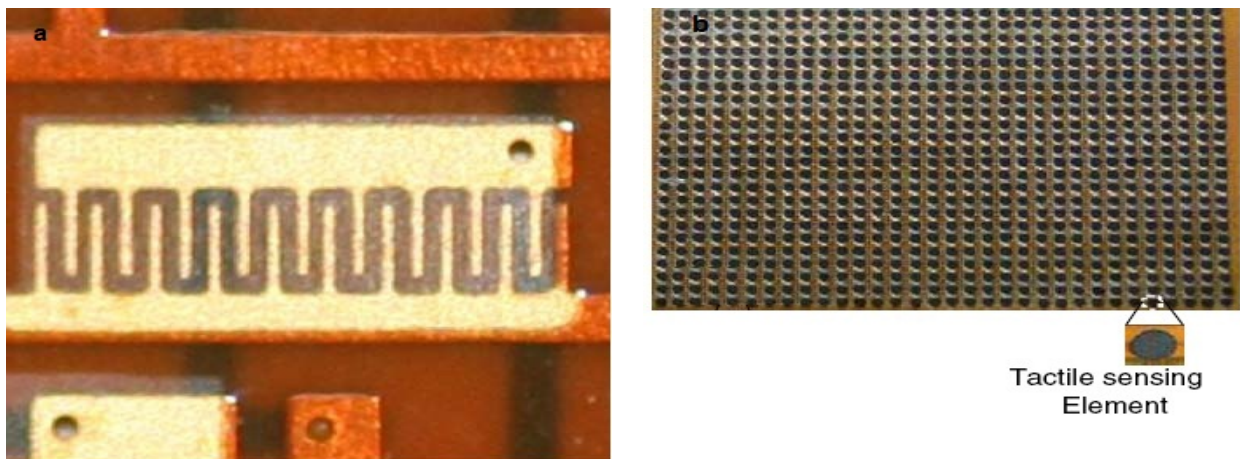

Fig. 4.6: Figure **a** show the interdigital electrodes for the tactile sensing elements. Figure **b** show the complete skin of the tactile sensor array.

4.1.2 A Tactile Sensor with electrical wires stitched

The work [16] develops [21]*a type of tactile sensor using pressure conductive rubber with stitched electrical wire. The sensor presented is thin an flexible and can cover three-dimensional object. Since the sensor adopts a single-layer composite structure, the sensor is durable with respect to external force. The sensor is employed for a robot hand, concretely for four fingers, where each finger is equipped with tactile sensor grasped sphere and column. They adopted a single-layer composite structure stitching electrodes into pressure-conductive rubber. They*

---

[20]The italized/emphasized text is a verbatim quotation from [15]
[21]The italized/emphasized text is a verbatim quotation from [16]

intended to keep the thin flexible property while improving durability with regard to the tangential force and deformation. The Figure (4.10) shows the structure of the sensor with the row of the electrodes are configured in the horizontal direction alternating back and forth, and the column of electrodes are configured in the vertical direction. The sensing element are configured in the intersection of the row and column electrodes.
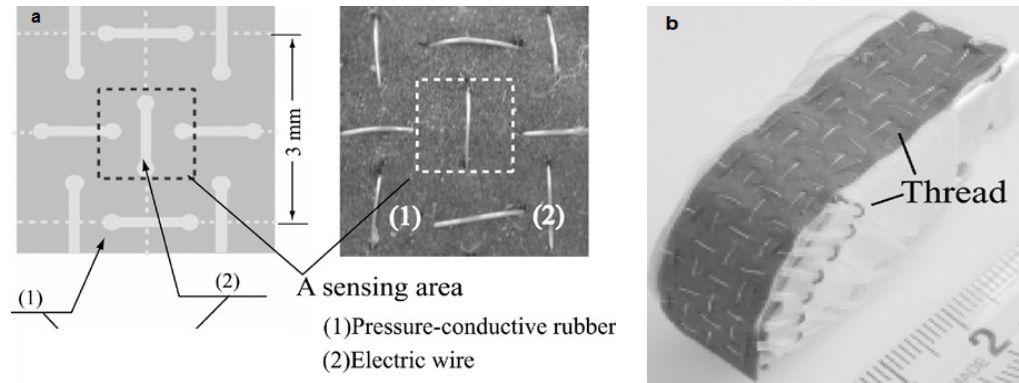

Fig. 4.7: Figure **a** shows the structure element where the wires are stitched into the rubber. Figure **b** shows the fingertip.

4.1.3   Pressure Sensor Grid for Humanoid Robot Foot

This report [17] presents [22]*a 32 × 32 matrix scan type high-pressure sensor for the feet of humanoid robots. Each sensing area is 4.2 mm × 4.4 mm and can measure vertical force of approximately 0.25-20[N]. They have used a electrodes grid which are overlaid with gold in order to suppress change of the contact resistance by the chemical change. They have get that thinness is better to achieve small time constant and sensitivity, so their system can realize higher scan rate.*

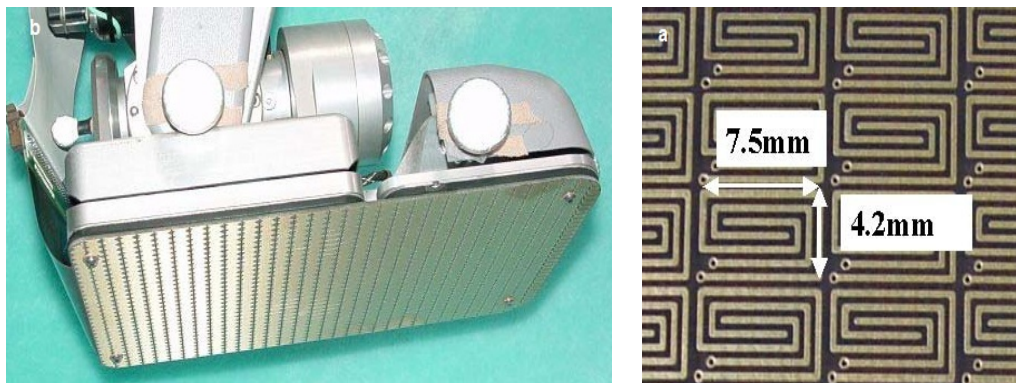[22]The italized/emphasized text is a verbatim quotation from [17]

Fig. 4.8: Figure **a** shows humanoid robot foot with pressure sensor grid. Figure **b** shows the sensor grid size.

4.1.4 Embedded Tactile Matrix Sensor

The work [20] presents [23]*a fully embedded tactile sensor to be installed on the phalanges of a robot hand is present in this paper. The sensor consist of a distributed array of analog tactile elements and an integrated three component force transducer. The tactile sensor is a matrix of electrodes etched a flexible printed circuit board (PCB), in order to conform to a curved surface, covered by pressure rubber. The sensor is composed by three modules: a three axis force sensor module, a matrix tactile transducer, and an data acquisition and processing module. This module are implemented in different PCB. They also presented a new technique based on the idea of contact centroid, in order to reduce the effect noise with respect to the actual pressure values. This technique allows to reduce the amount of data to be transmitted from the sensors to the control modules.*
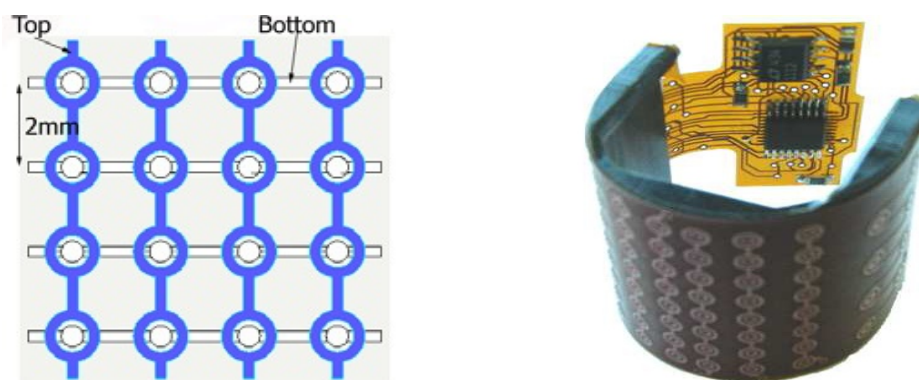

Fig. 4.9: Figure **a** shows the electrodes of the tactile sensor are etched on a double layer flex- PCB. Figure **b** shows the flex circuit conforms to the cylindrical phalange rigid cover.

---

[23]The italized/emphasized text is a verbatim quotation from [20]

4.1.5 Tactile Sensor Arrays of Robot for Three-dimension Force

This report [21] shows [24]*a new type of electrodes based on three electrodes a,b,c shaped sector and d electrode shaped round made on flexible PCB. The round area d serves as the common electrodes. The diameter of the sensor unit is 28 mm. They can measure the force in the three direction according to their experiments.*
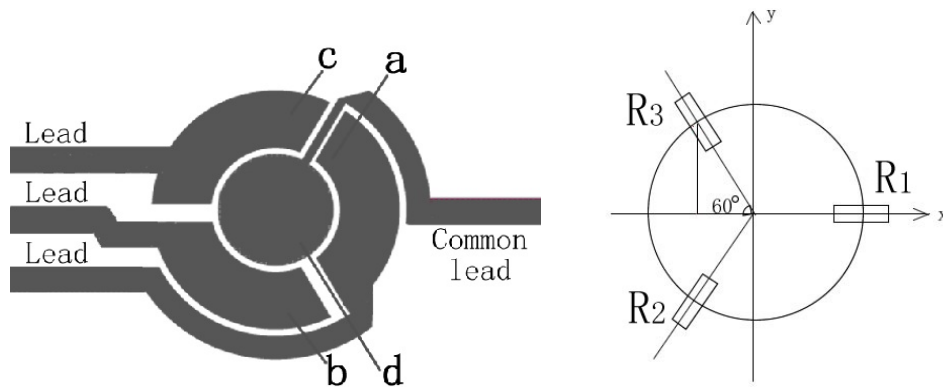

Fig. 4.10: Figure **a** shows the sensor unit structure. Figure **b** shows the equivalent resistance.

---

[24]The italized/emphasized text is a verbatim quotation from [21]

4.2 Readout Electronics for an Tactile Sensor based on conductive foam

[25]*The readout electronics are an important part of the sensor. The circuit has to read out a large amount of sensitive elements, and take the properties of the sensor into account. The electronics reduce the number of wires to the sensor and minimise the noise level, crosstalk and response time. An important measure to reduce the noise is to limit the length of the wires or to shield them. If not carefully designed, the electronics circuit can be a limiting factor for the bandwidth and sensitivity of the sensor. Especially for sensors with a large amount of taxels, the readout time of a single taxel has to be very short in order to reach an acceptable frame rate for the entire tactile sensor.*

Design of the readout circuit

[26]*In this section is presented several methods to measure multiple sensing elements of identical behaviour in N×M format arrays and the different problems arise in such topologies. The interconnection electrodes are used in row-column with all the sensor element having one of their ends connected to a column electrode and other end to a row electrode* as Figure (4.11) shows.
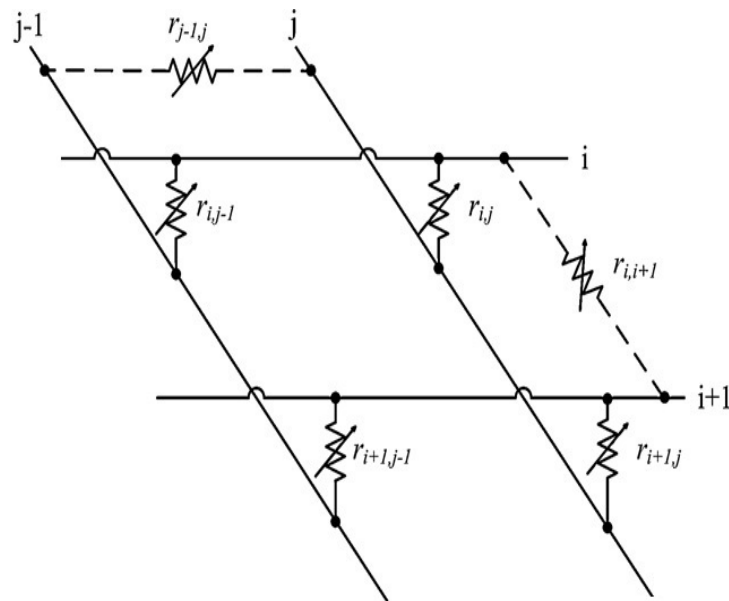

Fig. 4.11: Circuit with multiple sensing element of identical behaviour.

---

[25]The italized/emphasized text is a verbatim quotation from [9]

[26]The italized/emphasized text is a verbatim quotation from [33]

[27] *One of the major problems in the using of this topology is the crosstalk effect between adjacent elements, this can occur as long as the row-column electrode format is applied, which will change the value of the resistance read when attempting to read the voltage corresponding to a sensitive element. When it attempt to read the value of resistor R_{ij}, other parasitic paths of different lengths and resistance, such as the path composed of the three resistances $R_{ij_{-1}}$, $R_{i_1j_{-1}}$, $R_{i_{-1}j_{-1}}$ in series, appear in parallel to R_{ij}, Figure (4.11). They cause errors in the reading of the voltage. In the case of sensors made by polymer sheet, other paths appeared due to the bulk conductivity of the sheet, schematised by the parasitic resistances $R_{j_{-1}j}$ and $R_{i_{-1}i}$ (row-row and column-column) are present. Their magnitude depends on the materials and dimensions of the array and also on the pressure map.*
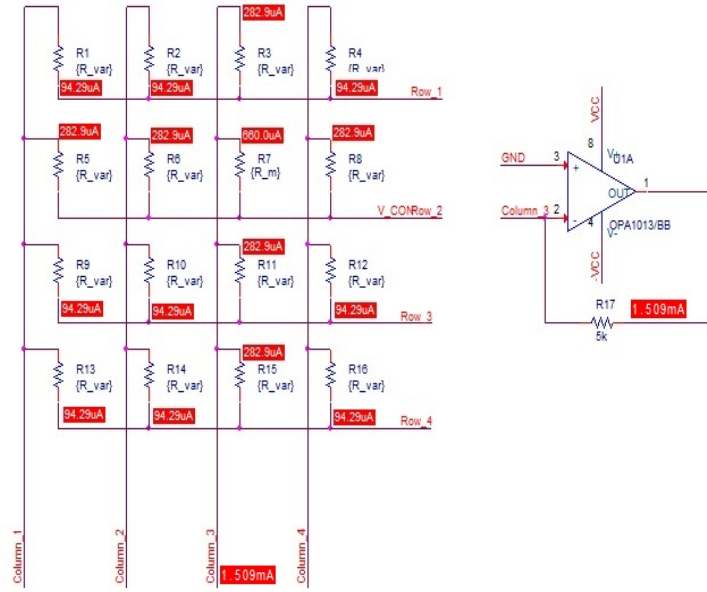

Fig. 4.12: shows crosstalk effect between adjacent elements.

This effect is shown in Figure(4.12) where is used current-voltage topology operational amplifier to read the drop of voltage in the resistance labelled as R_m. This simulation is carried out keeping fixed the resistance R_m and the surrounding resistances change their value in the same magnitude, they are labelled as R_{var}. The Figure (4.13) shows the reading of R_m. As it can be observed the drop of voltage in R_m changes when R_{var} changes because the current passes from some measuring points to others that are aimed, consequently the accurate resistance measurement cannot be done. How to exclude this undesirable current passes becomes a problem. Particularly in this type of the sensor, thus, it is necessary excluding the undesirable current passes per each element.

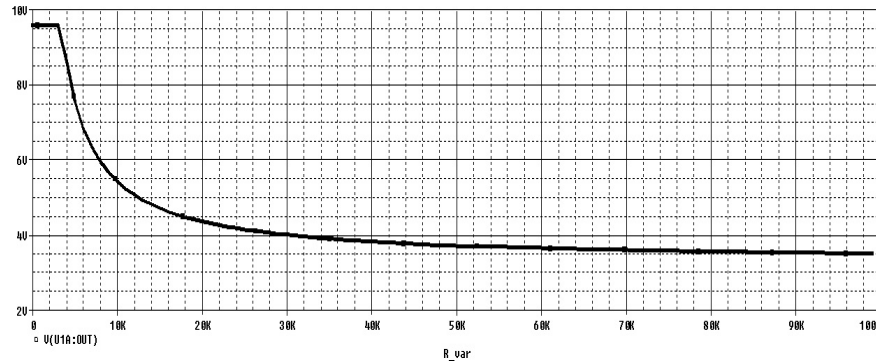[27]The italized/emphasized text is a verbatim quotation from [33]

Fig. 4.13: :shows the drop voltage in R_m when the surrounding resistance change.

The analysis and elimination of crosstalk effect have been extensively treated in the literature from different viewpoints, the most important are shown below:

- Method based on the zero potential.

- Method based on the voltage feedback.

- Method employed Analog/Digital converters on the column lines

In the readout system under study, the goals are four. Firstly, the readout system should be able to avoid the crosstalk effect. Secondly, to achieve acceptable speed sample, that is, the scanning time should be enough fast for no losing any type of contact. Thirdly, to achieve that the whole system is compacted, that is, to reduce the number of wires, to use the minimum of the devices. Finally, to achieve that the consumption is as low as possible, that is, one only tactel should be connected when the matrix is read. This last point is the most important when speak about large area. The previous methods connect every tactels when one row is selected. This presents a problem becuase if the resistances of the tactels are low the consumption is high, above all, when the rows are composed by many tactels. For this issue, the methods presented previously are not good candidates to use for large area. In this report is presented a novel method to be employed into large area. This novel method is shown in section (4.2.2) and is based on the measuring of each tatel independently.

Circuit based on zero potential method

[28]*The goal of this method is to get an equal potential zone to eliminate the crosstalk effect. In this method a voltage is applied to the row to be selected, and the others rows are tied*

---

[28]The italized/emphasized text is a verbatim quotation from [33]

to zero voltage. As for column direction is usually tied to negative input of the operational amplifier and other are also tied to zero voltage. As can be observed in the figure, when one row is selected, every tactels which are located over the selected row are activated. Thus, the consumption will be greater as increasing the number of tactels for row.
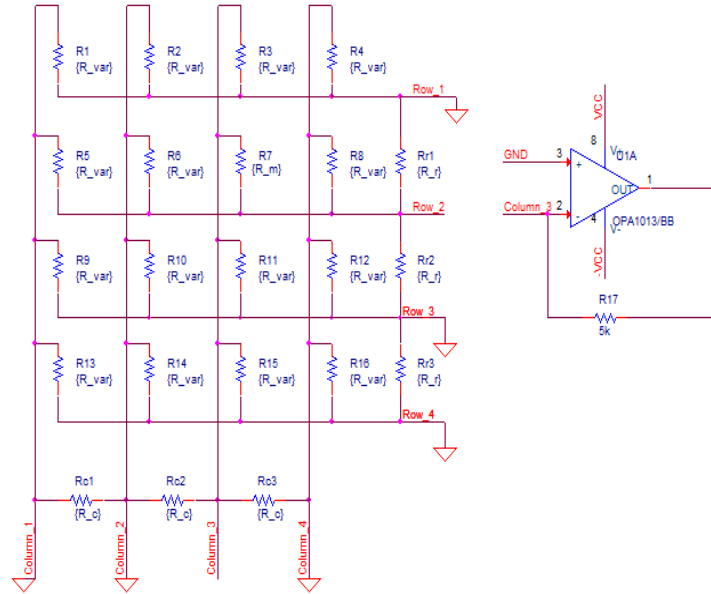

Fig. 4.14: shows crosstalk effect between adjacent elements.

The error due to the array scanning can be eliminated. Figure(4.14) shows the zero potential method and the Figure(4.15) shows that the drop of voltage on R_m is not affected when the surrounding resistances change their value. Furthermore, it is observed when the resistance surrounding are lower than 600 Ω the output decreases. This effect is explained in section (4.2.3).
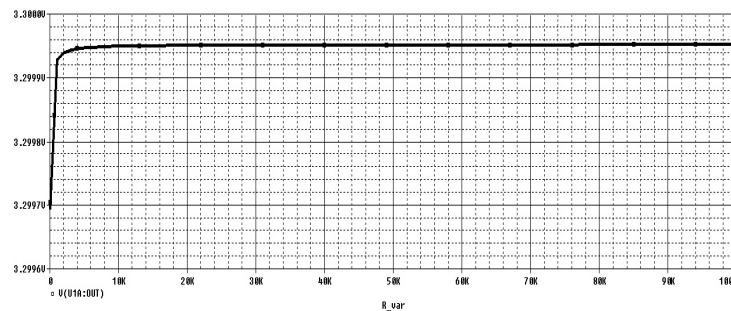

Fig. 4.15: shows the drop voltage in R_m when the surrounding resistance change.

To accomplish this method exists different alternatives. Figure (4.16) shows the typical circuit to accomplish this method where the circuit is composed by one microcontroller

(MCU), multiplexors and several operational amplifiers with as many columns as rows. The working of the circuit is very simple, [29]*for row scanning, one output port of the MCU provides the driving power to sensing elements and the row measured is tied to high level and other are tied to low voltage . For column scanning, another set of multiplexers is used to receive the data outputs from each sensor. A constant voltage is supplied, and the change of the current flowing through the resistor can be detected by the current-to-voltage converter, as shown in Figure (4.16). The scanned output voltages of tactile sensing arrays are transferred to analog-to-digital converter (ADC) of a MCU.* This configuration is used in [15],[16], [22].
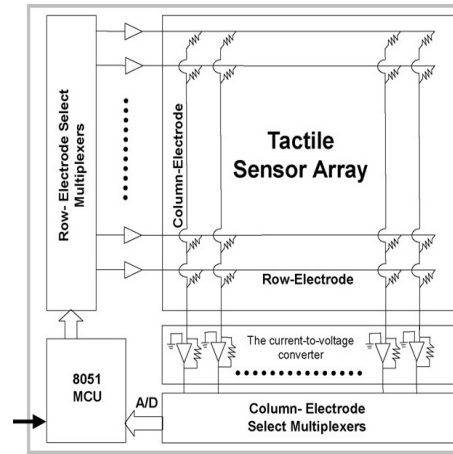
Fig. 4.16: Circuit based on zero potential method using MCU, multiplexor and ADC.[15]

Other way to carry out this configuration [18] is shown in Figure(4.17). This circuit has higher complexity than circuit shown in Figure(4.16), since this circuit uses at least two multiplexers, one switch and solely one operational amplifier. The quantity of devices depend on the number rows and columns the sensor has. [30] *The resistance $r_{i,j}$ is connected into the measurement loop through the multiplexers (mux_1 and mux_2); one end of the reference resistance R_{ref} is connected to the inverting input pin of the op-amp, and the other end is connected to the output pin of the op-amp; the driving voltage V_{dd} is applied on the current scanned driving electrode (the i-row electrode) by the mux_1, while the current scanned sampling electrode (the j-column electrode) is connected to the inverting input pin of the operational amplifier through the mux_2. The non-current scanned electrodes are connected to the ground by the switches. However, the non- current scanned sampling electrodes and the non-current scanned driving electrodes are connected to the ground.*

---

[29]The italized/emphasized text is a verbatim quotation from [15]

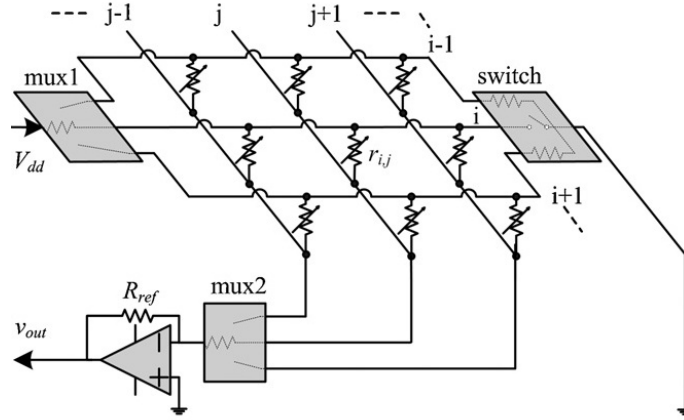[30]The italized/emphasized text is a verbatim quotation from [18]

Fig. 4.17: Circuit based on zero potential method [18].

The major drawbacks of both configurations are, they need many devices and depend on the size of the sensor. If the sensor has many columns it is necessary to use the same number of operational amplifiers for the first configuration, and it also needs as many outputs in MCU as rows the sensor has. Sometimes this is a restriction when this configuration is used for large area application.

In [19] is proposed a possible solution which avoids the use of many devices. The proposed circuit is shown in Figure (4.18) . [31]*As depicted in the Figure, the columns and the rows are connected to two digitally controlled SPDT (Single Pole, Double Throw) denoted in the Figure as switch. This allows the connection of any column to the load resistor R_L and any row to the output node of the operational amplifier. All other rows and columns stay connected to the ground. The element being accessed, comes in the negative feedback path of the operational amplifier. The other $N-1$ sensors connected to the selected column make a parallel combination across the two inputs of the operational amplifier, with non-inverting input connected to the ground. Similarly, $M-1$ elements connected to the selected row get connected to the output node of the operational amplifier with their other end grounded. The rest $(N-1) \times (M-1)$ elements, not physically connected to the element being accessed, have both of their ends at the ground.*

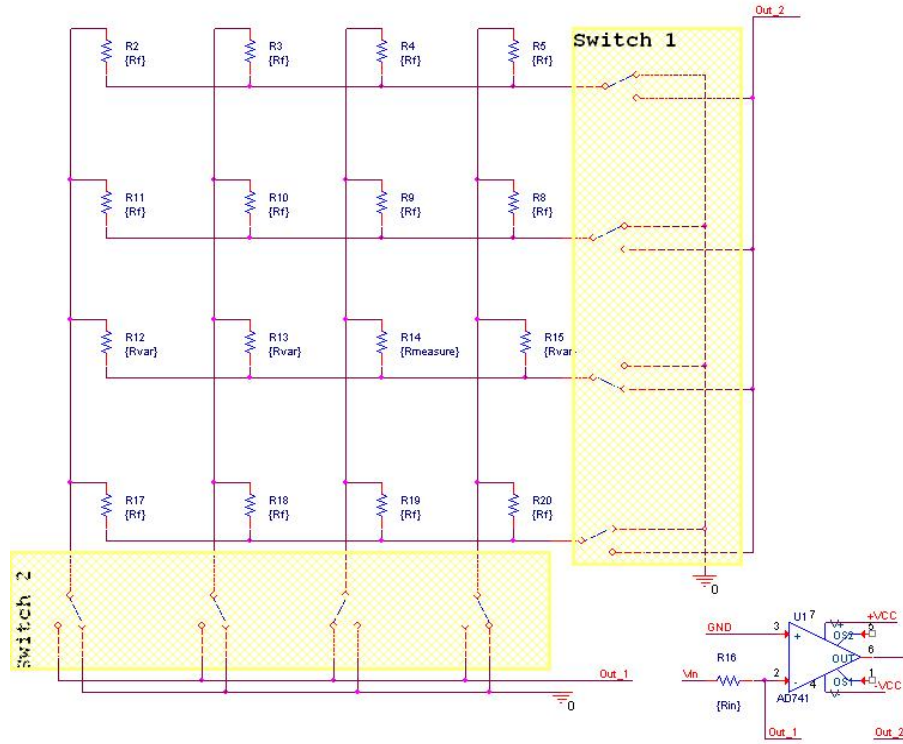[31]The italized/emphasized text is a verbatim quotation from [19]

Fig. 4.18: Schematic of the proposed circuit for implementing the ZPM.[19]

The effect of R_{var} over V_{out}, as depicted from Figure (4.19), is not significant. For a change of R_{var} from 1 to 500 Ω is observed an important change, this is explained in (4.2.3)
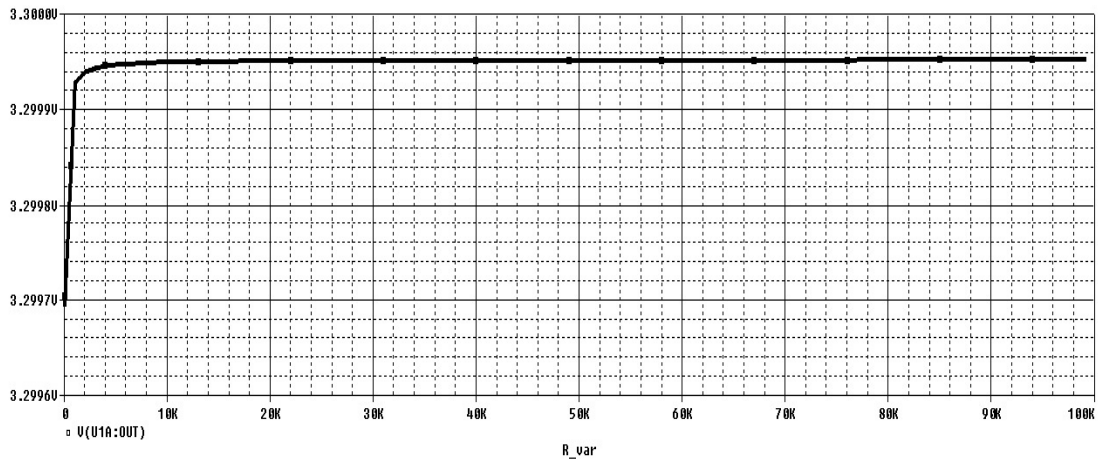

Fig. 4.19: The V_{out} of the circuit as a function of input resistance R_{var}.

4.2.1 Circuit based on the voltage feedback method

In [18] proposes the typical circuit which employ the voltage feedback method,shown in the Figure (4.23) . There are one operational amplifier, two multiplexor ans two switches. [32]*The resistance $r_{i,j}$ is connected into the measurement loop through the multiplexer(mux_1 and mux_2), one end of each reference resistance R_{ref} is connected to a column electrode, and the other end is connected to the ground; the voltage V_{dd} is applied on the current scanned driving electrode (the i-row electrode) by the mux_1, while the voltage of the current scanned sampling electrode (the j-column electrode) is exported via the mux_2 and the operational amplifier. Thus, V_{out} is fed back to the non-current scanned electrodes by the two switches.*
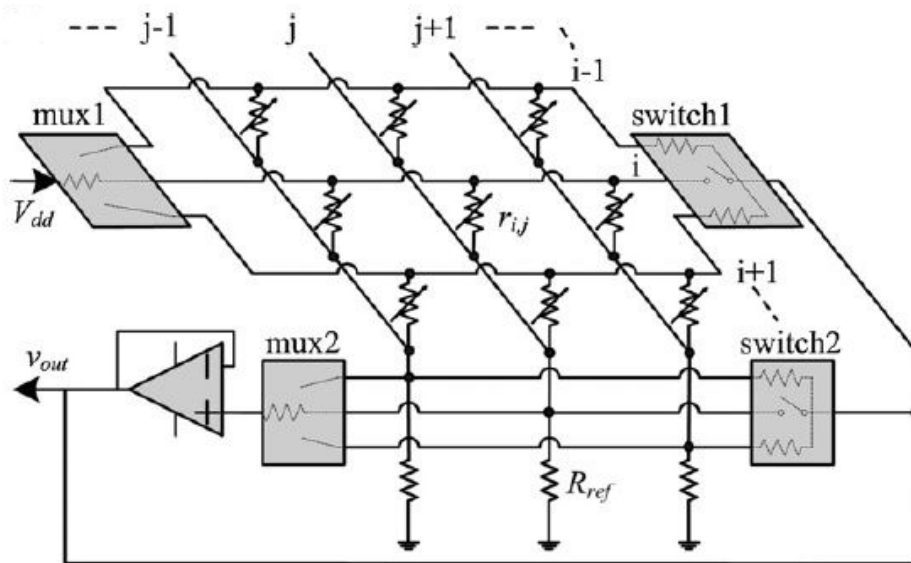

Fig. 4.20: Circuit based on Voltage feedback method [18].

---

[32]The italized/emphasized text is a verbatim quotation from [18]

Circuit based on the use of Analog/Digital converters on the column

Figure (4.21) shows the Analog/Digital converters method. This circuit is equipped with analog/digical converter on each columns and each rows of the sensor, this approach is proposed in [17] .
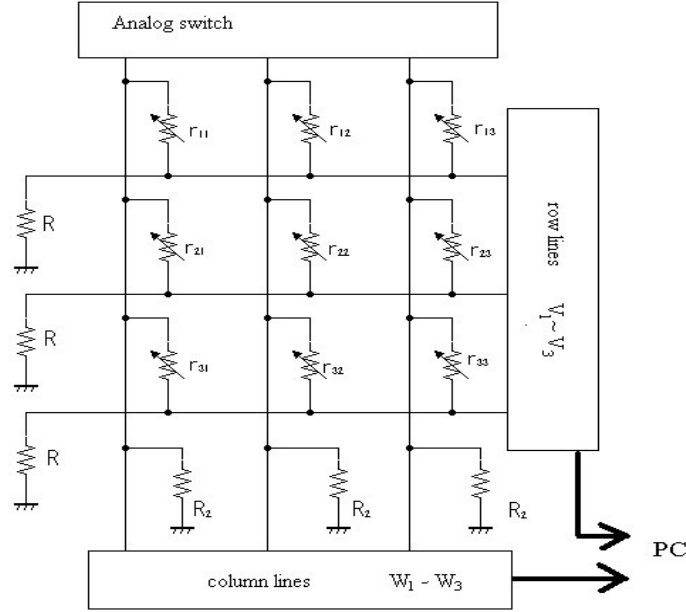

Fig. 4.21: Circuit based on Analog/Digital converters method [17].

When the column 1 is applied a fixed voltage , according to Kirchoff law, in top row the current is

$$\frac{^1V_1}{R} = \sum_j \frac{^1W_j - {}^1V_1}{r_{1j}} \tag{4.4}$$

So, for the i-th row and k-th column is

$$\frac{^kV_i}{R} = \sum_j \frac{^kW_j - {}^kV_i}{r_{ij}} \tag{4.5}$$

Let x_{ij} be $\frac{1}{r_{ij}}$

$$\frac{^kV_i}{R} = \sum_j \left({}^kW_j - {}^kV_i \right) \cdot r_{ij} \tag{4.6}$$

When $i=1$, the formula can be write as

$$V_1 = M_1 X_1 \qquad (4.7)$$

Therefore X_1 can be calculated as

$$X_1 = M_1^{-1} V_1 \qquad (4.8)$$

Thus, $i_t h$ X_i can be calculated as

$$X_i = M_i^{-1} V_i \qquad (4.9)$$

[33]*Value of resistance r_{ij} is found by taking the reciprocal of each element of vector X_i.*

Obviously, this method can only be used for small array because when is used for large area the computational cost can be very high, further, it is necessary having many input for each ADC.

---

[33]The italized/emphasized text is a verbatim quotation from [17]

4.2.2 Novel method based on measuring of each tactel independently (MEI)

In this report has been developed a new method to measure the tactels inspired on the common camera CMOS, this readout circuit is shown in the Figure (4.22). The readout circuit is based on the measuring of the elements independently, achieving that one only tactel is activated when one row is selected. So, it can be achieved a low consumption and can be employed for large area. The readout circuit employ as many Mosfets as resistances, thus, one end of each resistance is connected to the source pin of the Mosfet, and on the other end the resistance is connected to the measurement loop through a multiplexer, one end of each reference resistance R_{ref} is connected to the multiplexor output. The voltage V_{dd} is applied on all drain pin of the Mosfets, thus, when the gate pin of the Mosfet is set up to high level, that is to say shorted, the end resistor connected with source pin is tied to the voltage applied.
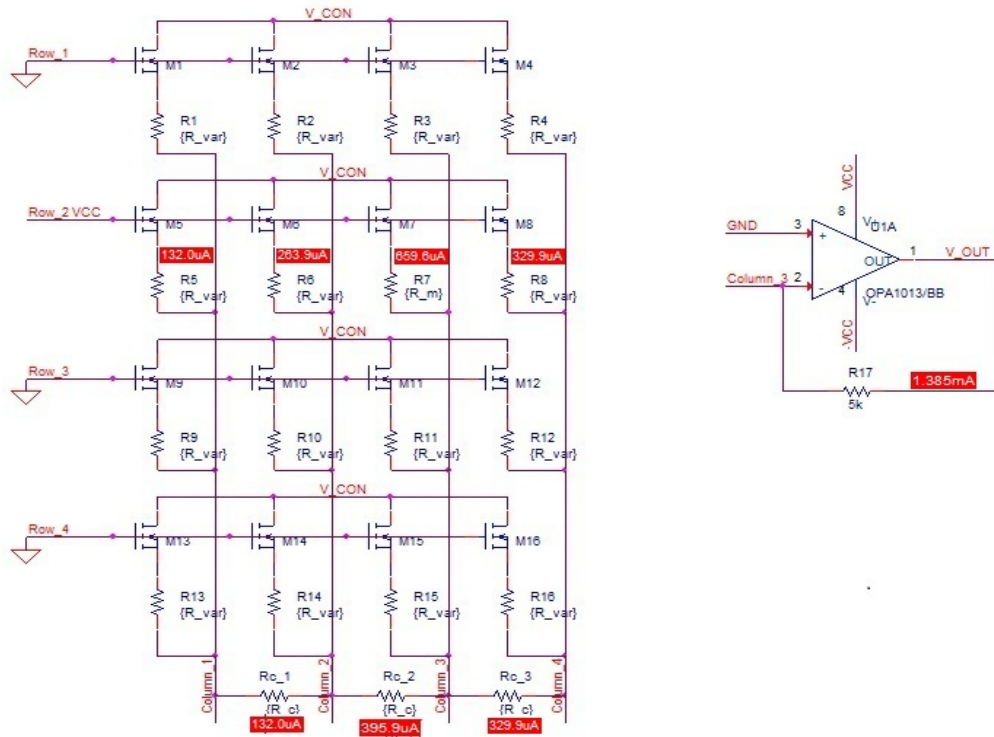

Fig. 4.22: Circuit based on Voltage feedback method.

Figure (4.23) shows the output voltage when R_m is measured. It is observed that the drop voltage in R_m is not linear due to the resistances R_c which connect the columns one to each other. Using this configuration appears the crosstalk effect due to the resistances between rows which make currents to appear on the other resistances, joining them with the output.
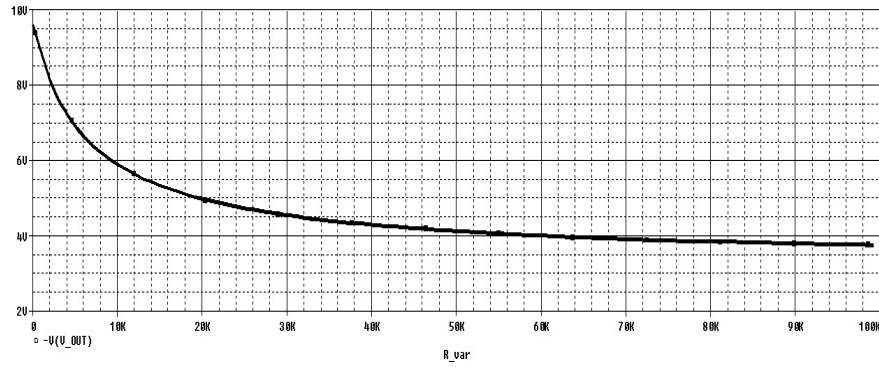

Fig. 4.23: Measure R_m when R_{var} changes.

To avoid this effect the easiest solution would be to use a small circular piece of conductive foam instead of polymer sheet. The small pieces are placed on an electrode pair which is patterned on the substrate described in previous subsection. This solution is shown in Figure (4.24), further, this solution was implemented in previous work as [15], [23].
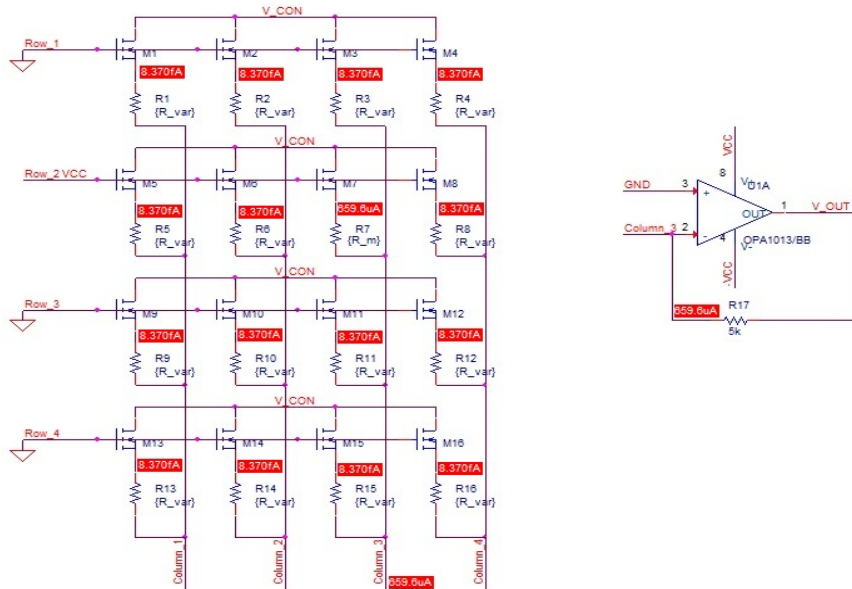

Fig. 4.24: Circuit based on Voltage feedback method without crosstalk effect.

Furthermore, with this solution is accomplished that only one resistance has a drop voltage because other resistances in the same selecting row are floating. Therefore the consumption in this type of configuration is ideal for large area tactile sensor, because this topology reaches a size of matrix very large. Figure(4.25) shows the output when the resistances R_{var} and R_m are measured. With this configuration the crosstalk effect is avoided.
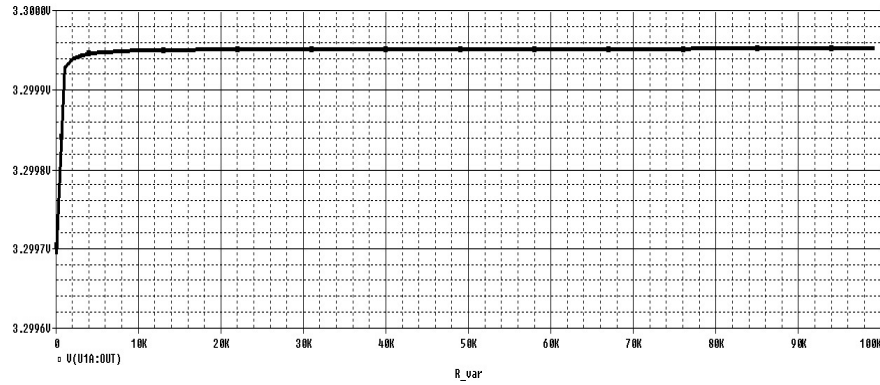

Fig. 4.25: Measure R_m when R_{var} changes.

4.2.3   Errors due to scanning Circuit

Effect of Output Resistance of Row Electrode Driver

There are a resistance between the row electrodes, denoted as r_r, it is called r_{j1j} in Figure (4.11) . This resistance is jointed in parallel with resistance value of the row electrodes at drive line, denoted as r_{row} , according to (4.10), [6]

$$\frac{1}{r_{row}} = \sum_{j=1}^{N} \left(\frac{1}{r_{smj}} \right) + \frac{1}{r_r} \tag{4.10}$$

where N is the number of column, r_{smj} is the resistance to measure, j is the column selected.

r_o is the output resistance of the device of the row–electrode driver, this resistance depends on the device used such as multiplexor, quick-switch, operational amplifier... [34]*The drive current, flowing where the voltage drop occurs in the row electrodes, and the voltage V_d at the drive points* are expressed in (4.11), [6]

$$V_d = \frac{r_o}{r_o + r_{row}} V_i \tag{4.11}$$

According to (4.11), if $r_o << r_{row}$ the voltage V_d will be the same as V_i, therefore it can be considered r_o negligible. So that there will be to choose the resistance of the device the lowest possible to sure this condition.

Effect of Loop Gain of Operational Amplifiers

The Figure (4.26) *shows the equivalent circuit when jth column of operational amplifiers is considered. r_{columj} represents the synthesized resistance of the resistance r_{sij} of the sensing element connected to the column electrodes and the leak resistance r_c between column electrodes.*
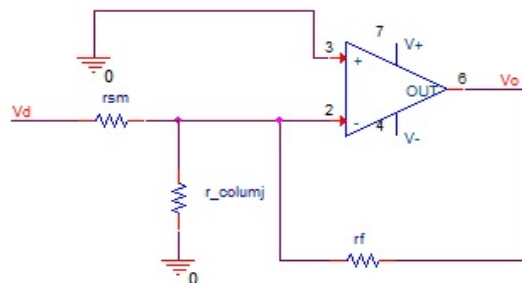

Fig. 4.26: Equivalent circuit for one column the zero potential scanning method.

---

[34]The italized/emphasized text is a verbatim quotation from [6]

Since this circuit is a summing circuit, if the value of r_{colum_j} is not extremely low, the values of r_{sm} the resistance could be measured from the output. However, when the value of r_{colum_j} becomes extremely low, the lowering of the loop gain A_L, shown in (4.13), results, and problems appear, such as the deviation from the imaginary zero voltage at the input of operational amplifiers. β represents the feedback factor, and is expressed in (4.14),[6]

$$\frac{1}{r_{colum_j}} = \sum_{i\neq j}^{N}\left(\frac{1}{r_{sij}}\right) + \frac{1}{r_c} \tag{4.12}$$

$$A = A_L \cdot \beta \tag{4.13}$$

$$\beta = \frac{r_{sm}r_{colum_j}}{r_f(r_{sm} + r_{colum_j}) + r_{sm} \cdot r_{colum_j}} \tag{4.14}$$

where A is the open-loop gain of the operational amplifiers and r_{sij} is the resistance value of the sensing element in the ith row connected to the jth columns of the operational amplifier. m is the electrode number of the connected row, for which r_{sm} should be measured. In order to maintain the imaginary zero voltage under the condition of varying β, it is necessary to select the operational amplifiers having high open-loop gain over a wide frequency range.

There is also another condition. The output voltage of the operational amplifier must be within the source voltage. Therefore, it is necessary to satisfy (4.15),[6].

$$V_{source} > \frac{r_f}{r_{sm}}V_i \tag{4.15}$$

This condition collapses when the value of r_{sm} becomes lower. Then, the zero voltage condition breaks, thus r_f should be selected to satisfy (4.15).

Effect input resistance on the frequency

[35]The differential open loop gain in an amplifier is not infinite, rather, is finite and decrease with the frequency. If it is considered a inverting amplifier topology, the closed-loop gain is given in (4.16), assuming a finite operational amplifier open-loop gain A,[7]

$$G = \frac{\frac{-r_f}{r_{smj}}}{1 + \frac{(1+\frac{r_f}{r_{smj}})}{A}} \tag{4.16}$$

The opened-loop gain in an operational amplifier of a typical general purpose is a low-filter pass that correspond, given by the next equation [7]

$$A = \frac{A_o}{1 + \frac{s}{w_b}} \tag{4.17}$$

---

[35]The italized/emphasized text is a verbatim quotation from [7]

where A_o correspond the gain dc and w_b denotes the corner frequency, that is to say, where the frequency falls down 3-dB.

Substituting (4.17) from (4.16) is obtained [7]

$$\frac{V_o(s)}{V_i(s)} = \frac{-r_f/r_{smj}}{1 + \frac{1}{A_o}\left(1 + \frac{r_f}{r_{smj}}\right) + \frac{s}{w_t/(1+r_f/r_{smj})}} \qquad (4.18)$$

where w_t is the frequency when $|A|$ reaches $0dB$. If it is assumed $A_o \gg 1 + r_f/r_{smj}$, which is usually the case, [7]

$$\frac{V_o(s)}{V_i(s)} = \frac{-r_f/r_{smj}}{1 + \frac{s}{w_b/(1+r_f/r_{smj})}} \qquad (4.19)$$

which is the same shape as low-pass filter network, thus with a dc gain given by r_f/r_{smj} and the frequency cut-off give by [7]

$$w_{3db} = \frac{w_t}{1 + r_f/r_{smj}} \qquad (4.20)$$

So the frequency decreases due to small resistance at the opamp input r_{smj} as it can be seen in (4.20).

4.3 Implementation of the Readout Circuit

In this section are presented two readout circuits based on the measuring of each tactel independently and the zero potential method. It is shown the devices selected to carried out both topologies. The readout circuit should be able to achieve a sample rate at least of 0.5 seconds to measure all tactels. This sample rate is the minimum rate which is possible to reach with the current DAQ boad.

4.3.1 First scanning electronic design

The electronic is based on measuring the elements independently **(MEI)**, which was explained in the section (4.2.2). Figure (4.27) depicts the blocks diagram which this method employs. There are five blocks where the proposing of the first one is to connect the host computer with the electronic. This block is responsible for sending the correct measuring sequence to each tactel through the Multiplexor block.
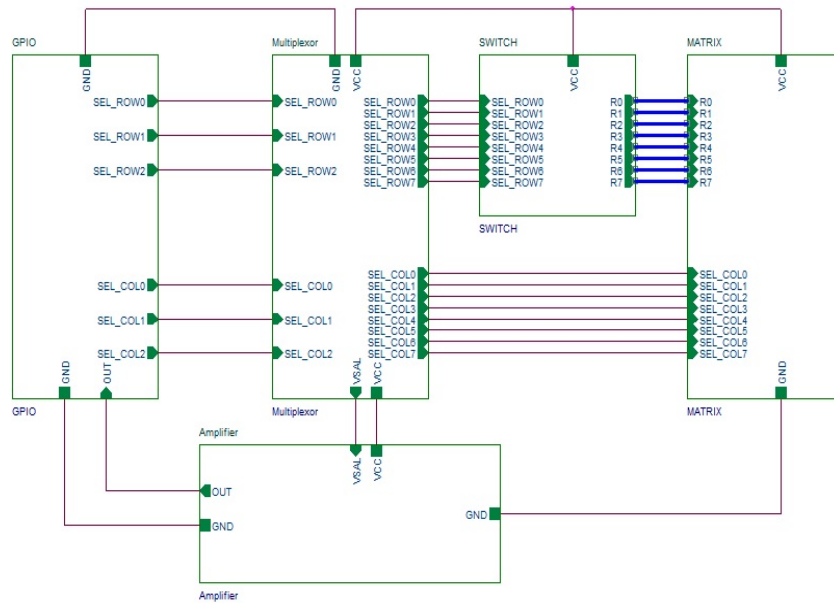

Fig. 4.27: Schematic for measuring of the elements independently method.

The $DT9816$ [30] is responsible of this. The device provides the communication between the host computer and the electronic via USB, moreover, the manufacture provides the software to tie the device with Data Acquisition Tool from Matlab. The principals features are:

- Up to 50 kS/s per channel (DT9816).

- 6 simultaneous analog inputs (16-bit).

- 16 digital I/O lines.

- Analog input ranges: ± 10V and ± 5V.

- Compatible with LabVIEW and MATLAB through available interface tools.

The LSB is possible to reach with $DT9816$ from differential voltage reference:

$$LSB = \frac{V_{ref}(+) - V_{ref}(-)}{2^N} = \frac{10 - (-10)}{2^16} = 305\mu V$$

The $DT9816$ sends the sequence to the multiplexers. There have been used two multiplexers: the first one (Mux1 in Figure (4.28)) is used to select one of the eight rows through the switches. The second one is used to connect the column selected with the amplifier block input (labelled as VSAL in Figure(4.28)).
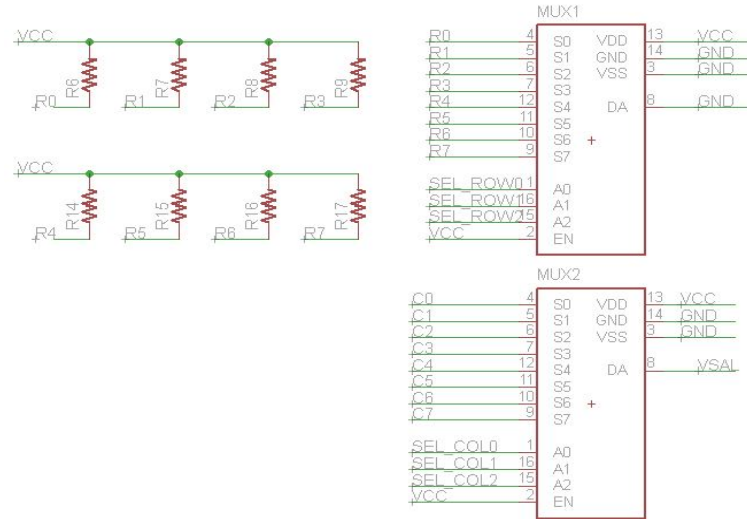
Fig. 4.28: Electronic for Multiplexor block.

The $ADG708$ is low voltage, CMOS analog multiplexers comprising eight single channels. The $ADG708$ switches one of eight inputs ($S1$ to $S8$) to a common output, D, as determined by the 3-bit binary address lines $A0$, $A1$, and $A2$. The principal features are:

- Single supply with 3V and 5V and $\pm$ 2.5 dual-supply rails.

- Low R_{on} where the resistance typical is 3 Ω

- 14 ns switching times.

- Low power consumption.

- TTL/CMOS compatible inputs.

The switch block are composed by switches should be enabled with inverse logical, this means that the switch ties the input with the output when on the enable pin is set up as Low Level, on the opposite, when the enable pin is as High Level the switch remains at High Impedance. For this issue, it is necessary to use one series of $pull-up$ resistances, in such way, when one row is selected through the multiplexer, this sets up the enable pin with Low Level due to the multiplexer input,D, is tied to ground. While the rest enable pins of the switches remain in High Level due to the $pull-up$ resistances, that is to say to High Impedance. When one switch is shorted, one end of the tactel is found with the voltage applied on the port A of the switch. To select the column desired it can be done thought Mux 2, which connects other end of the tactel with the input amplifier.
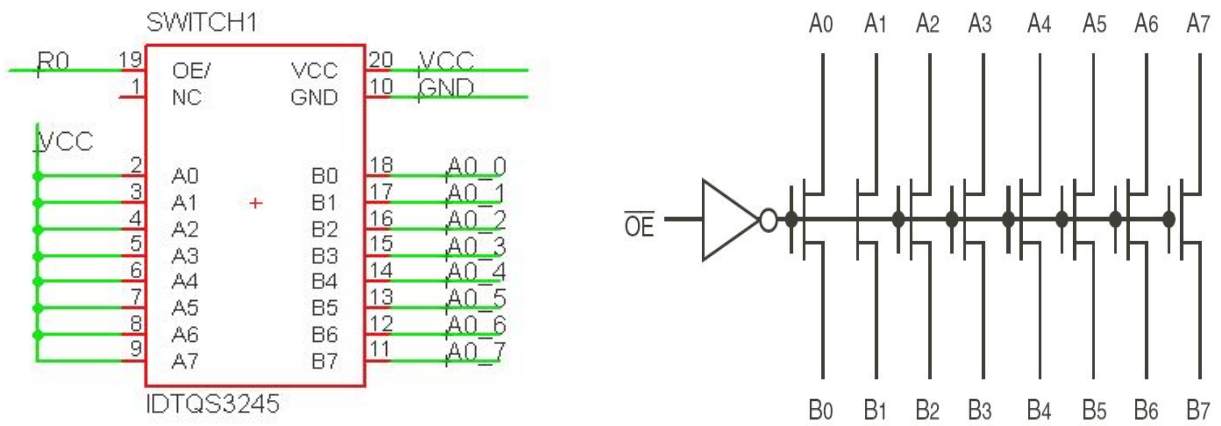

Fig. 4.29: Electronic for Matrix block.

The $QS3245$ provides a set of eight high-speed CMOS TTL. The low ON resistance allows inputs to be connected to outputs without adding propagation delay and without generating additional ground bounce noise. The $QS3245$ provides an order of magnitude faster speed than conventional logic devices. The principal features are:

- Enhanced N channel FET with no inherent diode to V_{cc}.

- 5 Ω bidirectional switches connect inputs to outputs.

- Low power CMOS proprietary technology.

- Zero propagation delay, zero ground bounce.

- TTL-compatible control inputs.

The Vsal signal obtained should be amplified, for accomplishing a adequate range is necessary to use the Amplifier block, Figure (4.31). The configuration chosen is based on current-voltage converter .It need to use two operational amplifiers due to the first stage accomplishes a negative voltage, so the second stage convert it to positive voltage, moreover, it is used as low pass-filter. The output is connected to analog input of the $DT9816$.
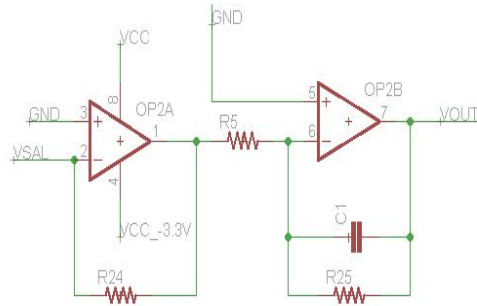

Fig. 4.30: Electronic for Amplifier block.

The $OPA2705$ are optimized for applications requiring rail-to-rail input and output swing. The $OPA2705$ offers excellent dynamic performance and unity-gain stability. The principal features are:

- Rail-To-Rail input and output.

- Wide supply range: dual Supplies from ± 2 to ± 6

- Low offset: $0.5mV$.

- High speed: $1MHz$, 0.6V/μs.

- Low input bias current: $1pA$.

The resistance R_{24} is chosen according to the material used because each one has different sensitivity. The resistance $R-5$, R_{25} and the capacitor $C1$ should be chosen depending to the bandwidth that the readout circuit employed. In this case, it has been chosen 0.5 [s] to read the whole matrix 8 x 8, so for each tactel is employed 7.8 [ms], that is, 0.2 [KHz]. Thus, the topology used in the second operational amplifier is an inverter low pass. At low frequencies the capacitors impedance is very high, much higher than R_{25}, and so does not affect the circuit ($X_{C1} \parallel R_{25} = R_{25}$). At high frequencies the capacitors impedance is very low, much lower than R_{25}, and thus limits the impedance of the parallel combination ($X_{C1} \parallel R_{25} = X_{C1}$). The gain follows to decrease as frequency increases beyond the cutoff frequency. The cutoff frequency given by:

$$H(jw) = \frac{R_{25}}{R_5(1 + jwR_{25}C_1)}$$

Thus, to get a cutoff frequency of 0.2 $[kHz]$ with unit gain ($R_{25} = R_5 = 1\ [K\Omega]$), there is obtained a $C_1 = 1.2\ \mu F$. The Bode diagram of the low pass is shown below:
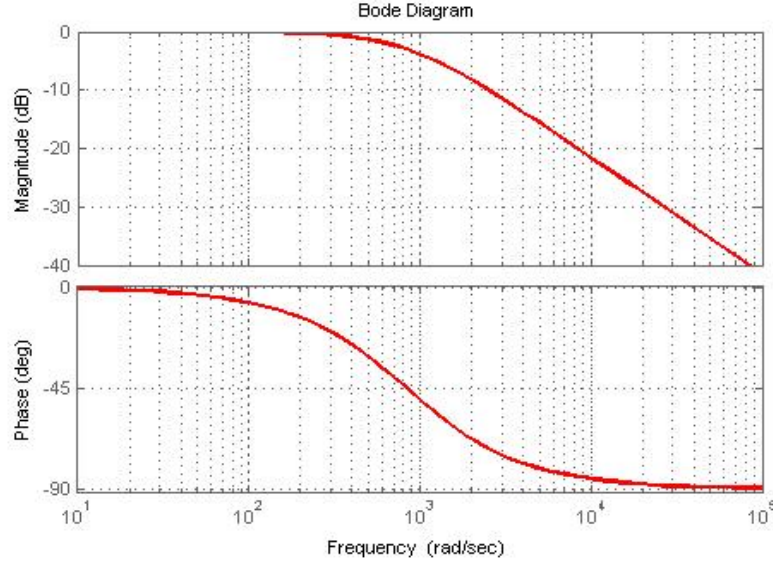

Fig. 4.31: Diagram bode for inverter amplifier low pass.

4.3.2   Second scanning electronic design

This electronic model is based on zero potential method **ZPM**,concretely the third circuit explained based on SPDT, shown in section (4.2). Figure (4.32) depicts the blocks diagram which this method employs. There are five blocks where GPIO block, Multiplexor block and Amplifier Block have the same operated for both methods. The matrix block uses the same configuration depicted in Figure(4.12). This means that the interconnections electrodes are used in row-column with all the the sensor elements having one of their ends connected to one column electrode and other end to a row electrode.
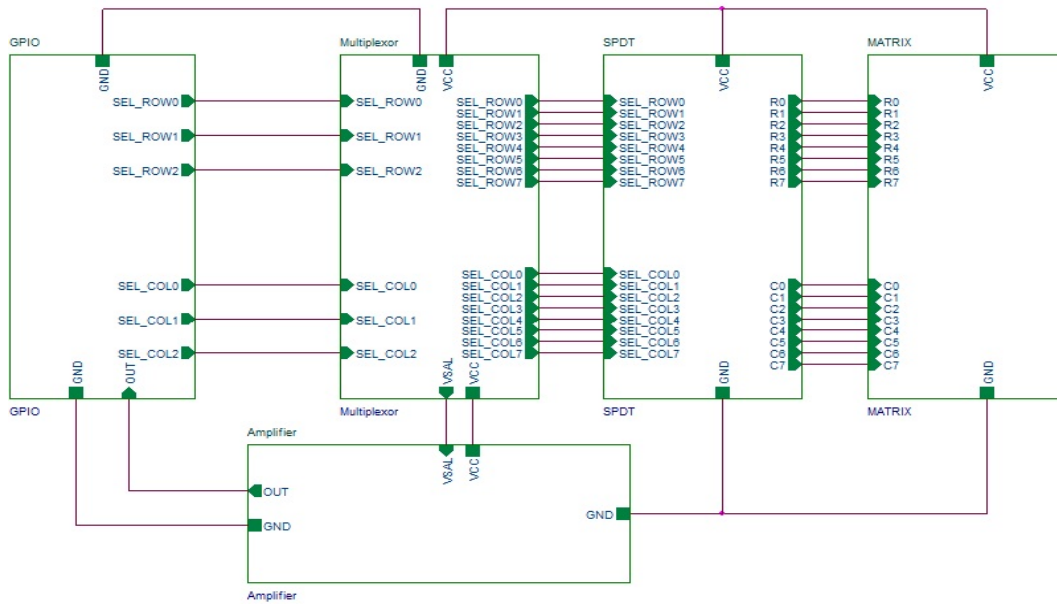
Fig. 4.32: Schematic for measuring of the elements using the zero potential method.

The Multiplexor block selects the row and column to be measured. The outputs of each multiplexer are connected to the inputs of the SPDT block, as it is shown in Figure(**??**). Each SPDT is selected independently, thus, the multiplexer output is connected to IN pin of the SPDT, when this pin is set up as Low Level, the output D, which is connected to each row, is tied to SB, that is to say, the row is selected, while others inputs are set up as High Level, thus their outputs are tied to ground through SA. To select one column is developed the same process.
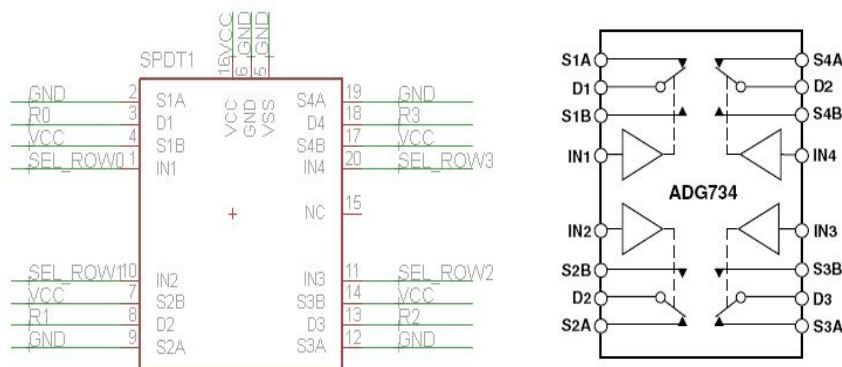
Fig. 4.33: Electronic for SPDT block.

The ADG734 is low voltage, CMOS device comprising four independently selectable SPDT (single pole, double throw) switches. All channels exhibit break-before-make switching

action preventing momentary shorting when switching channels. The principal features are:

- Single power supply from 1.8V to 5.5V and Dual supply ± 2.5V.

- 2.5 Ω On Resistance.

- 19 ns Switching Times.

- Low Power Consumption.

- TTL/CMOS Compatible Inputs.

5 Selection of the tactel of the shape

The behaviour of the conductive when no pressure is applied is as it was isolated, that is to say the fibres are distributed along the conductive foam without touching each other. When pressure is applied over conductive foam the particles come together and its electrical resistance is reduced, so that the interface resistance decreases. This effect is shown in Figure (4.3). Thus, the tactile sensor performances is governed by the interface effect between the conductive material and the electrodes. The output of the sensor is based on three single resistors. This is shown in Figure(4.5). The equivalent resistance of a tactel is given by [14]

$$R_{eq} = R_{inn} + R_{vol} + R_{out} \tag{5.1}$$

where

- R_{inn} is the resistance at the inner interface.

- R_{out} is the resistance at the outer interface.

- R_{vol} is the resistance of the path between both electrodes.

[36]*The resistance depends on the effective contact area that depends also on the pressure that is proportional to the area of the electrode*, so this effect can be written as [11]

$$R_{in} = \frac{1}{A_{in}P} \qquad\qquad R_{out} = \frac{1}{A_{out}P} \tag{5.2}$$

where A_{in} and A_{out} are the inner area and outer area of the electrode, respectively, and P is the pressure applied over conductive foam. It is obvious that the summation of both areas is constant due to the area of the electrodes is fixed. *So $A_{in} + A_{out} = A$, where A is a constant.* If it is considered the pressure to be constant and given and the R_{out} is also considered constant, is obtained that [11]

$$R_{eq} = \frac{1}{A_{in}} + \frac{1}{A_{out}} \tag{5.3}$$

From (5.3) is obtained R_{eq} is a constant. Furthermore, the largest sensitive is obtained when the value of R_{eq} is minimum. From (5.3) and (5.1), it is obtained that R_{eq} has a minimum value for $R_{in} = R_{out}$, that is to say that $A_{in} = A_{out}$. To show this, there have been fabricated different electrodes with different shape, different inner areas, outer areas and different gaps between areas. These different electrodes with their respectively areas are shown in Table (5.1).

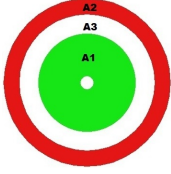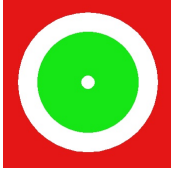[36]The italized/emphasized text is a verbatim quotation from [11]
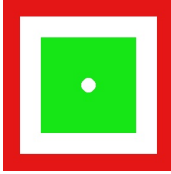
Shape 1	Shape 2	Shape 3
$A_1 = 19{,}62$ [mm^2]	$A_1 = 19{,}62$ [mm^2]	$A_1 = 19{,}62$ [mm^2]
$A_2 = 19{,}62$ [mm^2]	$A_2 = 35{,}48$ [mm^2]	$A_2 = 29{,}81$ [mm^2]
$A_3 = 18{,}85$ [mm^2]	$A_3 = 18{,}85$ [mm^2]	$A_3 = 8{,}63$ [mm^2]
$A_2/A_1 = 1$	$A_2/A_1 = 1{,}82$	$A_2/A_1 = 1{,}52$

Shape 4	Shape 5	Shape 6
$A_1 = 19{,}62$ [mm^2]	$A_1 = 19{,}81$ [mm^2]	$A_1 = 25$ [mm^2]
$A_2 = 20{,}42$ [mm^2]	$A_2 = 19{,}39$ [mm^2]	$A_2 = 24{,}04$ [mm^2]
$A_3 = 4{,}124$ [mm^2]	$A_3 = 18{,}81$ [mm^2]	$A_3 = 20{,}36$ [mm^2]
$A_2/A_1 = 1{,}04$	$A_2/A_1 = 0{,}98$	$A_2/A_1 = 0{,}96$

Table 5.1: Shape and size of electrodes make with PCB technology

The experiments have been done with five different conductive foams. The first one is Conductive Polyethylene(PE)Foam Model AE [26], the second one is Conductive Polyurethane (PU) Foam Model 1105 series [25], the third one is Conductive Rubber Foam (Rubber) Model C-4255 [27], the fourth one is a Conductive Polyethylene (PEF) Foam whose features are not known and fifth one is a CS57-7RSC [24]
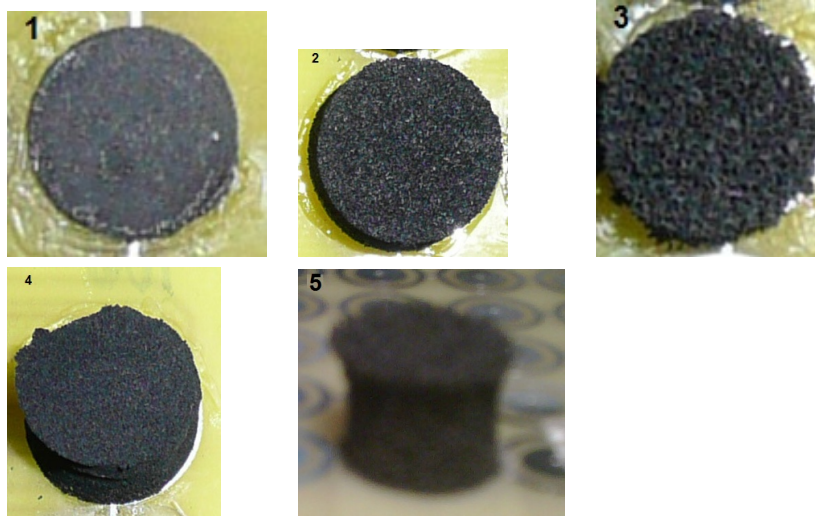
Fig. 5.1: depicts the material used where the picture labelled as **1** is the material CS57-7RSC, **2** is PE, **3** is PEF, **4** is Rubber and **5** is PU

5.1   Experiments

The experiments have been done with the devices shown in Figure(5.2) where appears a weight, syringe, a glass with plane bottom and an empty bottle where the bottom has been cut. The experiments have been carried out filling and empting with water the bottle. The water amount is measured with the weight. When the bottle is being filling, the pressure over foam increases, the interface area between the foam and the electrodes increases and it is produced one changing in the voltage proportional to water amount deposes. The same effect occurs when the bottle is being emptied where is produces a decreased of the voltage. The emptying is performed with the syringe shown. Thus, it can also be measured the hysteresis for each shape and for each material.
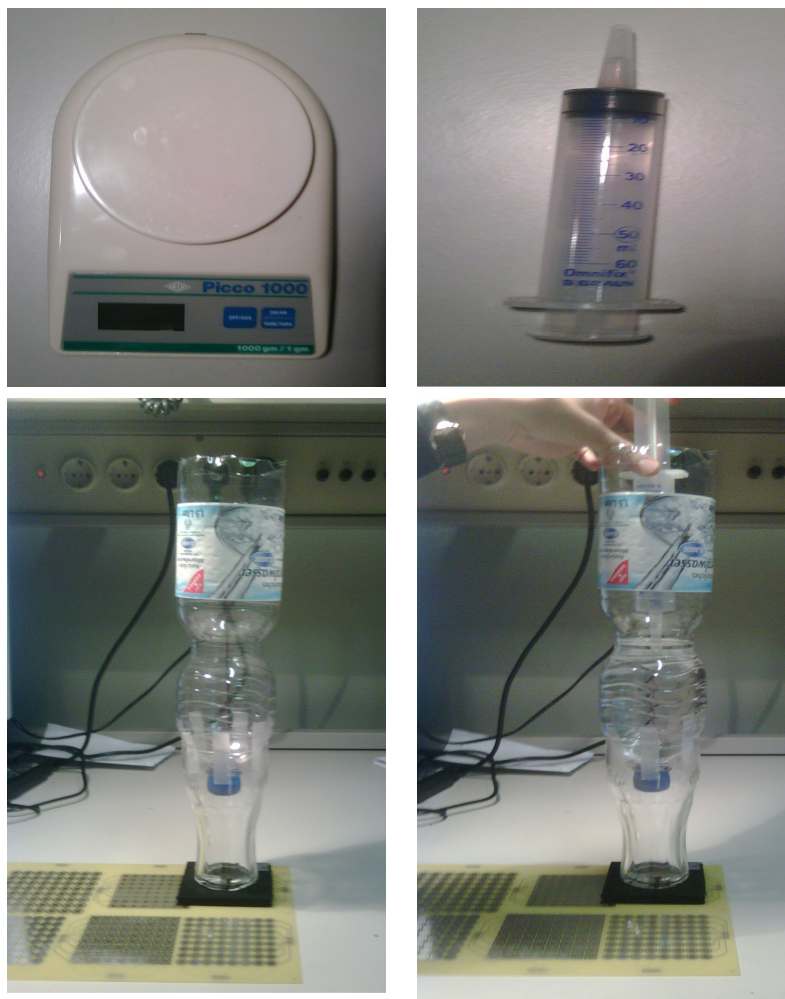

Fig. 5.2: Material used to perform the experiments.

In the Figure (5.3) is shown the electronic used to measure the drop of voltage in the four elements measured independently, the block labelled as MATRIX_BOARD corresponds with the different electrodes shape employed. Furthermore, the Figure shows where the voltage has been measured.
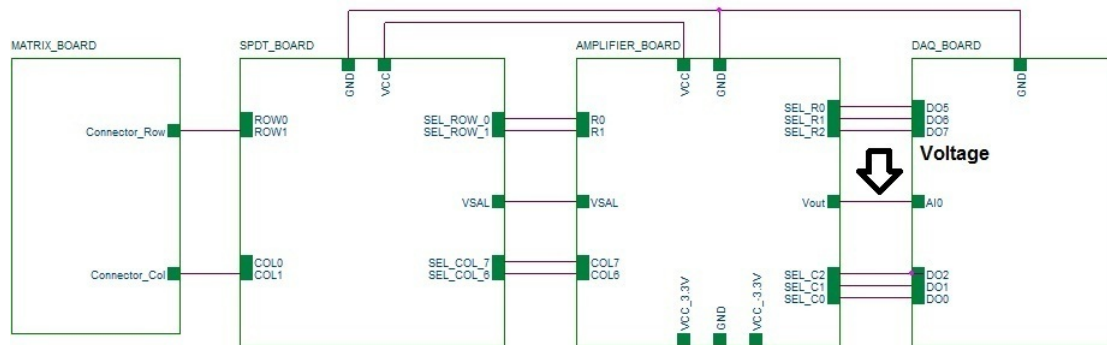

Fig. 5.3: depicts the circuit employed to measure the drop of voltage in the four elements employed.

5.1.1 Experiments with Conductive Polyurethane (PU)

The graphics obtained with Conductive Polyurethane for each shape are shown below. The first picture shows the voltage of the four tactels measure versus applied pressure, the second one is the average voltage from the previous picture. The third is the hysteresis into one tactel and the fourth one is the resistance from the second picture. The resistance R_{24} used in the Figure (4.31) to obtain the measurements is 10 KΩ.
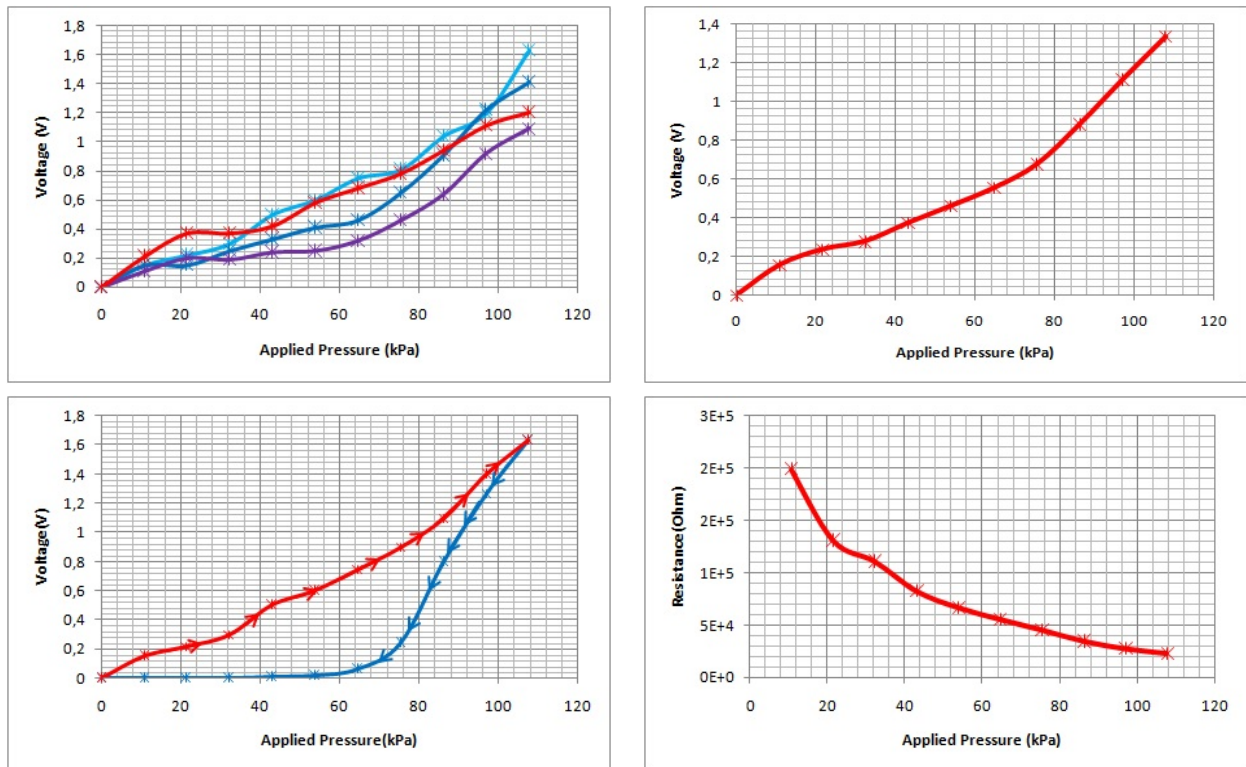
- Shape 1

Fig. 5.4: Measure with the shape 1 electrode and PU foam.
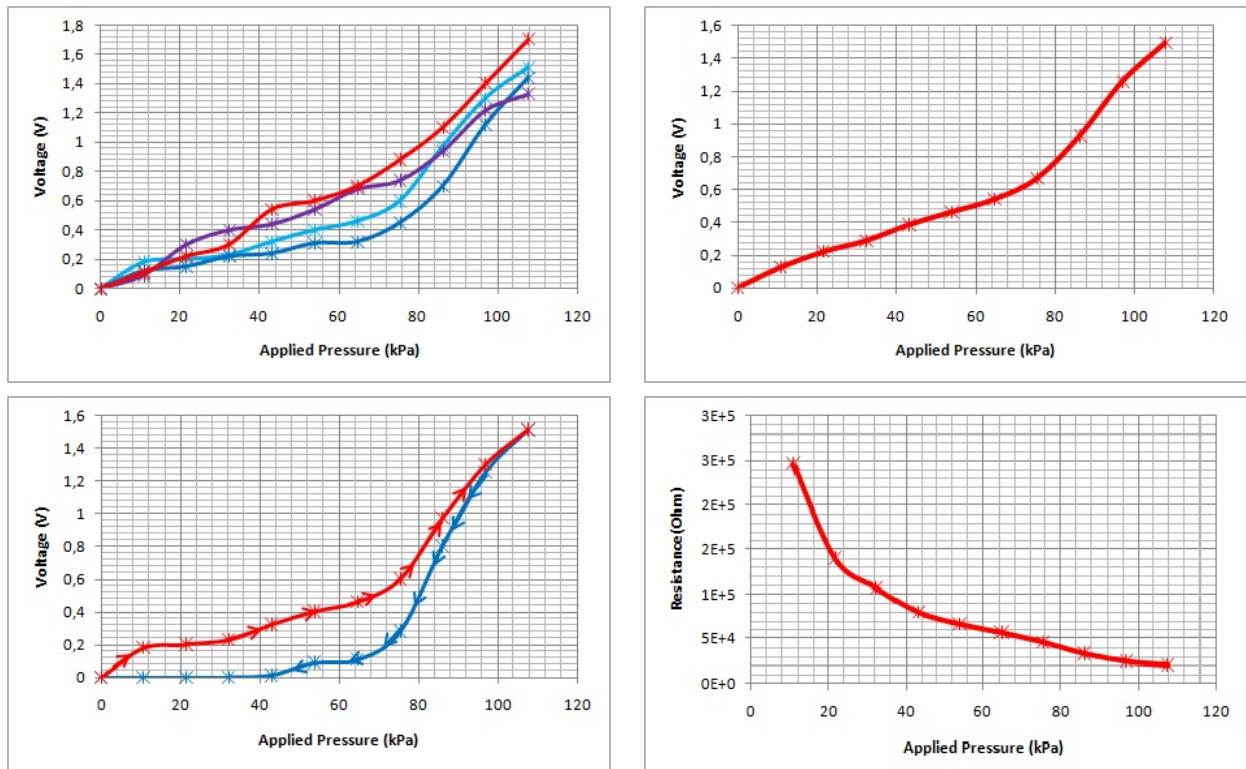
- Shape 2

Fig. 5.5: Measure with the shape 2 electrode and PU foam.
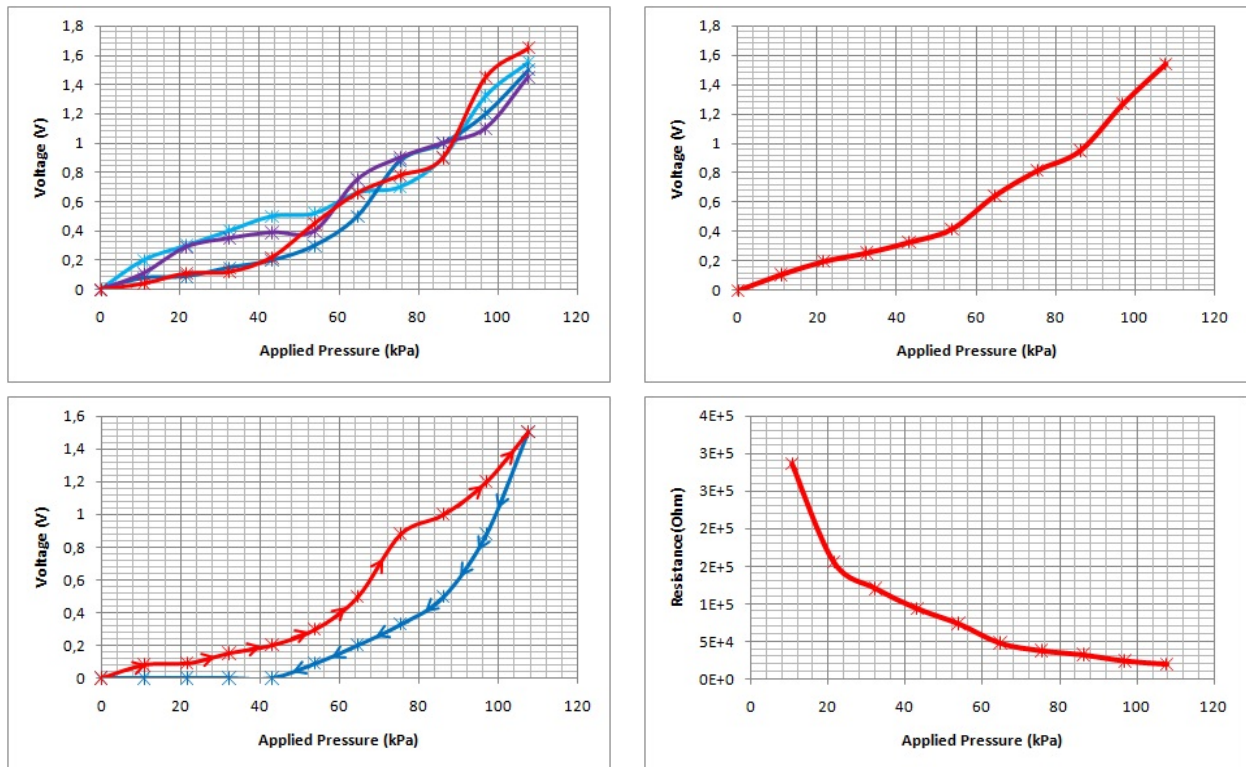
- Shape 3

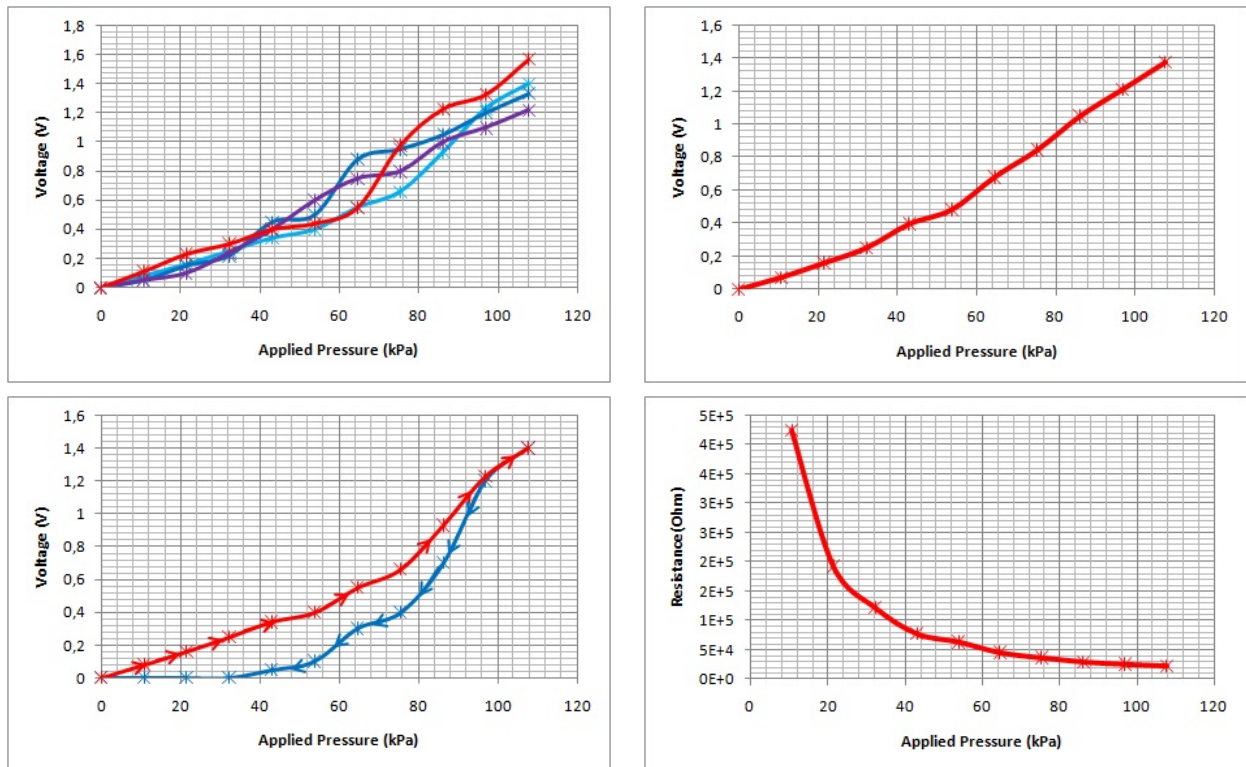Fig. 5.6: Measure with the shape 3 electrode and PU foam.

- Shape 4

Fig. 5.7: Measure with the shape 4 electrode and PU foam.

- Shape 5

Fig. 5.8: Measure with the shape 5 electrode and PU foam.

- Shape 6

Fig. 5.9: Measure with the shape 6 electrode and PU foam.

5.1.2 Experiments with Conductive Rubber Foam (Rubber)

The graphics obtained with Conductive Polyurethane for each shape are shown below. The first picture shows the voltage of the four tactel's measure versus applied pressure, the second one is the average voltage from the previous picture. The third is the hysteresis into one tactel and the fourth one is the resistance from the second picture. The resistance R_{24} used in the Figure (4.31) to obtain the measurements is 2.7 KΩ.

- Shape 1

Fig. 5.10: Measure with the shape 1 electrode and Rubber foam.

● Shape 2

Fig. 5.11: Measure with the shape 2 electrode and Rubber foam.

- Shape 3

Fig. 5.12: Measure with the shape 3 electrode and Rubber foam.

- Shape 4

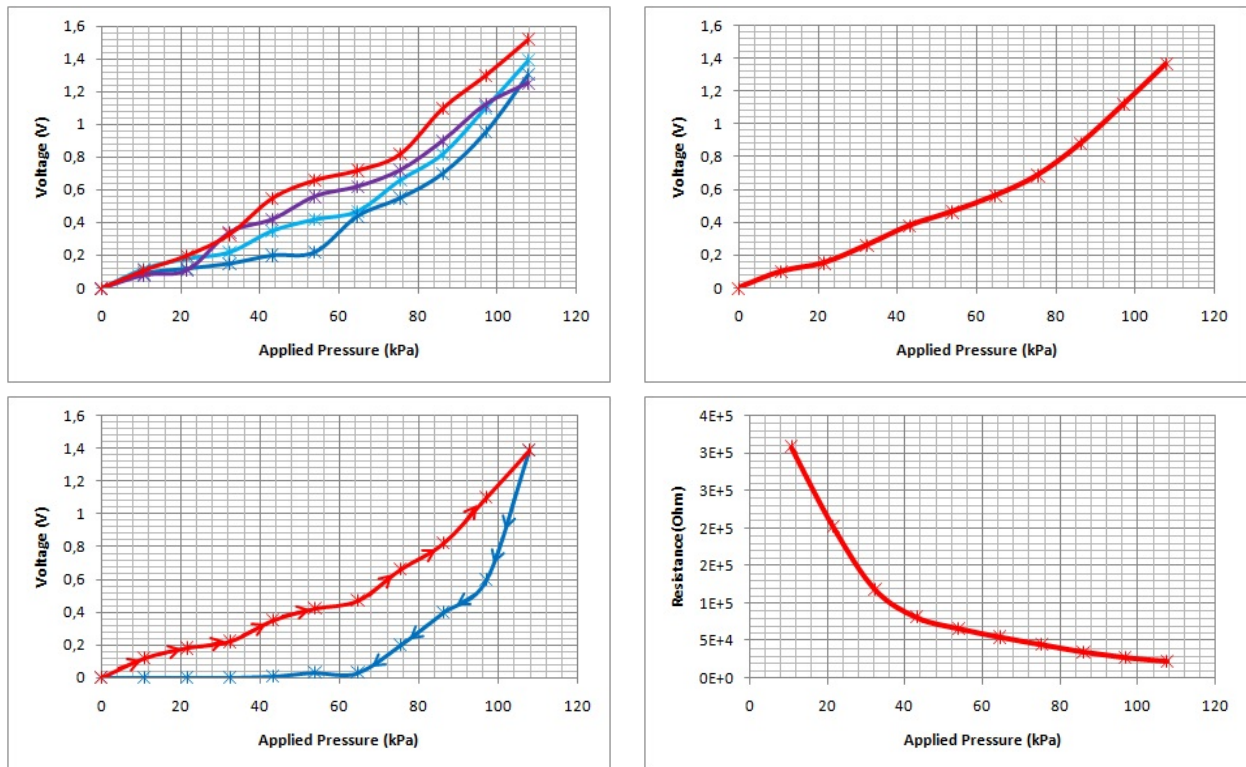Fig. 5.13: Measure with the shape 4 electrode and Rubber foam.

- Shape 5

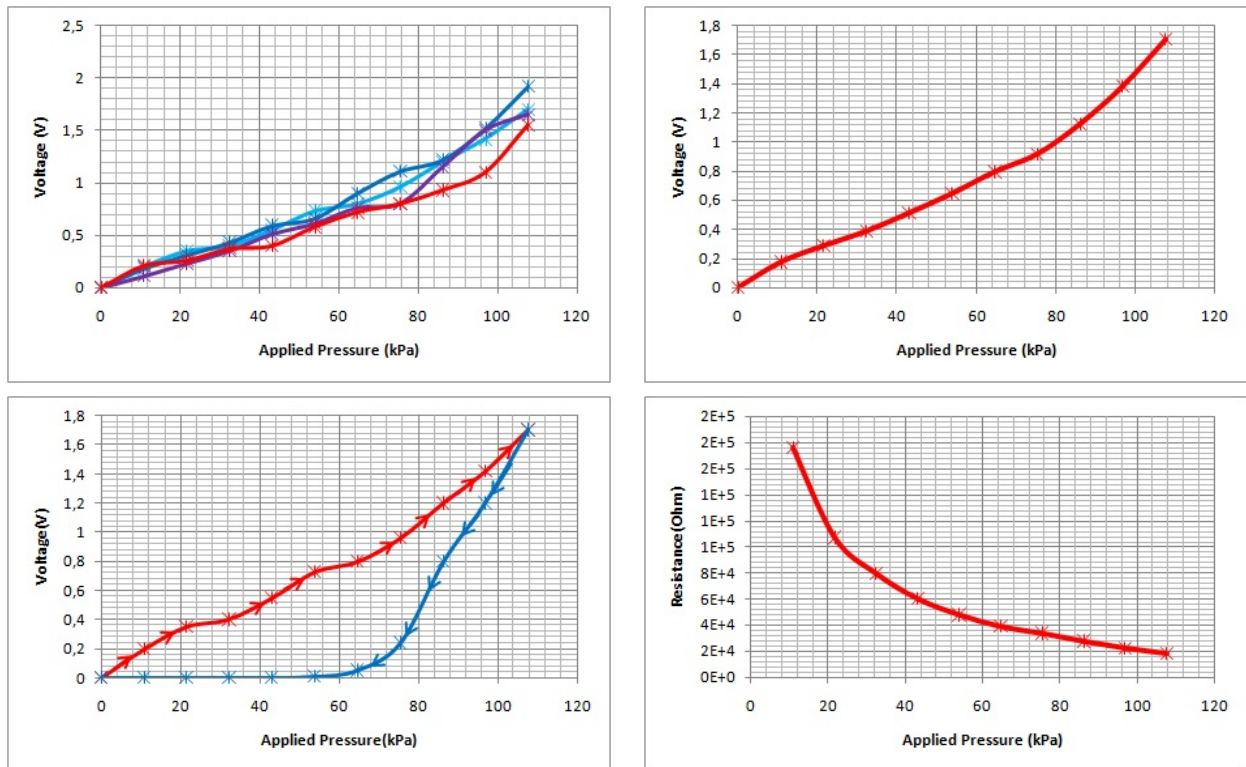Fig. 5.14: Measure with the shape 5 electrode and Rubber foam.

- Shape 6

Fig. 5.15: Measure with the shape 6 electrode and Rubber foam.

5.1.3 Experiments with Conductive Polyurethane (PE)

The graphics obtained with Conductive Polyurethane for each shape are shown below. The first picture shows the voltage of the four tactel's measure versus applied pressure, the second one is the average voltage from the previous picture. The third is the hysteresis into one tactel and the fourth one is the resistance from the second picture. The resistance R_{24} used in the Figure (4.31) to obtain the measurements is 10 KΩ.

- Shape 1
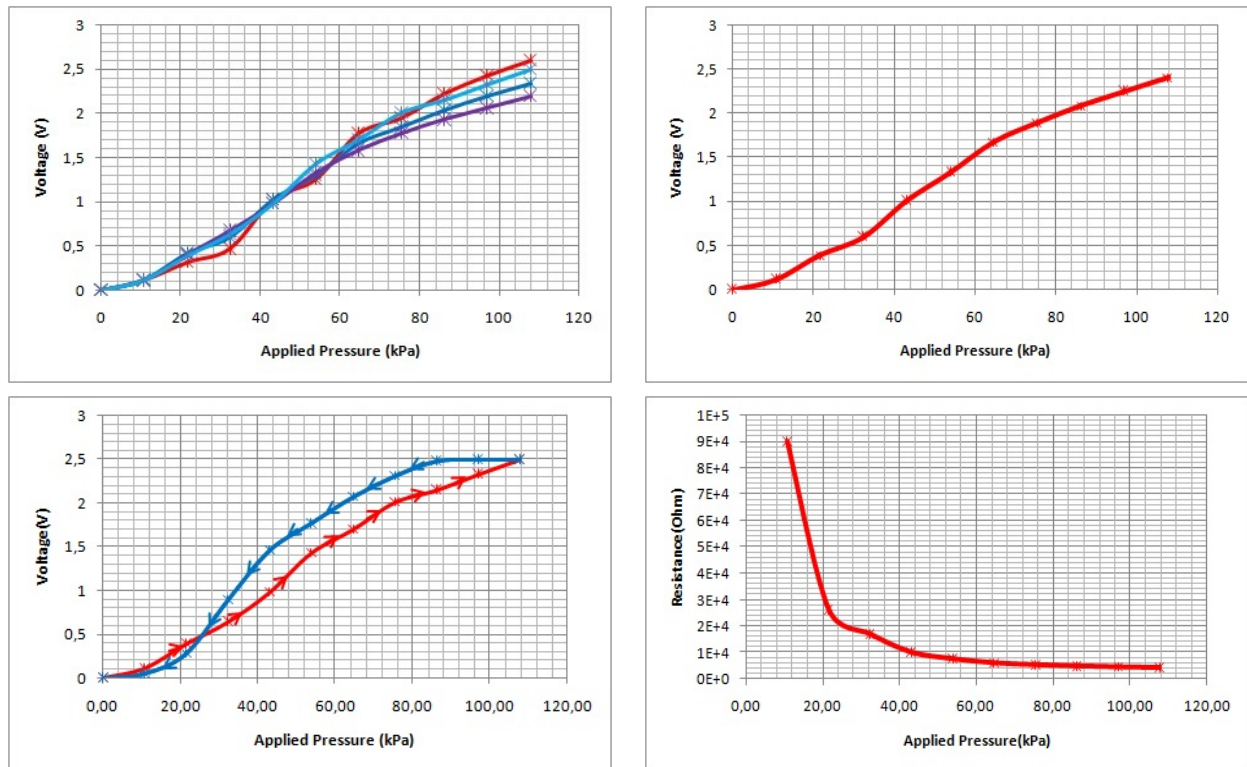

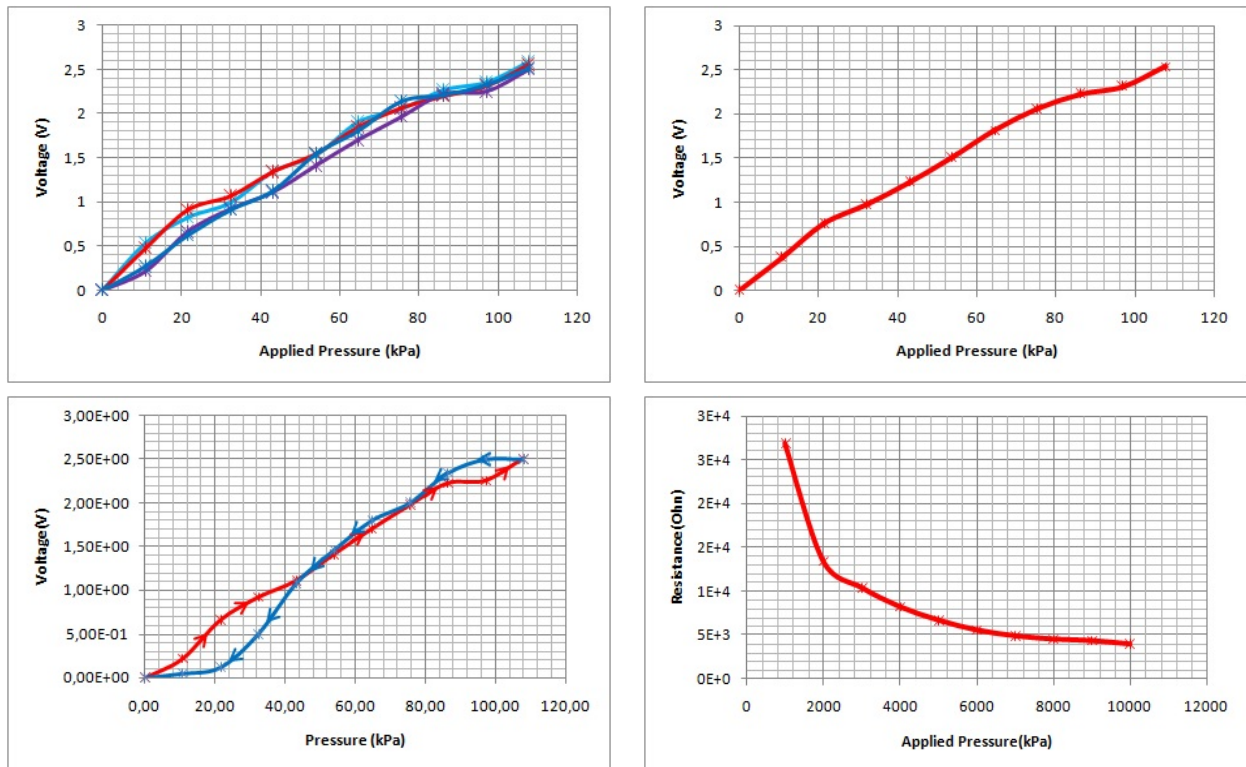Fig. 5.16: Measure with the shape 1 electrode and PE foam.

- Shape 2

Fig. 5.17: Measure with the shape 2 electrode and PE foam.

- Shape 3

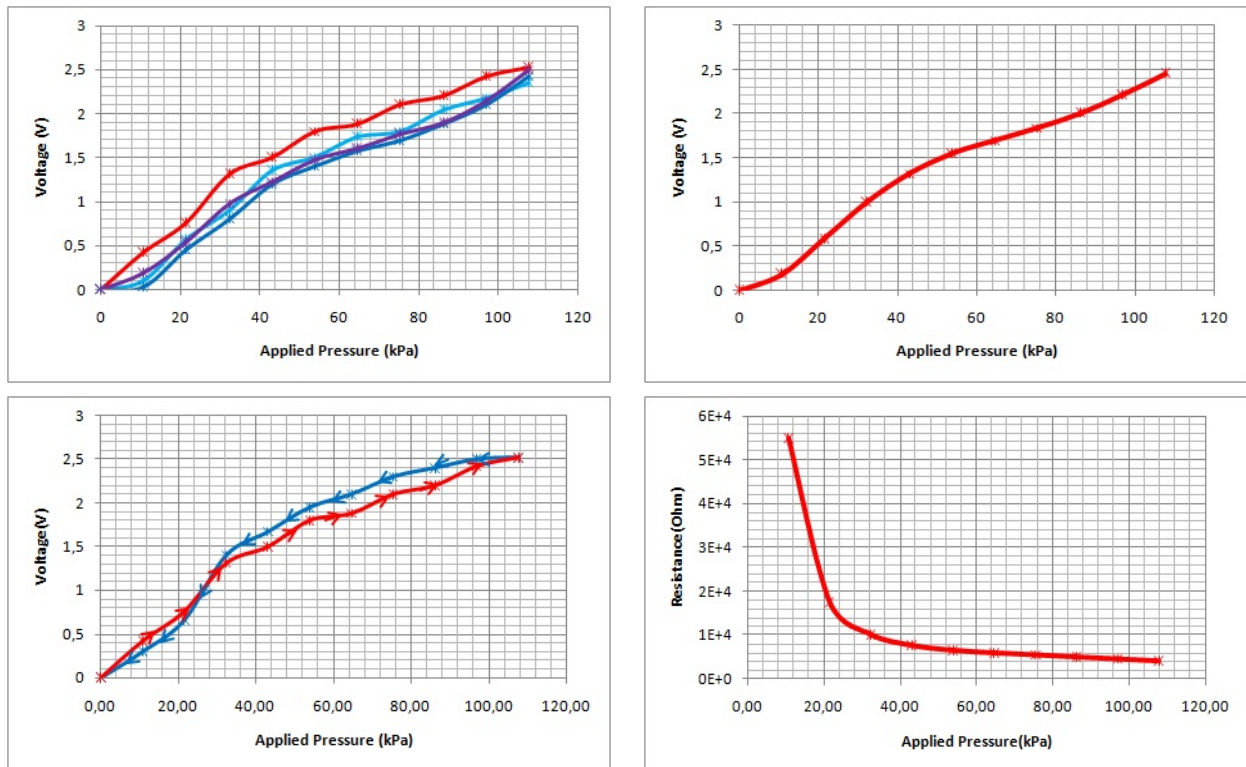Fig. 5.18: Measure with the shape 3 electrode and PE foam.

- Shape 4

Fig. 5.19: Measure with the shape 4 electrode and PE foam.

- Shape 5

Fig. 5.20: Measure with the shape 5 electrode and PE foam.

- Shape 6

Fig. 5.21: Measure with the shape 6 electrode and PE foam.

5.1.4 Experiments with Conductive Polyurethane (PEF)

The graphics obtained with Conductive Polyurethane for each shape are shown below. The first picture shows the voltage of the four tactel's measure versus applied pressure, the second one is the average voltage from the previous picture. The third is the hysteresis into one tactel and the fourth one is the resistance from the second picture. The resistance R_{24} used in the Figure (4.31) to obtain the measurements is 2.7 KΩ.
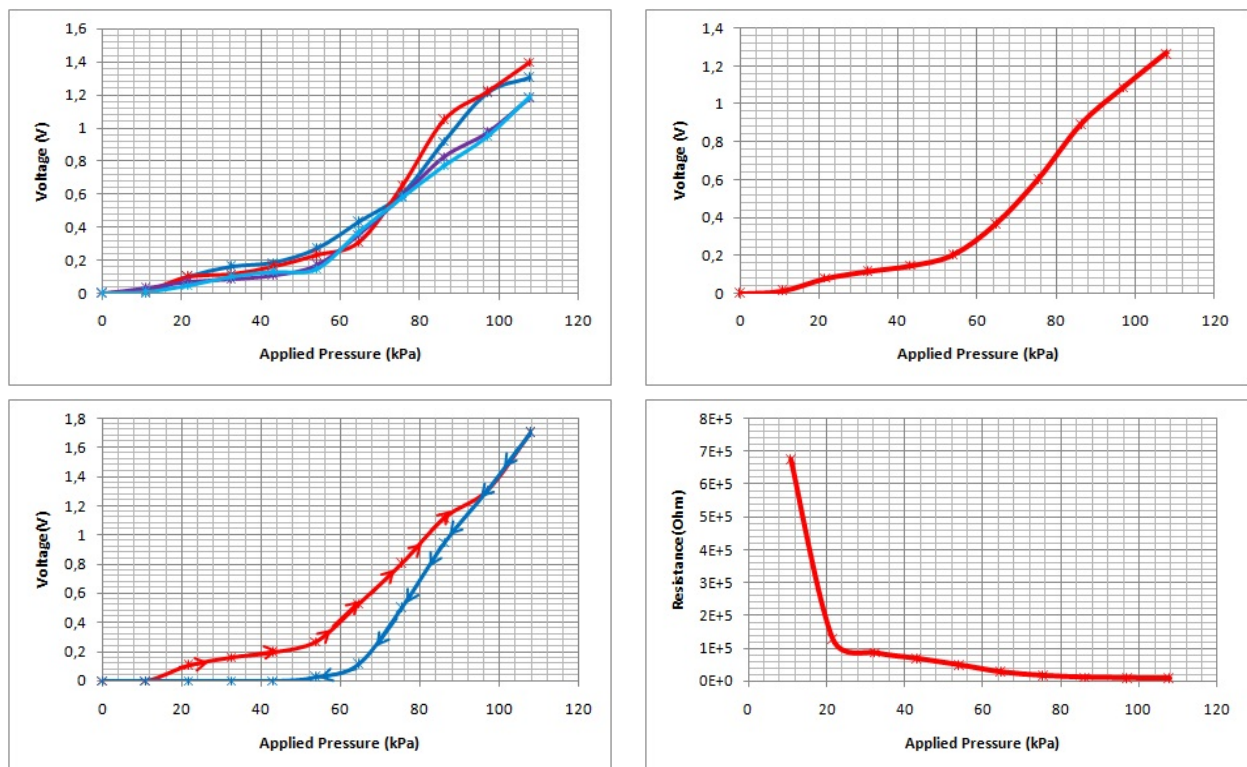
- Shape 1

Fig. 5.22: Measure with the shape 1 electrode and PEF foam.

- Shape 2
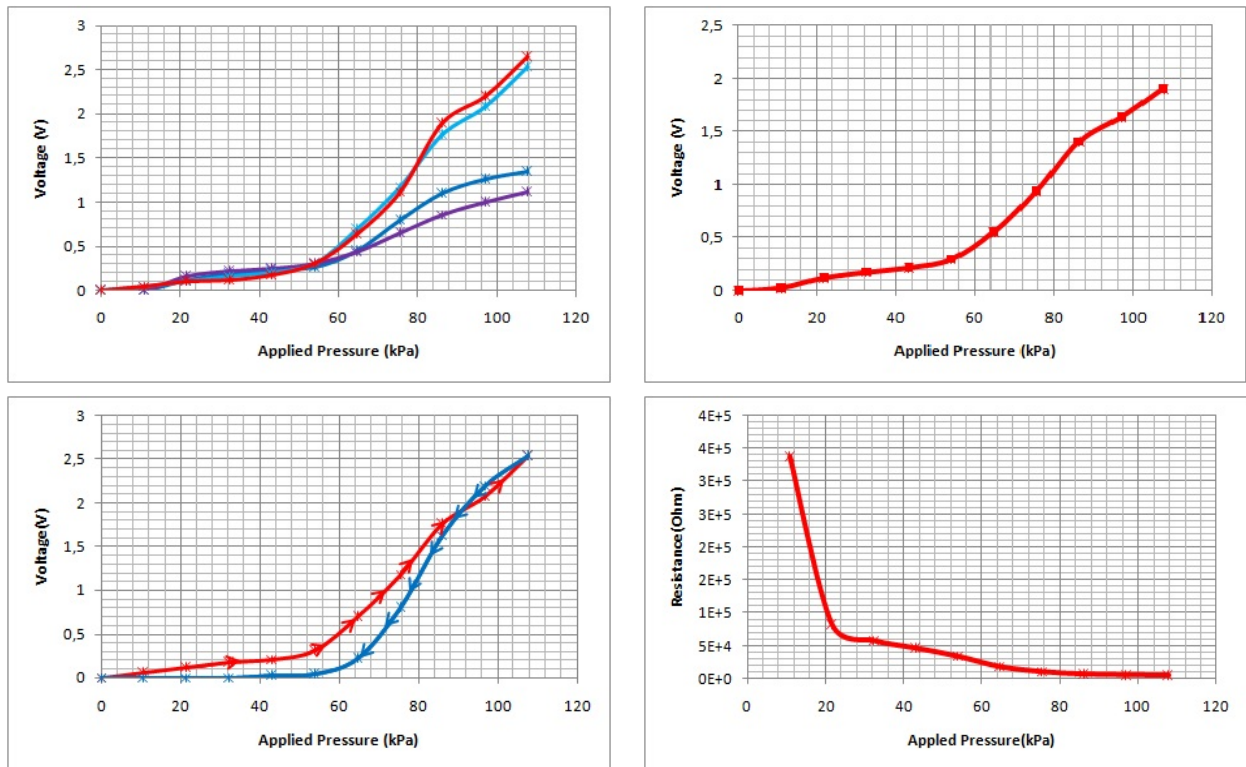
Fig. 5.23: Measure with the shape 2 electrode and PEF foam.

- Shape 3
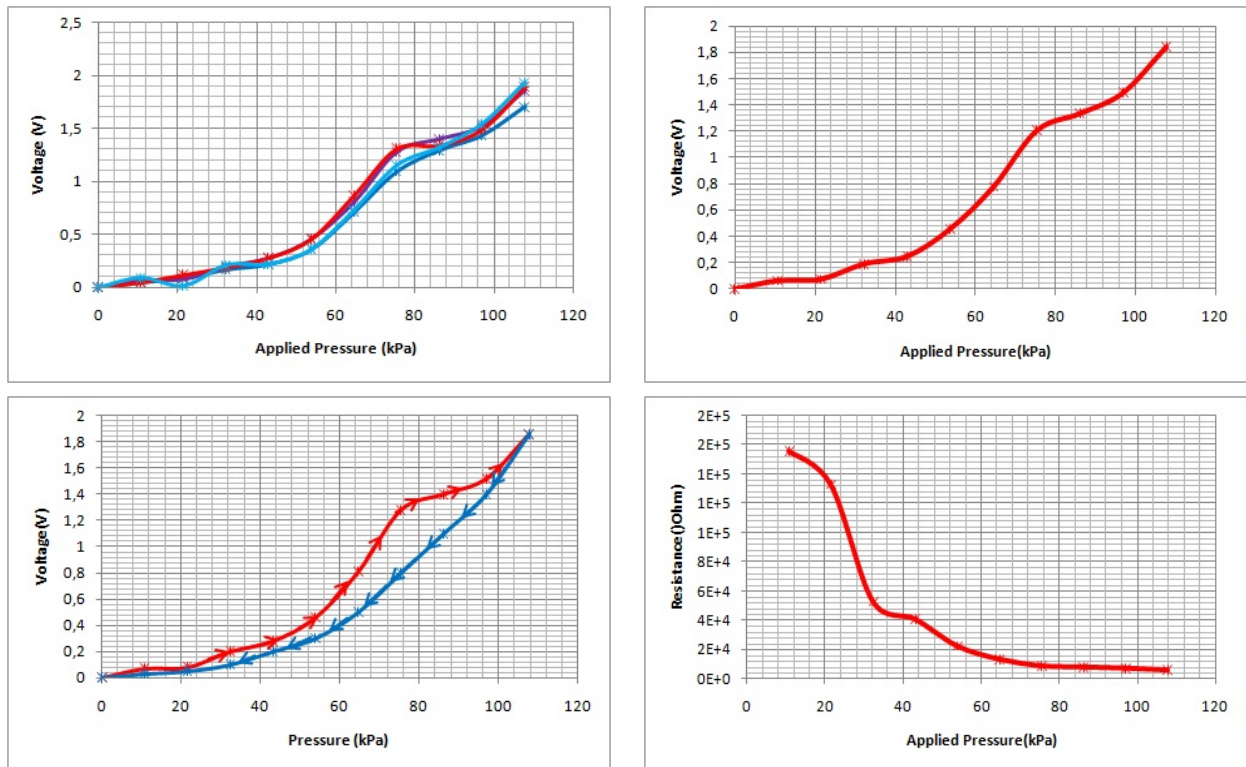
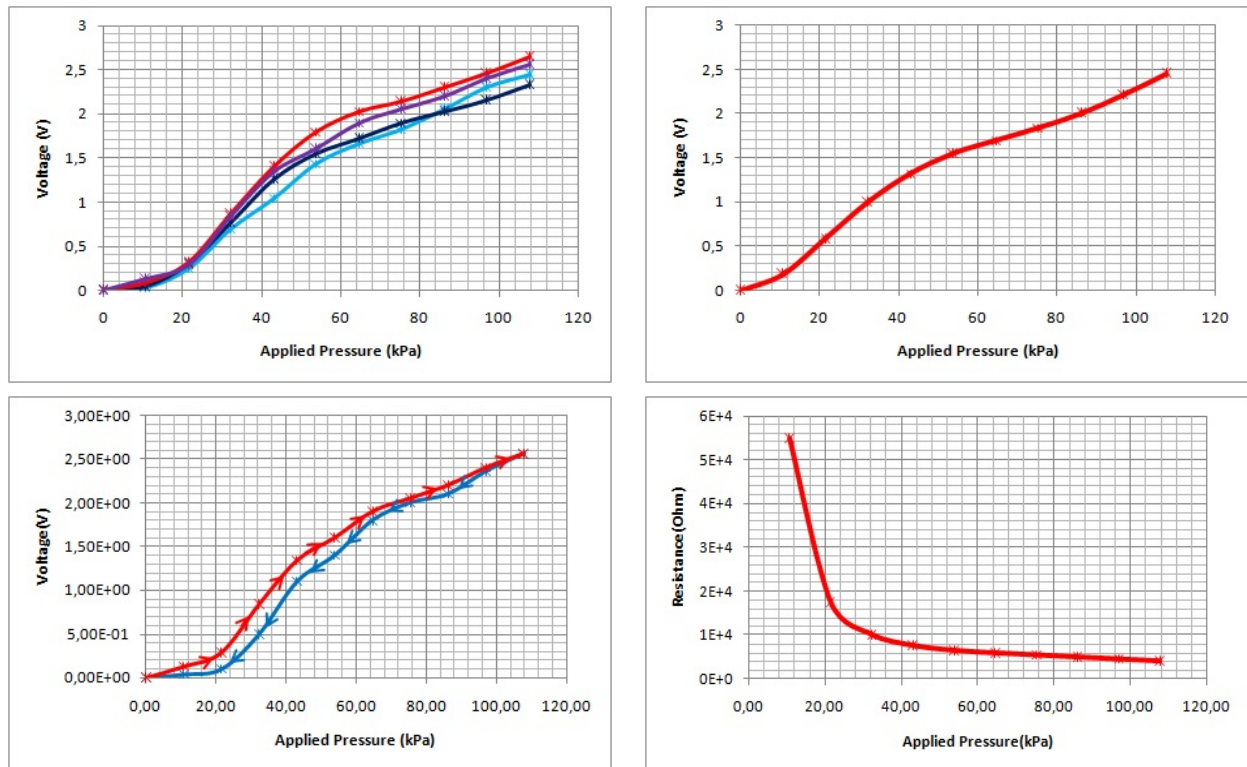Fig. 5.24: Measure with the shape 3 electrode and PEF foam.

- Shape 4
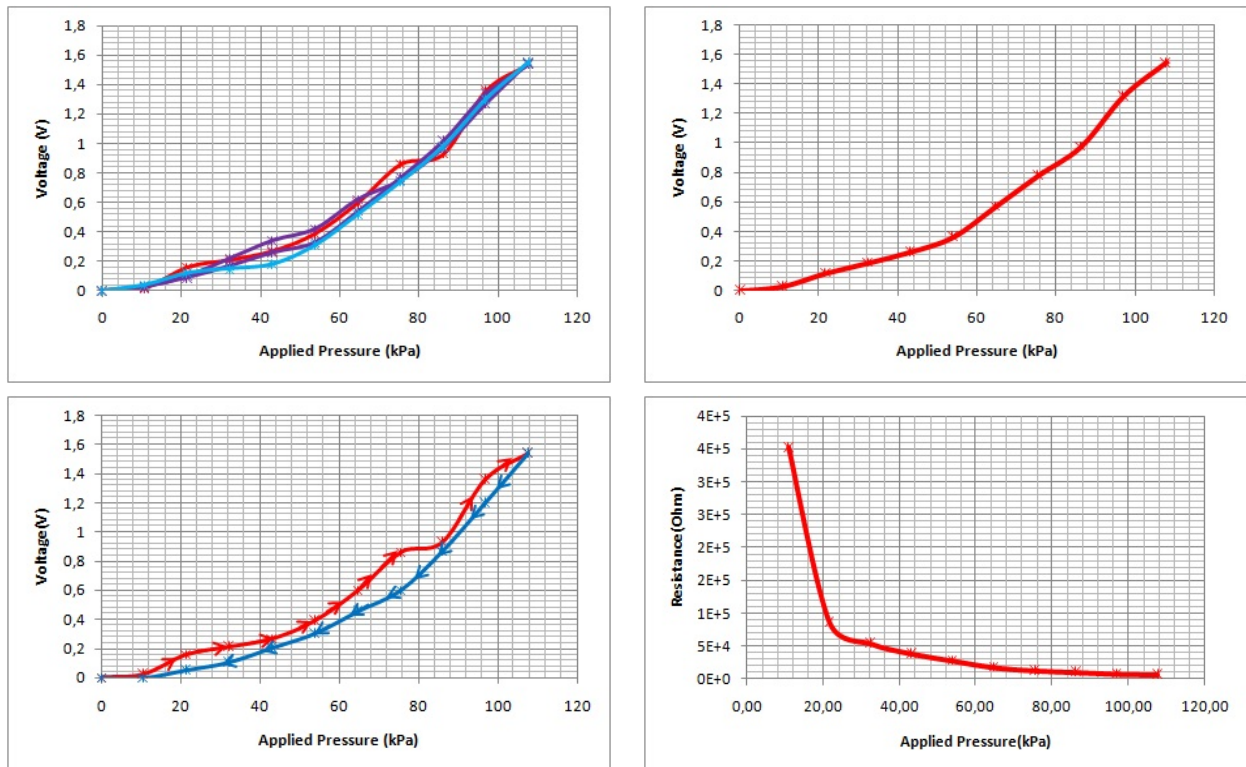
Fig. 5.25: Measure with the shape 4 electrode and PEF foam.

- Shape 5
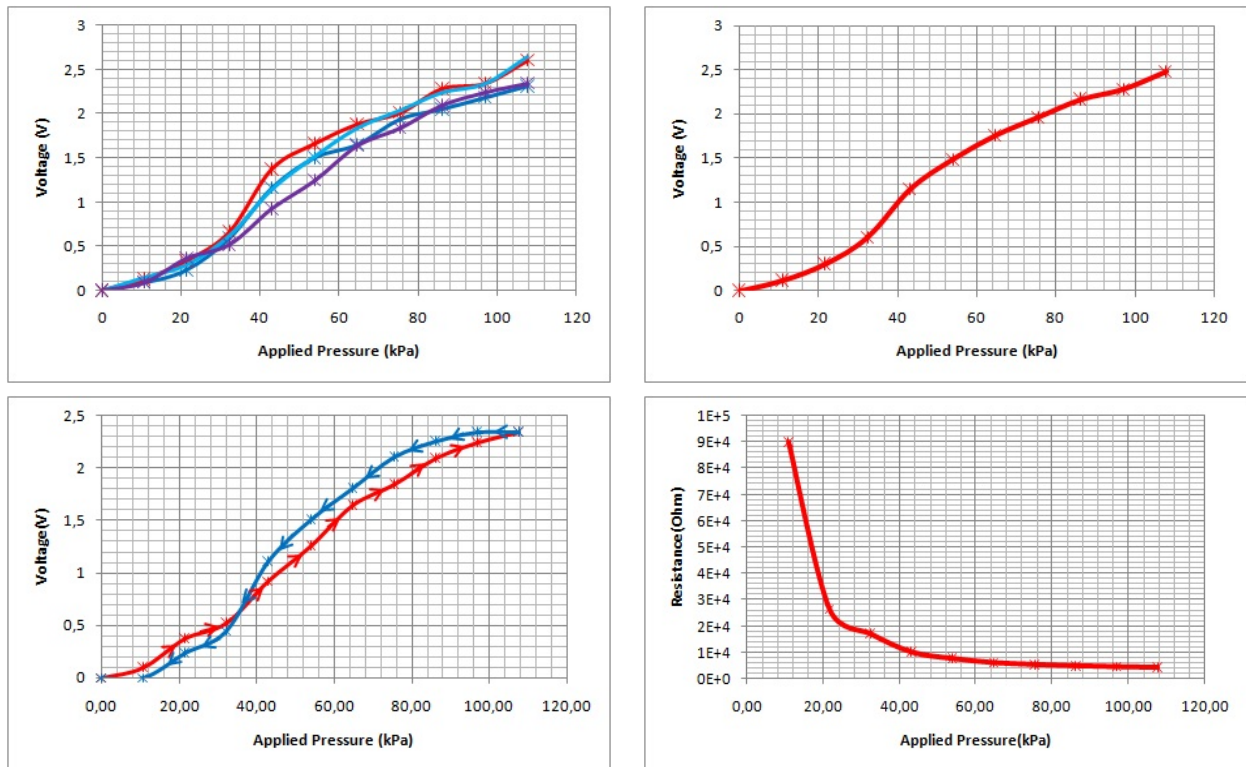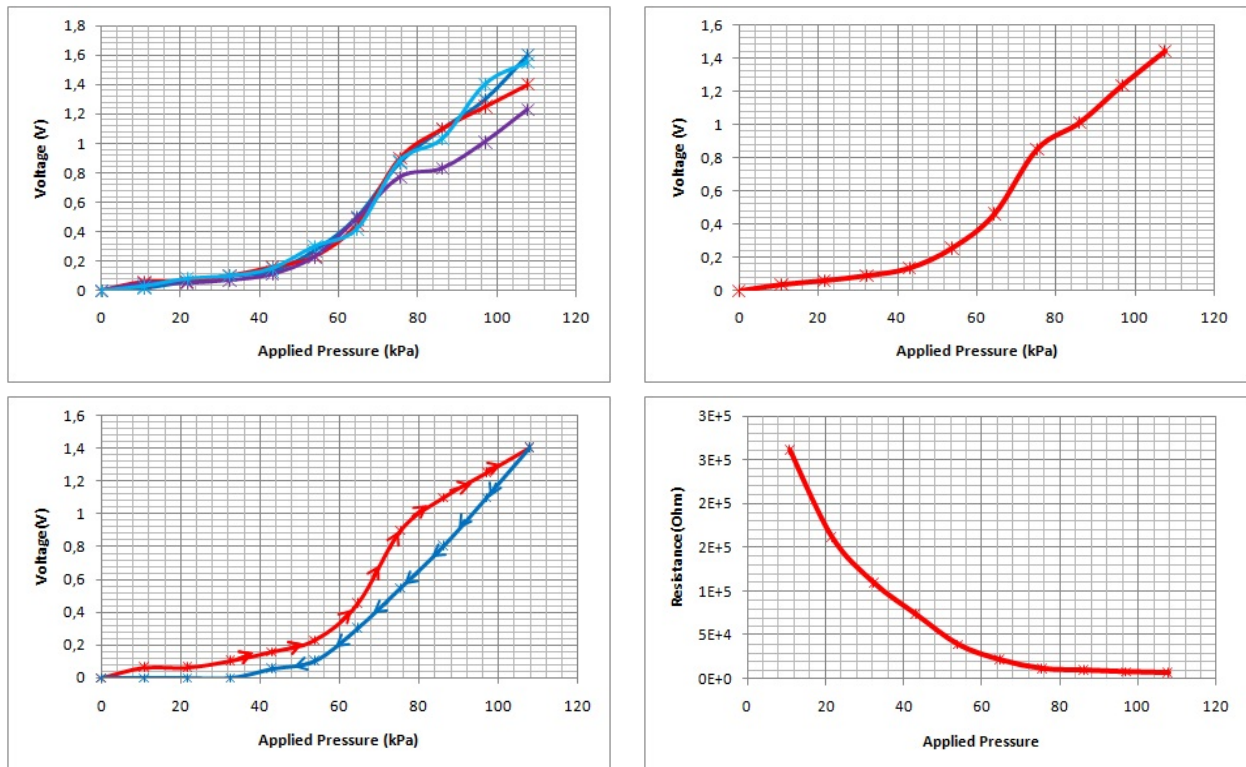

Fig. 5.26: Measure with the shape 5 electrode and PEF foam.

- Shape 6
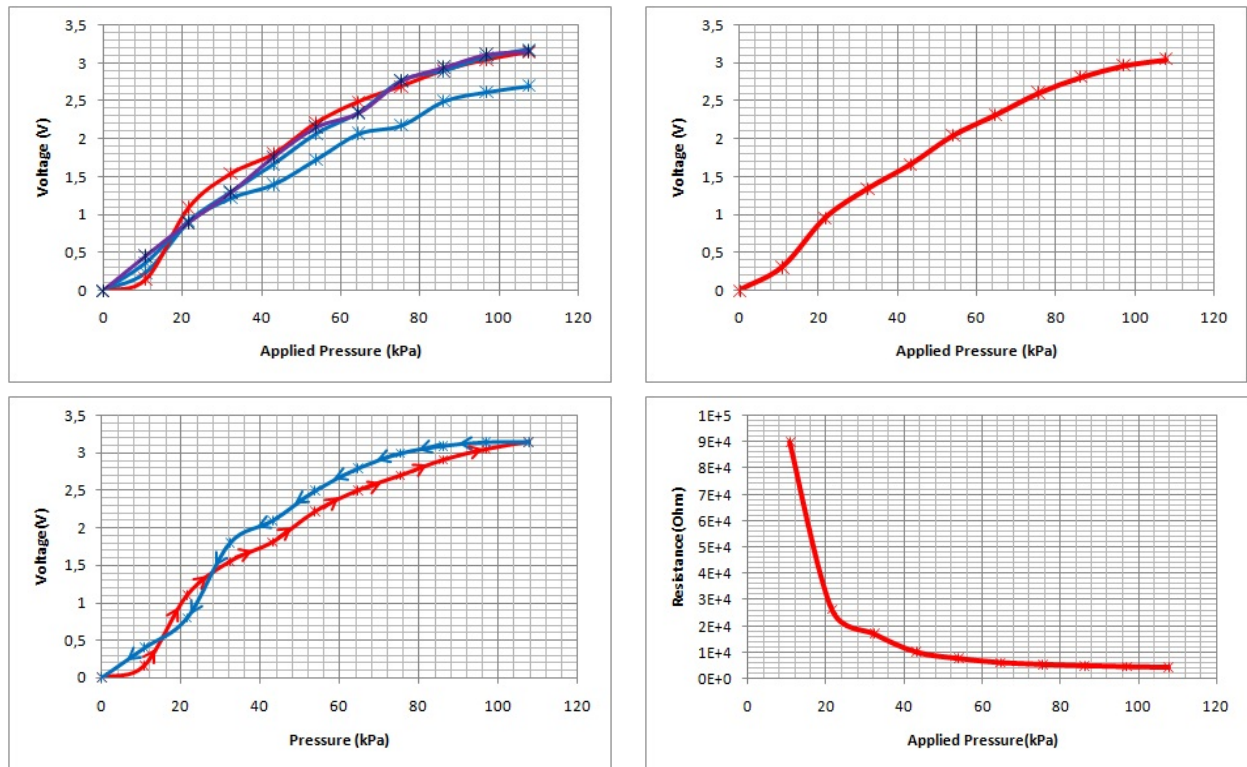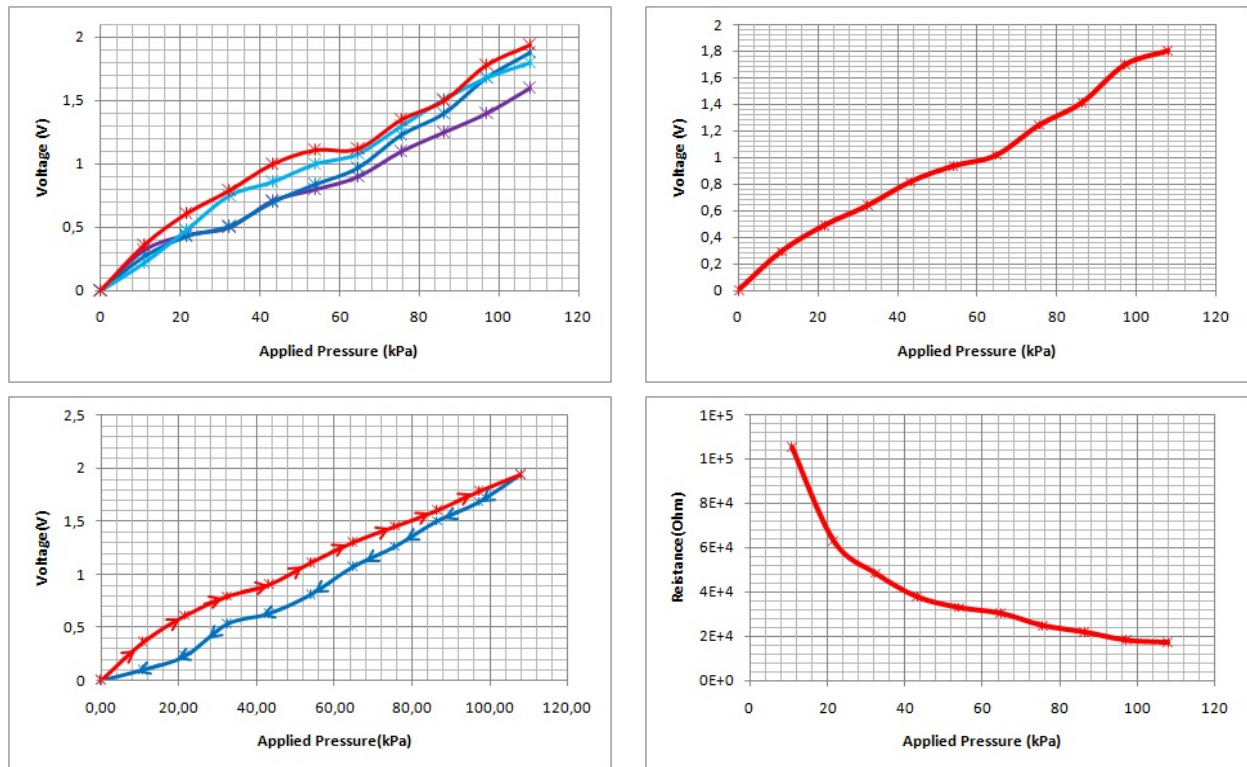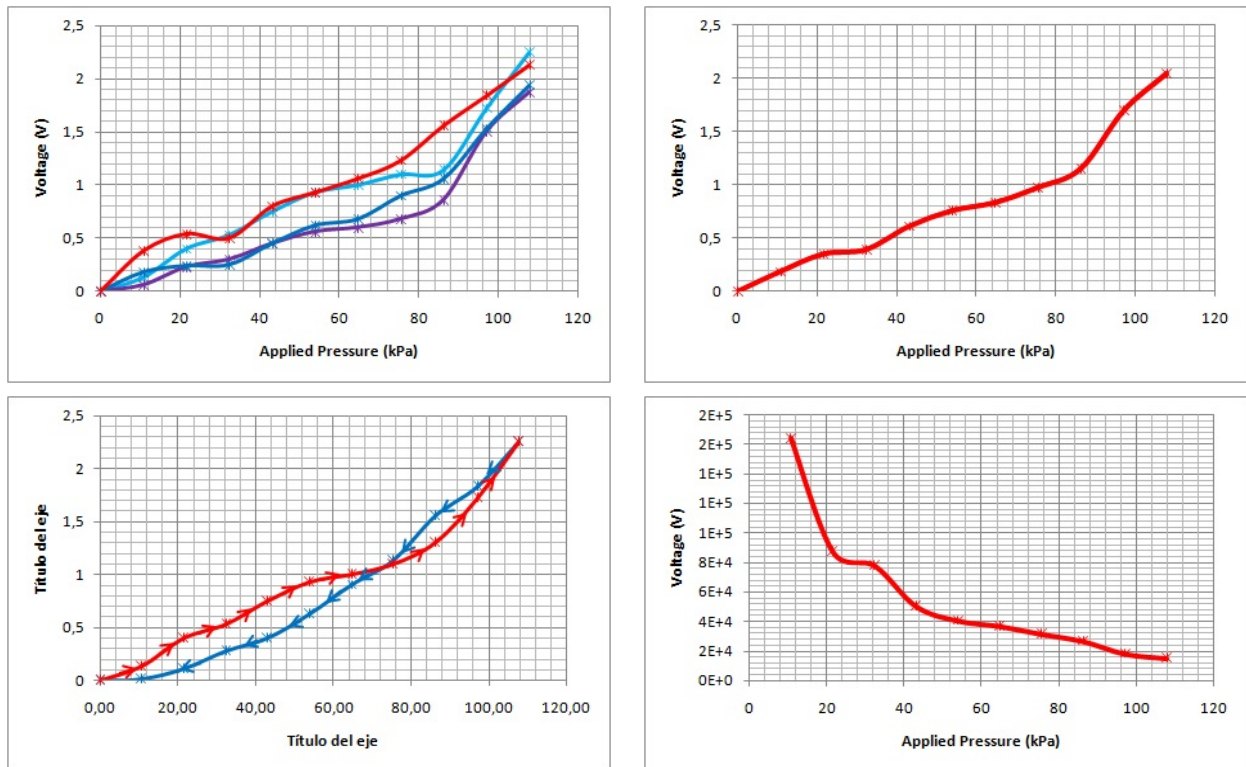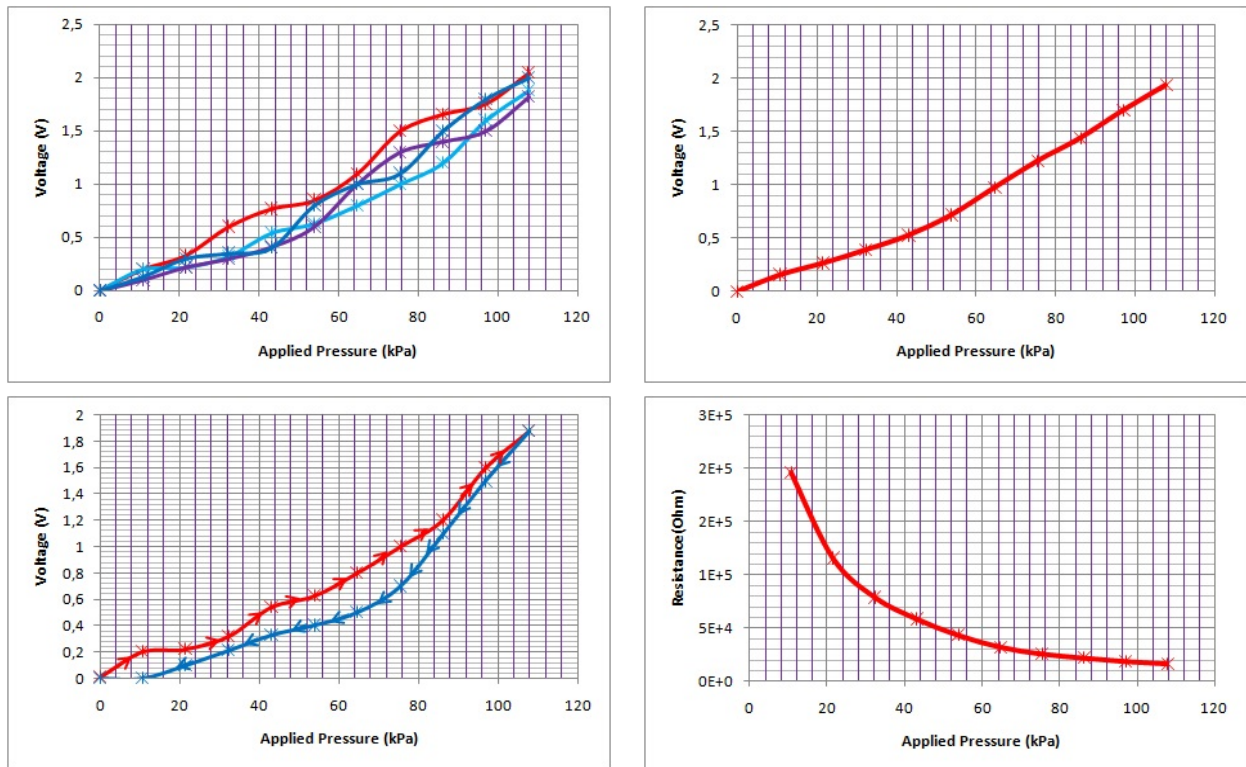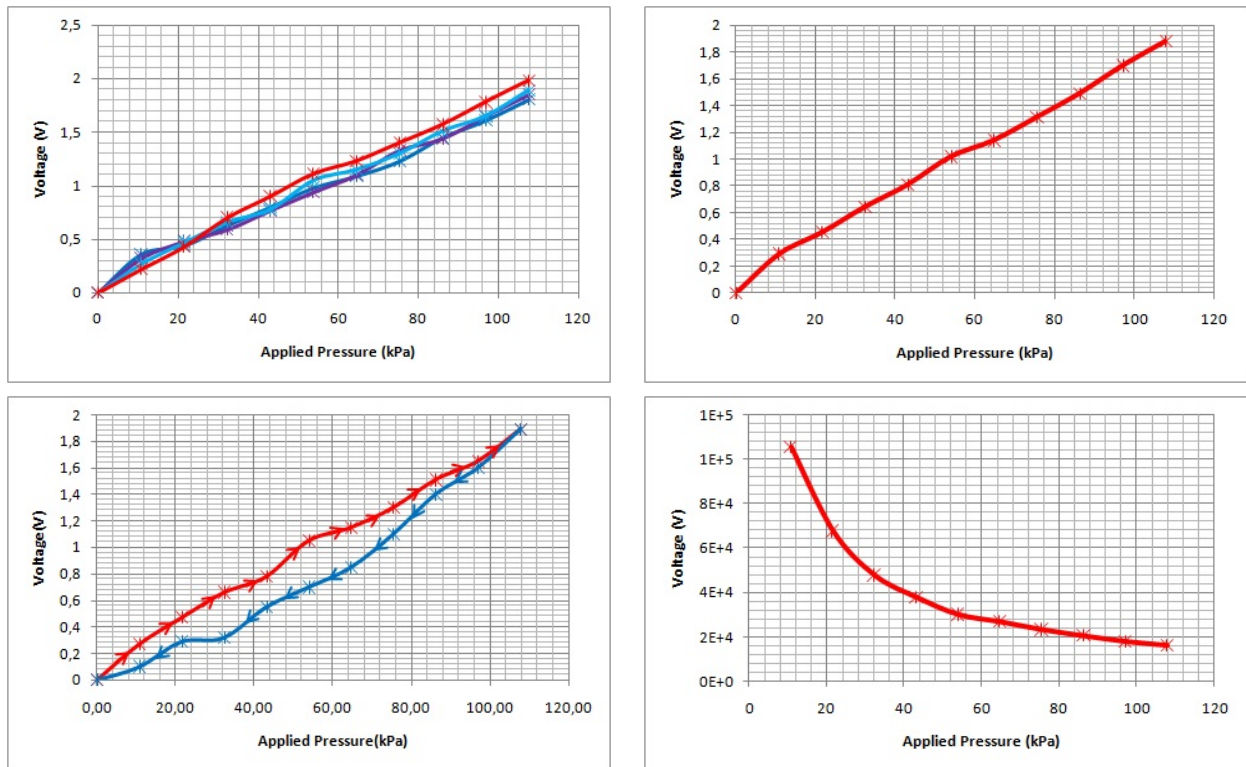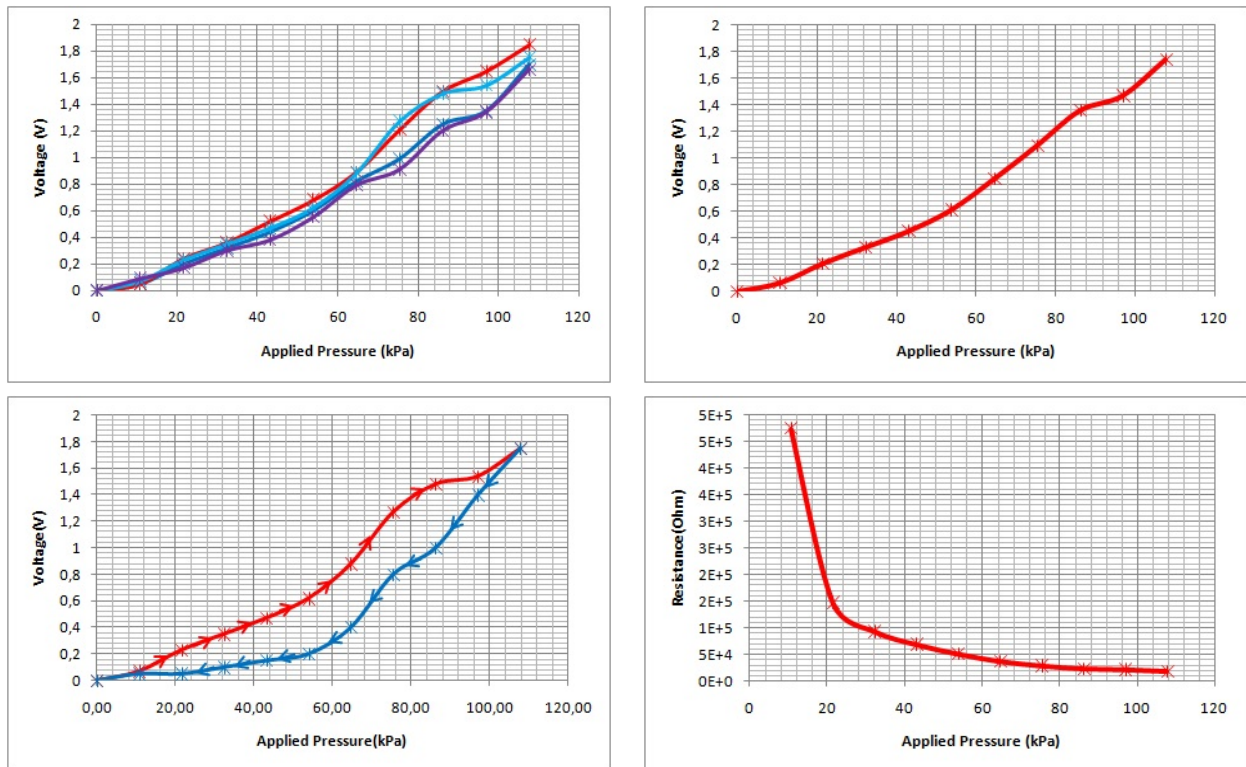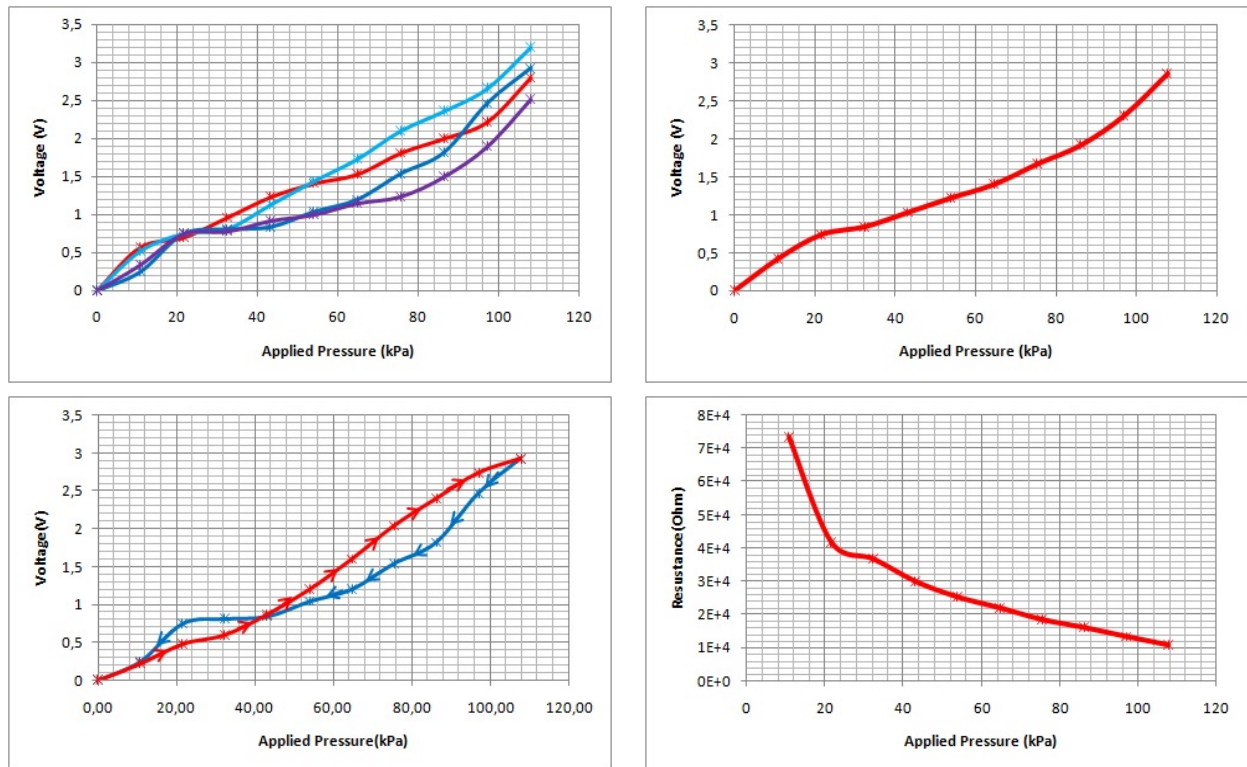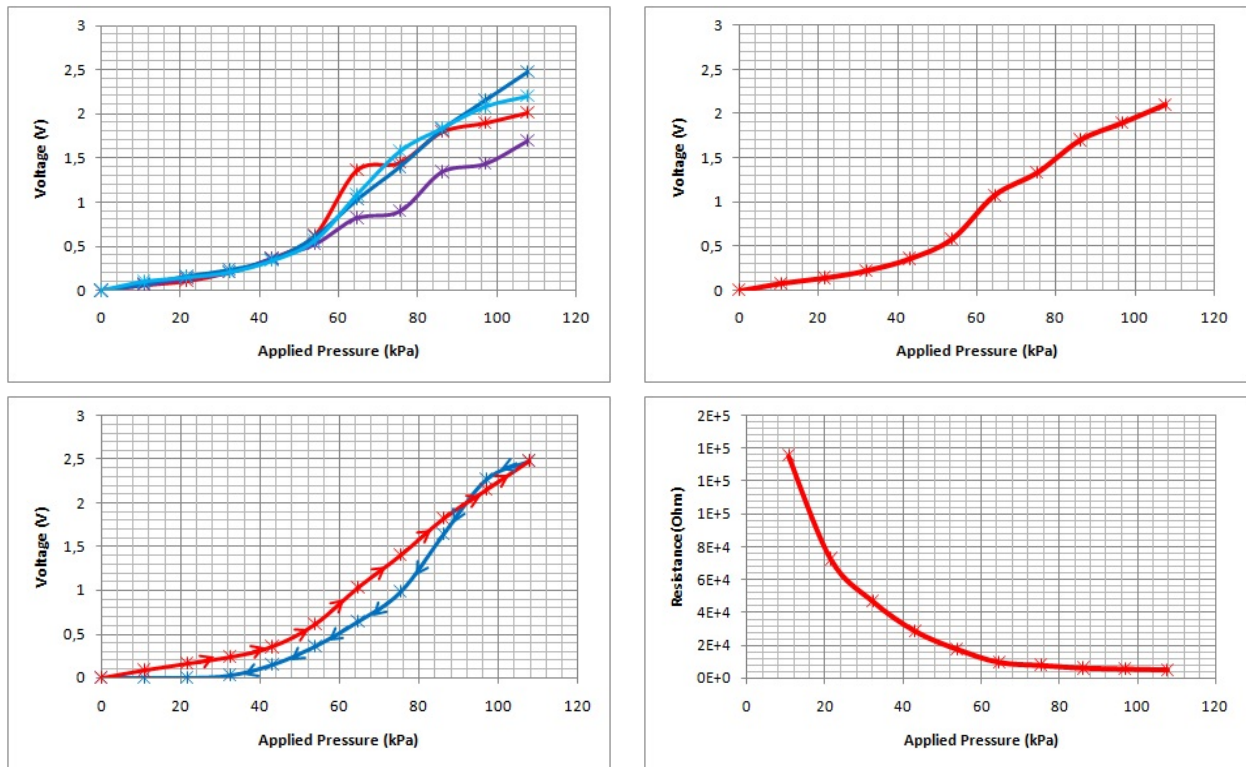

Fig. 5.27: Measure with the shape 6 electrode and PEF foam.

5.1.5 Results

The experiments show that the foam labelled as Rubber has better sensitivity than other foams. On the opposite, the foam labelled as PU shows the lowest sensitivity, moreover, this foam has higher hysteresis as it appears in the experiments.

During the experiments the foam labelled as PU lost properties as tests were carried out, however, other foams keep almost invariable their properties.

Calibration of the tactels

Other issue to highlight is, some undesired source of errors such as mismatching, hysteresis or drift are presented when it is performed the measurements on the tactels. These effects are quiet important in this kind of sensor. To reduce it, it is necessary to use a strategy for calibrating the measurements of the tactels.
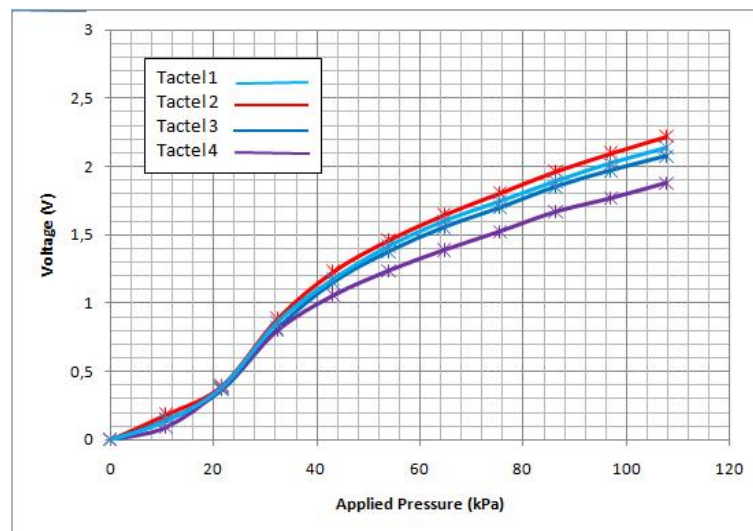
Fig. 5.28: depicts the average curve for each one of the four tactels measured, using the Rubber foam over the Shape 4.

The calibration of the sensor has been accomplished applying an uniform pressure level simultaneously over all tactels. This experiment has been performed over Shape 4, using the Rubber foam and the voltage has been obtained using the circuit shown in the Figure (5.3). Four tactels have been measured independently. For each tactel there have been obtained six different curves (corresponding to the six experiments accomplished). Further, there has been obtained the average curve for each tactel, shown in (5.28). From these four curves, there has been obtained the average curve, labelled as $mean_{cb}$. It is obtained the standard deviation of each tactel respect to the $mean_{cb}$. This means, for each level of

pressure there are six different measurements, so it is obtained the standard deviation of each measurement respect to the corresponding pressure value in $mean_{cb}$.

Pre.[kPa]	Tactel$_1$[V]	Tactel$_2$[V]	Tactel $_3$[V]	Tactel$_4$[V]	mean$_{cb}$
0	0.0	0.0	0.0	0.0	0.0
10.7	0.14	0.19	0.15	0.10	0.14
21.5	0.39	0.40	0.37	0.38	0.38
32.3	0.86	0.89	0.82	0.80	**0.84**
43.1	1.18	1.23	1.15	1.06	1.15
53.9	1.42	1.46	1.38	1.24	1.37
64.7	1.60	1.65	1.56	1.39	1.55
75.4	1.75	1.81	1.70	1.52	**1.69**
86.2	1.89	1.97	1.85	1.67	1.84
97.0	2.03	2.10	1.97	1.77	1.97
107.8	2.14	2.22	2.08	1.88	**2.08**

Table 5.2: Voltage output for each one of the four tactels and the average curve from the four tactels. The voltage has been obtained using the circuit shown in Figure 5.3.

To reduce the standard deviation and so to fit the obtained curve for each tactel with the mean$_{cb}$, each tactel is affected by a correction factor, so that when the output of the tactel is multiplied by it the result is the same as the output of another sensor under the same pressure. Thus, if m_{ij} is the measurement from a tactel, the calibration can be made as [11]

$$m_{ij_{caibrated}} = m_{ij}\frac{mean_{cb}}{m_{ij}cb} \tag{5.4}$$

where $m_{ij}cb$ is the output average of the tactel for a given pressure at the calibration point and $mean_{cb}$ is the mean value of the outputs from all tactels at the calibration point. As calibrations points have been used (0.84[V] to 32.33 [kPa], 1.69 [V] to 75.43 [kPa], 2.08 [V] to 107.76 [kPa]). The first calibration point is applied to the first three data, the second point is applied to the following four data and the third point is applied to the rest. For instance, for a tactel there is the following:

Pre.[kPa]	Ex$_1$ [V]	Ex$_2$[V]	Ex$_3$[V]	Ex$_4$[V]	Ex$_5$[V]	Ex$_6$[V]	S.D.B[V]
0	0.0	0.0	0.0	0.0	0.0	0.0	0.0
10.7	0.13	0.11	0.08	0.07	0.06	0.12	0.05
21.5	0,48	0,44	0,33	0.36	0.33	0.33	0.06
32.3	0.90	0.83	0.74	0.73	0.86	0.74	0.08
43.1	1.15	1.00	1.04	1.05	1.15	0.94	0.12
53.9	1.30	1.16	1.20	1.27	1.38	1.11	0.16
64.7	1,42	1,30	1.38	1.45	1.52	1.26	0.18
75.4	1,51	1,43	1,50	1,60	1,70	1,40	0,20
86.2	1.61	1.56	1.68	1.77	1.84	1.54	0.21
97.0	1.70	1.66	1.76	1.88	1.94	1.66	0.23
107.8	1.80	1.83	1.85	1.96	2.03	1.80	0.22

Table 5.3: Voltage output for each experiment of a tactel for a given pressure. S.D.B means Standard Deviation Before. The voltage has been obtained using the circuit shown in Figure 5.3.

The following Table shows the new voltage output when the algorithm (5.4) is employed:

Pre.[kPa]	Ex$_1$[V]	Ex$_2$[V]	Ex$_3$[V]	Ex$_4$[V]	Ex$_5$[V]	Ex$_6$[V]	S.D.A[V]
0	0.0	0.0	0.0	0.0	0.0	0.0	0.0
10.7	0.14	0.12	0.08	0.07	0.06	0.13	0,05
21.5	0.50	0.46	0.35	0.38	0.35	0.35	0,06
32.3	1.00	0.92	0.82	0.81	0.96	0.82	0.09
43.1	1.28	1.11	1.16	1.17	1.28	1.04	0.09
53.9	1.44	1.29	1.33	1.41	1.53	1.23	0.10
64.7	1.58	1.44	1.53	1.61	1.69	1.40	0.10
75.4	1.67	1.58	1.66	1.77	1.88	1.55	0.11
86.2	1.78	1.73	1.86	1.96	2.04	1.70	0.12
97.2	1.88	1.84	1.95	2.08	2.15	1.84	0.12
107.8	1.99	2.02	2.05	2.17	2.25	1.99	0.10

Table 5.4: Calibrated voltage output for each experiment of a tactel for a given pressure. S.D.A means Standard Deviation After. The voltage has been obtained using the circuit shown in Figure 5.3.

The Figure (5.29) shows the new obtained curves when is used an algorithm. It can be observed that if an algorithm is used the mismatching between tactels decrease.
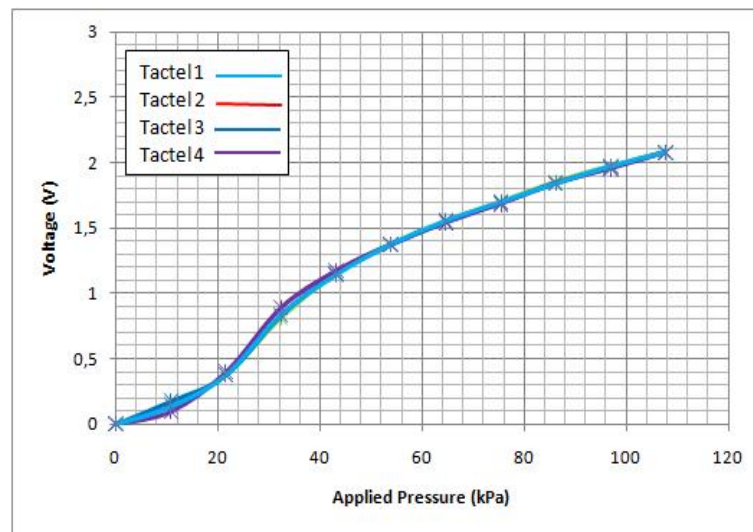
Fig. 5.29: depicts the average curve for each one of the tactel measured with a calibration applied, using the Rubber foam over the Shape 4.

Mismatching over the foam

There was another error source found when the experiments were carried out. Despite the foams used are isotropic they don't have a constant behaviour in all zones of the foams. This means that the result changes depending of the zone of the foam used to measure. In Figure (5.30) is shown the result obtained when it is measured on different zones on the same foam and shape, where can be observed the different result achieved.
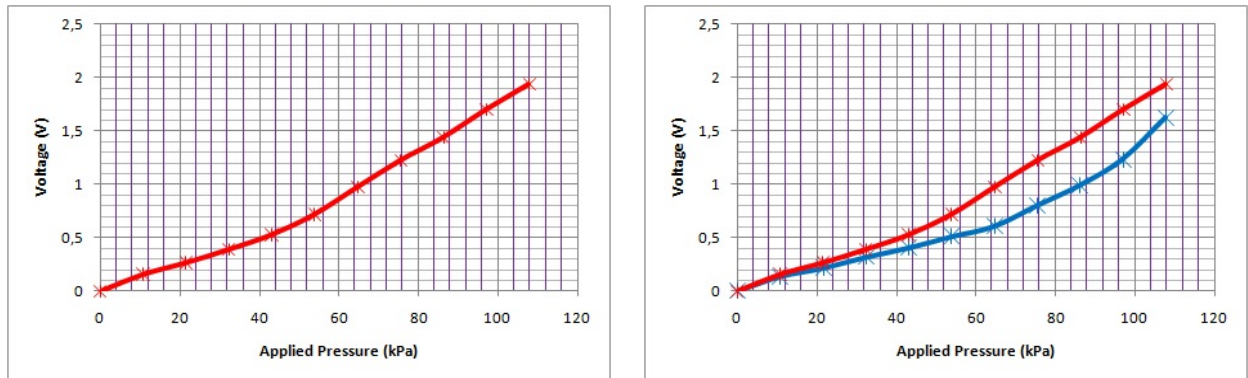
Fig. 5.30: Different result with measuring in different zone on the foam.

Clamping of the foam over the electrode

To carry out the electronic based on the measuring of the element independently, it is necessary clamping the conductive material over the electrodes through a conductive glue because when it is used a conductive foam appears crosstalk effect among tactels. The glue employed should meet certain requirements, as a low resistance in the force direction and a high resistance in the same plane of the electrodes. The material chosen has been the 3M Electrically Conductive Adhesive Transfer Tape 9703[29] which is a pressure sensitive adhesive (PSA) transfer tape with anisotropic electrical conductivity. The PSA matrix is filled with conductive particles which allow interconnection between substrates through the adhesive thickness (the "Z-axis") but are spaced far enough apart for the product to be electrically insulating in the plane of the adhesive. The principal features are:

- Insulation Resistance 3.4 x 1014 Ohms.

- Contact Resistance 1.25 milliOhm-in^2

- Minimum Gap 15 mil (0.4 mm).

- Minimum Overlap Area 5000 mil^2 (3.2 mm^2).

There has been made an experiment to show the difference between clamping the conductive material over the electrode with adhesive tape or depositing the conductive material over the electrode directly. The experiment made is shown in the Figure(5.31) where there have been selected the foams labelled as PE, Rubber and CSA. On each one has been applied a normal force and the drop of voltage has been captured.
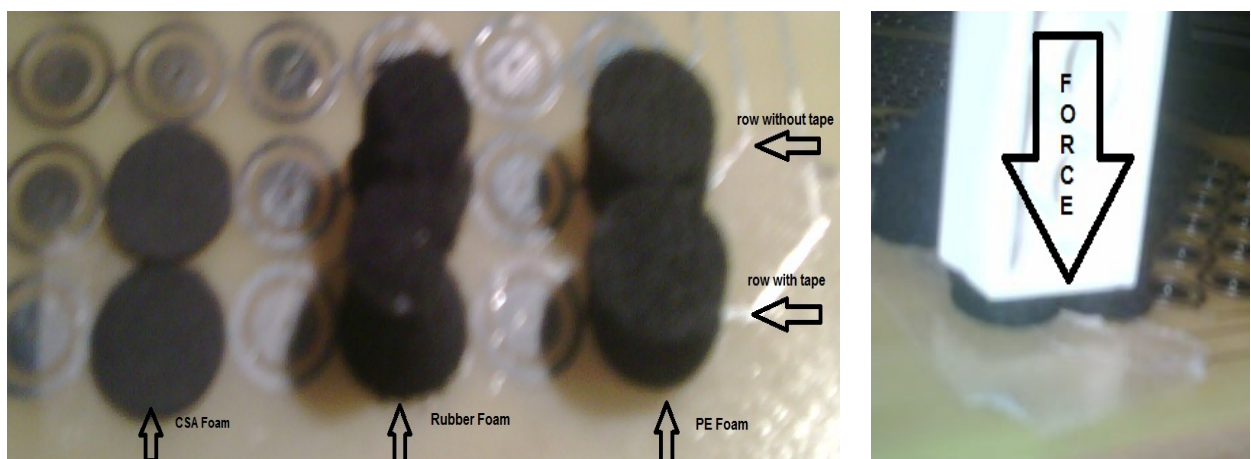
Fig. 5.31: Experiment carries out to obtain the mismatching with and without the using of the adhesive tape.

The Figure (5.32) shows the changing of the voltage and resistance when a normal force is applied. It does not show a significant changing with the applied force. To validate this, there has been performed another experiment with the PE foam, and it is obtained the same result. Therefore, with this assumption is accomplished the same behaviour shown by Weiβ in [14].
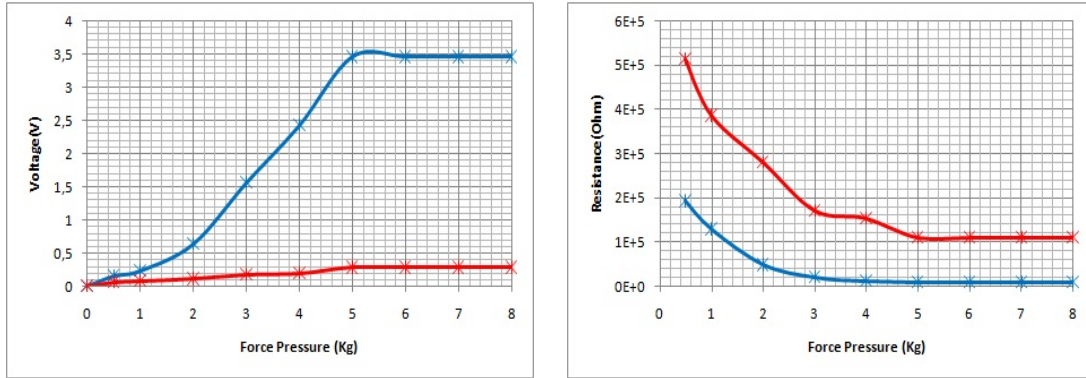
Fig. 5.32: depicts the difference of voltage and resistance in Rubber foam when is employed an adhesive tape to clamp the foam over the electrode. The red line corresponds with the measure with adhesive tape and blue line corresponds to the measure without adhesive tape.

This conclusion leads to the assumption of the working principle explained in section (4.1), where the contact resistance plays the most important role in the decreasing of the resistance and the bulk resistance can be considered negligible.
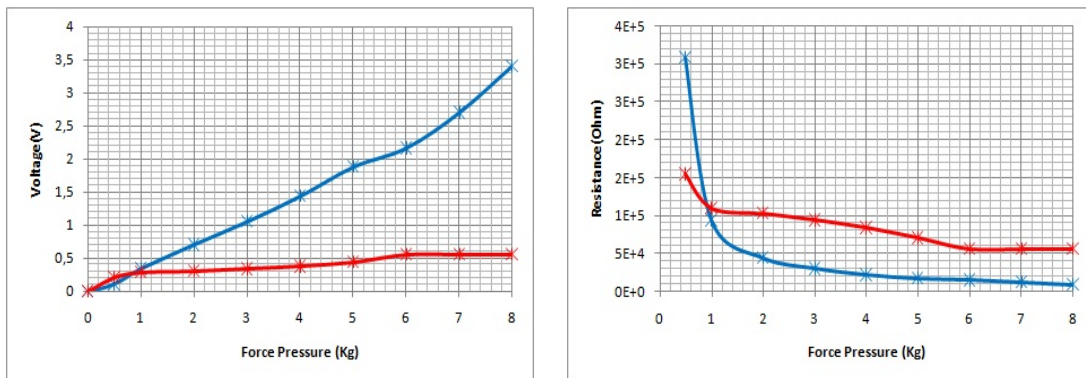
Fig. 5.33: depicts the difference of voltage and resistance in PE foam when is employed an adhesive tape to clamp the foam over the electrode. The red line corresponds to the measure with adhesive tape and blue line corresponds to the measure without adhesive tape.

The previous experiments have shown that the EMI/STATIC Shield conductive materials are not good candidates when they are clamped over the electrode. The CSA material is an isotropic conductive material designed to be used as sensor element. The Figure (5.34) depicts the difference when the conductive material is clamped through the adhesive tape or is deposited directly. The experiment shows that when is used an adhesive tape to clamp the foam, is obtained less sensitivity with the same applied force. But despite this, the response is quite linear with the applied force.
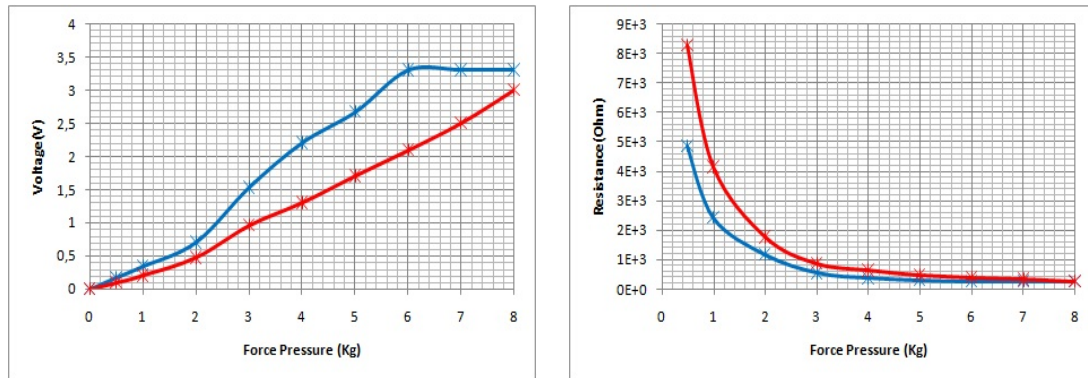
Fig. 5.34: depicts the difference of voltage and resistance in CSA foam when is employed an adhesive tape to clamp the foam over the electrode. The red line corresponds with the measure with adhesive tape and blue line corresponds to the measure without adhesive tape.

Once has been shown that the EMI/STATIC Shield conductive materials do not work when they are clamped with adhesive tape, in this report is shown a special way of clamping the foam over electrodes without changing the sensitivity. This special way is based on clamping the foam over the electrode with glue for commercial use. The key will be the commercial glue does not touch the electrodes because this kind of glue is not conductor. This new strategy has been implemented and is accomplished the same sensitivity when the foam is clamped over the electrode directly. This is shown in the Figure (5.35).
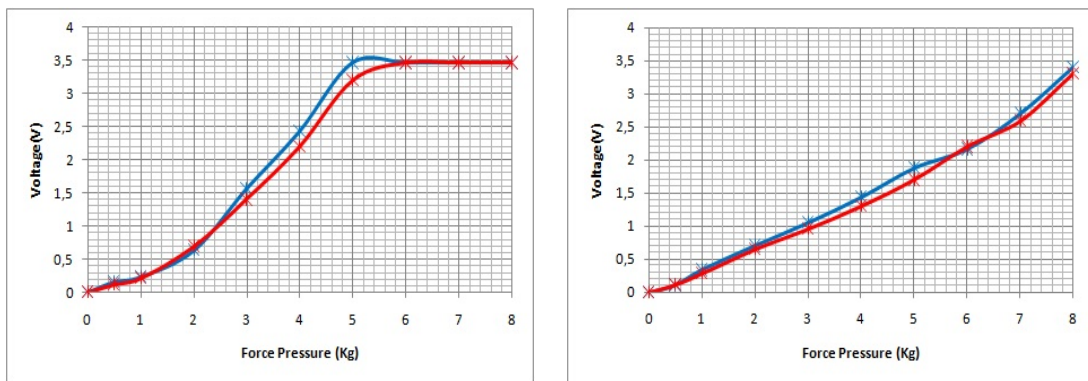
Fig. 5.35: depicts the difference of voltage and resistance with Rubber foam and PE foam when is employed an commercial glue to clamp the foam over the electrode. The red line corresponds with the measure with commercial glue and blue line corresponds to the measure without commercial glue.

5.2   Selection of the shape of the electrode

In the Table (5.5) is shown the maximum values obtained for each foam on each shape, this means the sensitivity. If it is compared the Shape 1 with the Shape 5 in Table (5.1), it is observed that both have the same area therefore the sensitivity should be almost the same. If it is observed the sensitivity for both shapes in the Table (5.5), the sensitivity has practically the same value for both. Thus, it is confirmed that the shape of the electrode does not have too much influence over the sensitivity.

	Shape 1	Shape 2	Shape 3	Shape 4	Shape 5	Shape 6
PU	1.35 [V]	1.5 [V]	1.54 [V]	1.38 [V]	1.34 [V]	1.71 [V]
Rubber	2.43 [V]	2.54 [V]	2.45 [V]	2.49 [V]	2.45 [V]	3.05 [V]
PE	1.81 [V]	2.05 [V]	1.94 [V]	1.88 [V]	1.74 [V]	2.86 [V]
PEF	1.37 [V]	1.91 [V]	1.85 [V]	1.55 [V]	1.40 [V]	2.10 [V]

Table 5.5: shows the maximum voltage when a pressure of 107.8 [Kpa] is applied on the tactels for each shape shown in the Table (5.1) from the experiments shown in the section (5.1). The voltage has been measured according to the Figure (5.3).

Other important conclusion is, that the area between electrodes (A_3) does not have much influence in the measure, at least if this area has the same size than the other areas, Shape 1 and Shape 4. In the Table (5.5) is observed if the area A_3 is smaller, the sensitivity is a little bigger. Thus, the best would be that this area is the smallest possible.

Furthermore, to see the influence of the area of the electrodes on the sensor performance it is compared the Shape 1 against to Shape 2 and Shape 3. The three shapes have the same inner area and the Shape 2 and Shape 3 has the outer area bigger than Shape 1. As it is obvious, the voltage with Shape 2 and Shape 3 should be much higher, approximately the same sensitivity obtained in Shape 6, however, the sensitivity is much more smaller. Thus, the performance of the sensor is determined mainly by the area of the smaller one.

One of the most important conclusions is , that even when the electrode has a smaller total area (obtained summing the inner and outer area of electrodes) it is achieved a higher sensitivity with similar areas. This can be seen if it is compared the Shape 2 against to Shape 6 where is obtained that the output with shape 2 electrode is lower than the shape 6 electrode.
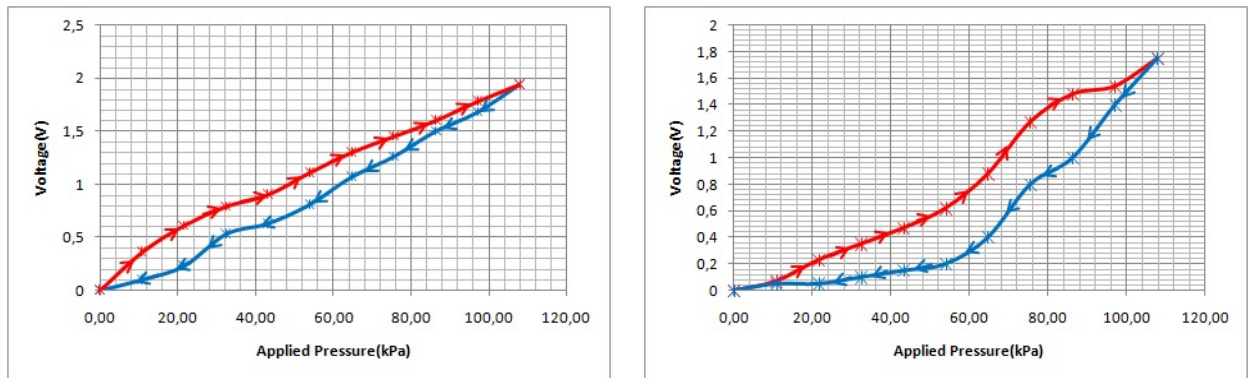
Fig. 5.36: Measure obtains with the shape 1 and shape 5 electrode and PE foam.

Other conclusion is, that the electrodes with round shape have lower hysteresis than square shape, as is shown in the experiments done. Figure (5.36) shows this effect.

Once there have been presented the results with the four materials and six shapes, there have been obtained the following conclusions:

- The electrode shape does not have too much influence over the sensitivity.

- The best would be that the gap between electrodes is the smallest possible.

- The performance of the sensor is determined mainly by the area of the smaller one.

- The round shape seems to have lower hysteresis than the square shape.

Other requirement that should be considered, is the change of the resistance versus time. In Figure (5.37) is shown this effect for each foam.
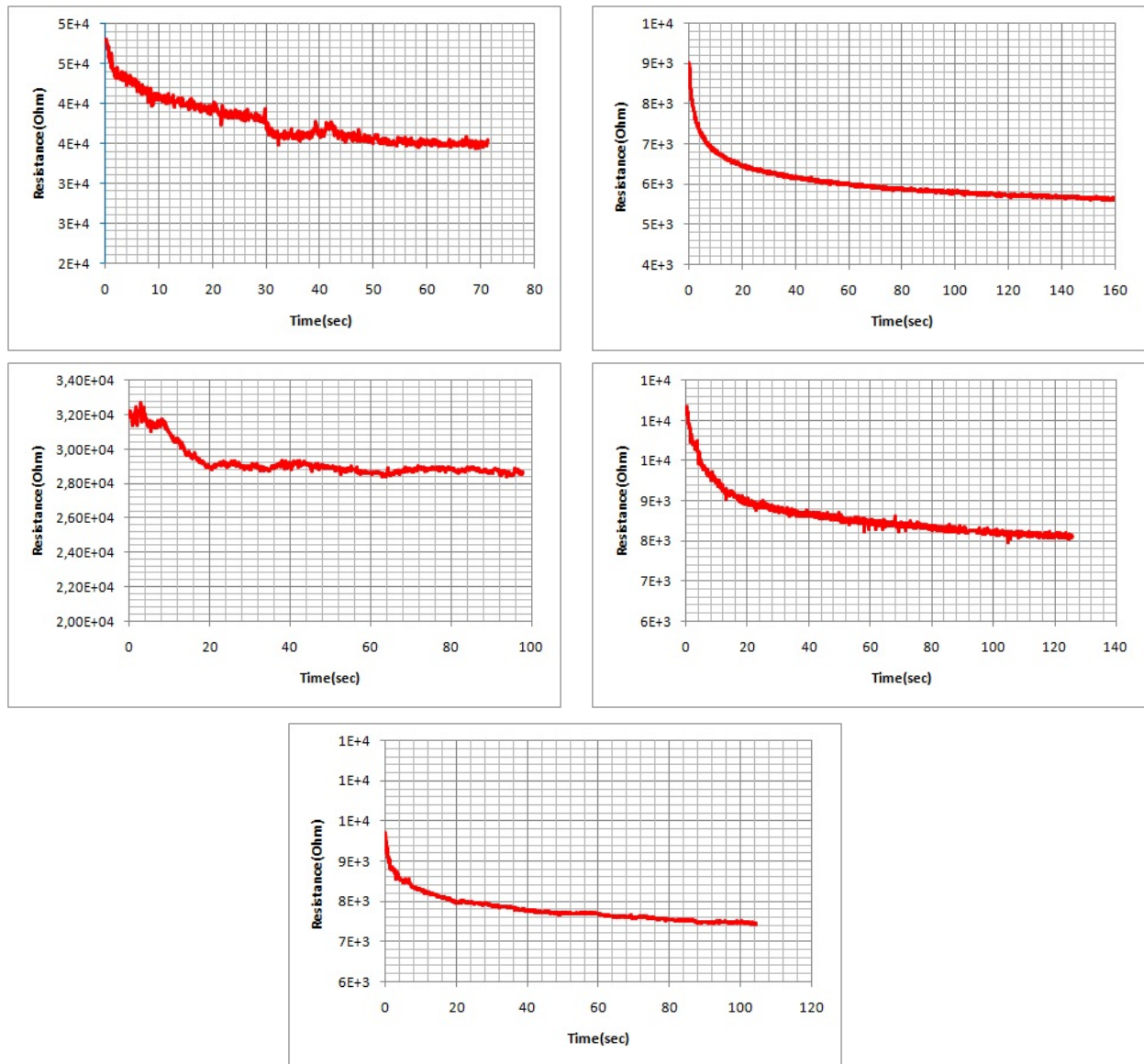
Fig. 5.37: Resistance versus time for each foam. The first picture is PU foam, the second picture is Rubber foam, the third picture is PE foam, the fourth picture is PEF and the fifth picture is CSA.

The Table (5.6) shows the drop resistance against time for each interval. The foam labelled as Rubber has the largest drop resistance and the lowest is the foam labelled as CSA. Furthermore, this table shows that the maximum drop resistance is produced in the interval from 1 second to 5 seconds. This consequence means that for a precise pressure measuring the four first foams would need to be loaded at least from 5 to 15 seconds and the CSA foam would need to be loaded at least one second.

	1s	5s	15s	30s	60s
PU	7,72%	3,58%	7%	7%	4,6%
Rubber	10,1%	11,5%	8%	4,5%	4,61%
PE	2,4%	2,5%	4,2%	2,3%	1,7%
PEF	4,3%	9,5%	7,3%	3,8%	3,9%
CSA	7,5%	5,2%	4,4%	3,0%	2,5%

Table 5.6: Drop resistance versus time for each interval.

5.3 Selection the best material

In this section is selected the best material attending to the sensitivity, the hysteresis, behaviour, durability and the price. Each feature is classified with a mark from 1 to 5, being 1 the best mark and 5 the worst mark. Furthermore, no all features have the same importance, so the features with more relevant are labelled with 1 and the features with less importance are labelled with 2 or 3. Thus, the material with less mark will be the material with better features to employed in the tactile sensors.

Material	Sensitivity	Hysteresis	Durability	Price	TOTAL
PU	5	5	5	1	2*5+1*5+2*5+3*1=28
Rubber	2	1	1	3	2*2+1*1+2*1+3*3=16
PE	3	2	2	2	2*3+1*2+2*2+3*2=18
PEF	3	3	4	3	2*3+1*3+2*4+3*3=26
CSA	1	2	1	5	2*1+1*2+2*1+3*5=21

Table 5.7: depicts the classification of each material attending to the Sensitivity, Hysteresis, Durability, Price. Furthermore, the features have been classified from their relevant.

6 Implementation of the tactile sensor

In this section is shown the consumption for each topology, as well as the consumption for each device used into each topology. Furthermore, there are shown the differences between the system based on zero potential method **(ZPM)** using the readout electronic shown in the section (4.3.2) and system based on the measurement of the tactels independently **(MEI)** using the readout electronic shown in the section (4.3.1), developed in this report. In both case the resistance R_{24} used in the Amplifier Block is 2.7 KΩ.

Moreover, in this section is explained a novel method to scan the matrix only when the sensor has been touched, while the sensor is not pressured, it will remain in stand by state.

6.1 Consumption in the steady state

In the Table (6.1) are shown the components used into each topology, as well as the consumption for each one of them and the total consumption for each topology. As can be observed the resistance has the maximum power consumption, highlight that one only resistance is activated for each multiplexer, since one only row or column is selected at the same time. The ZPM circuit needs two resistances activated while the MEI circuit needs only one resistance activated. The maximum current consumption is the operational amplifier where the consumption is the same in both methods because they use the same configuration, shown in the Figure (4.31) . These points should be changed in the future improvements.

ZPM						
Device	**N^o**	**V.(+)[V]**	**V.(-)[V]**	**C.(+)[mA]**	**C.(-)[mA]**	**T.C.[mW]**
O.P	2	3.3	-3.3	0.29	0.30	1.98
Multiplexer	2	3.3	-	0.002	-	0.007
SPDT	4	3.3	-	0.004	-	0.0132
R. 1 MΩ	16	3.3	-	0.006	-	43.56
Total				**0.29**	**0.29**	**45.56**
MEI						
Device	**N^o**	**V.(+)[V]**	**V.(-)[V]**	**C.(+)[mA]**	**C.(-)[mA]**	**T.C.[mW]**
Regulator 5/3.3	1	5	-	0.14	-	0.75
O.P.	2	3.3	-3.3	0.29	0.29	1.98
Multiplexer	2	3.3	-	0.002	0	0.007
Switch	8	5	-	0.008	-	0.04
R. 1 MΩ	8	5	-	0.005	-	25
Total				**0.44**	**0.29**	**27.77**

Table 6.1: depicts the voltage, current and consumption for each device used into each topology, as well as the total current and total consumption for each topology.

6.2 Comparison between ZPM and MEI

In this section are shown the differences between ZPM circuit and MEI circuit when one only tactel is pressured, one whole row is pressured and when one row is pressured but one tactel is not activated. The Figure (6.1) depicts how the current consumption has been taken.
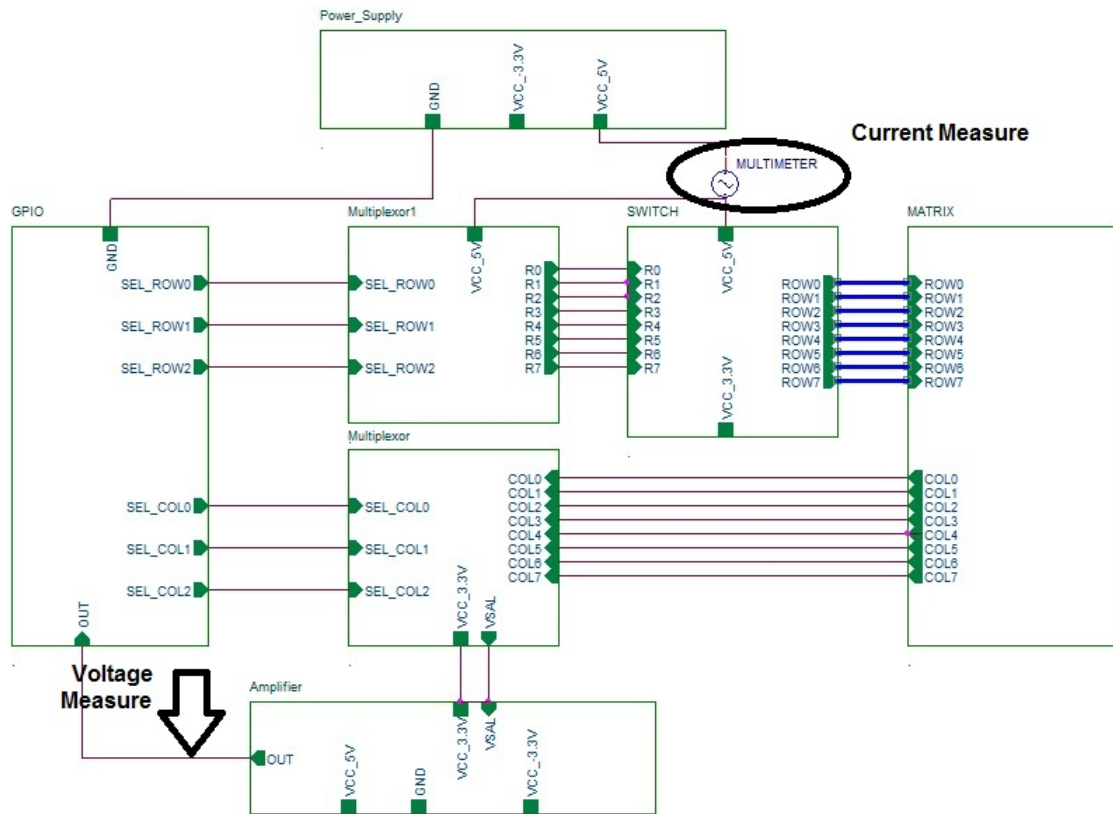

Fig. 6.1: depicts the blocks diagram for MEI circuit and how the current consumption has been taken.

Measurement of a tactel

There has been carried out an experiment to show the difference between both systems when a tactel is pressured. There have been taken the values for different output voltages and the currents have been measured. The Figure (6.2) shows the experiment that has been carried out for both systems where one tactel is activated. The negative voltage is not included in the Table (6.2) because the consumption is the same in both methods, as can be observed in the previously section.
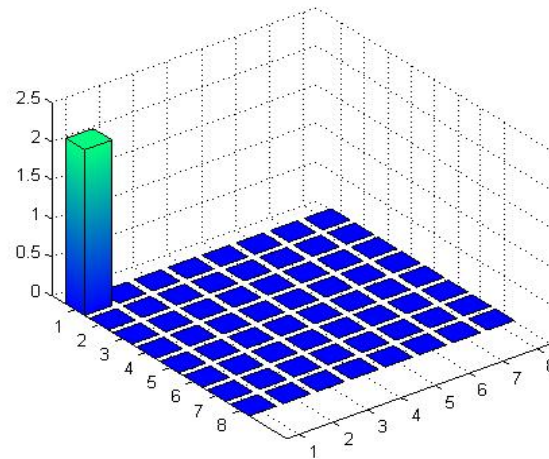
Fig. 6.2: Measurement of one tactel with both systems.

In the Table (6.2) is shown the current obtained for each voltage from each system. It can be observed the ZPM circuit has lower current than the MEI circuit in the steady state because the MEI circuit employs more devices. Moreover, the Power consumption is higher in MEI circuit because the voltage supply is 5 V instead of 3.3 V which is used by ZPM circuit.

ZPM											
Voltage[V]	0	0.23	0.38	0.62	0.9	1.2	1.5	1.8	2	2.33	2.5	2.85
Current[mA]	0.29	0.62	0.83	1.15	1.56	1.93	2.36	2.8	3.1	3.55	3.64	4.16
Power [mW]	0.96	2.04	2.8	3.7	5.1	6.3	7.7	9.2	10.2	11.7	12.0	13.7
MEI											
Voltage[V]	0	0.20	0.46	0.59	0.72	0.94	1.25	1.75	2.1	2.55	2.85	2.97
Current[mA]	0.44	0.64	1.06	1.22	1.42	1.72	2.18	2.80	3.30	4.00	4.40	4.56
Power [mW]	2.6	3.7	5.4	6.4	7.2	8.8	11	14.4	16.9	20.1	22.1	22.8

Table 6.2: Voltages and currents for each readout circuit. The ZPM uses a voltage supply of 3.3 V and MEI uses a voltage supply of 5 V.

Measurement of one row

There has been carried out an experiment to show the difference between both systems when one row is pressured and the current on each tactel has been measured. The Figure (6.3) shows the output for each system. This experiment is very important because it can be observed the working difference between both systems. While the ZPM circuit actives all tactels when one row is selected, the MEI circuit actives one tactel when one row is selected.
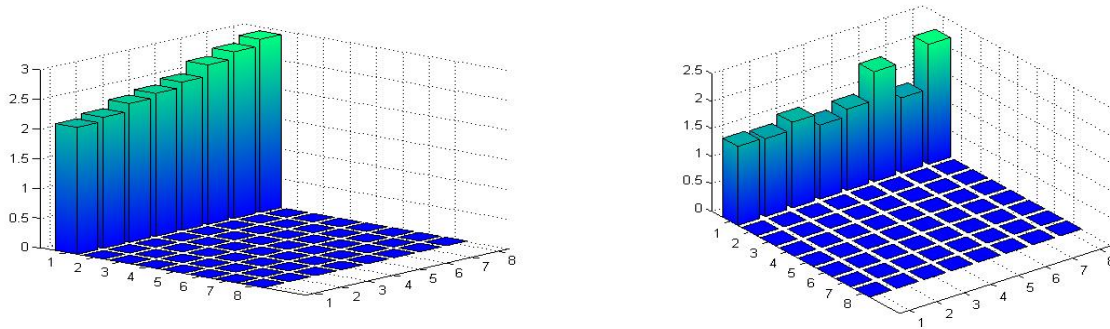
Fig. 6.3: shows the output when one row is pressured for each system. The picture on the left corresponds to ZPM circuit and the pictured on the right corresponds to MEI circuit.

As can be observed in Table (6.3) the consumption of ZPM circuit is higher than MEI circuit despite of a lower initial consumption in the steady state. Thus, when several tactels are pressured in the same row, the consumption is higher for the first system. Moreover, the consumption for MEI circuit is the same when one row is pressured or one only tactel is pressured, therefore, it can be affirmed that the MEI circuit has a better performance for large area applications.

ZPM								
	$T_{1,1}$	$T_{1,2}$	$T_{1,3}$	$T_{1,4}$	$T_{1,5}$	$T_{1,6}$	$T_{1,7}$	$T_{1,8}$
Voltage[V]	2.14	2.21	2.34	2.41	2.5	2,69	2.81	2.92
Current[mA]	9.72	9.82	9.94	10.05	10.13	10.32	10.55	10.65
Power [mW]	32.1	32.4	32.8	33.2	33.4	34.1	34.8	35.1
MEI								
	$T_{1,1}$	$T_{1,2}$	$T_{1,3}$	$T_{1,4}$	$T_{1,5}$	$T_{1,6}$	$T_{1,7}$	$T_{1,8}$
Voltage [V]	1.43	1.41	1.55	1.34	1.47	1.99	1.36	2.17
Current[mA]	2.40	2.37	2.60	2.30	2.46	3.15	2.34	3.41
Power [mW]	12.0	11.85	13.00	11.50	12.30	15.75	11.70	17.05

Table 6.3: Voltages and currents each readout circuit where $T_{i,j}$ means the tactel places on the row i and on the column j. The ZPM uses a voltage supply of 3.3 V and MEI uses a voltage supply of 5 V.

If it is compared the Table (6.2) with Table (6.3), it can be observed that the consumption is the same for MEI circuit, however, in the ZPM circuit the consumption rises significantly.

Measurement of one row with a tactel free

There has been carried out an experiment to show the difference between both systems when one row is pressured with one tactel not pressured and the current on each tactel has been measured. The Figure (6.4) shows the output for each system.

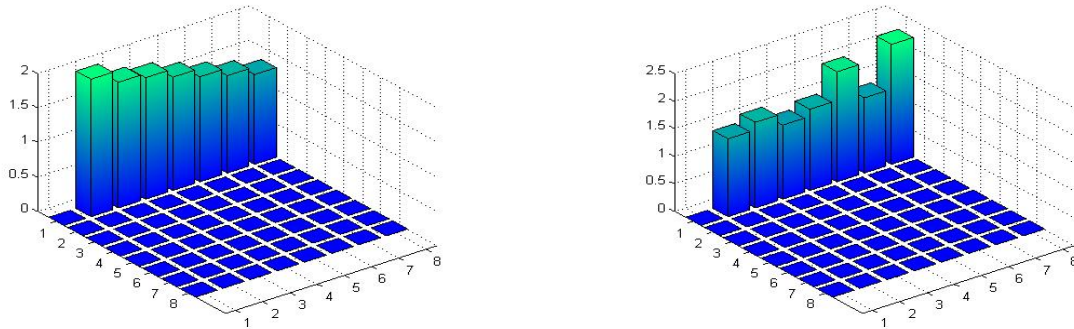

Fig. 6.4: shows the output when one row is pressured for each system with one tactel not pressured. The picture on the left corresponds to ZPM circuit and the pictured on the right corresponds to the MEI circuit.

As can be observed in Table (6.4) the consumption of ZPM circuit is higher than MEI circuit despite the initial consumption is lower. Thus, when several tactels are pressured in the

same row, the consumption is higher for the first system. Moreover, the consumption for MEI circuit is the same when one row is pressured or one only tactel is pressured. It can be also observed that when the output of one tactel is 0 ,that is without pressure, the output in MEI circuit is equal to Table (6.2), that is, the consumption is given as a result of the devices used but the drop of resistance has not influence. However, in ZPM circuit the drop of resistance of other tactels influences when one tactel is not pressured.

ZPM								
	$T_{1,1}$	$T_{1,2}$	$T_{1,3}$	$T_{1,4}$	$T_{1,5}$	$T_{1,6}$	$T_{1,7}$	$T_{1,8}$
Voltage[V]	0	1.99	1.82	1.76	1.64	1.52	1.41	1.3
Current[mA]	4.93	7.17	6.95	6.89	6.72	6.54	6.41	6.23
Power [kW]	16.3	23.7	22.9	22.74	22.2	21.59	21,16	20.56
MEI								
	$T_{1,1}$	$T_{1,2}$	$T_{1,3}$	$T_{1,4}$	$T_{1,5}$	$T_{1,6}$	$T_{1,7}$	$T_{1,8}$
Voltage [V]	0	1.41	1.55	1.34	1.47	1.99	1.36	2.17
Current[mA]	0.44	2.37	2.60	2.30	2.46	3.15	2.34	3.41
Power [kW]	2.20	11.85	13.00	11.50	12.30	15.75	11.70	17.05

Table 6.4: Voltages and currents for each readout circuit where $T_{i,j}$ means the tactel places on the row i and on the column j. The ZPM uses a voltage supply of 3.3 V and MEI uses a voltage supply of 5 V.

6.3   Resolution

Once the MEI method has been evaluated and shows a good performance, the next goal is set the size of the tactel. The initial approach for this report is to employ the tactile sensor for large area where the resolution and sensitivity is not the principal requirement. So, if it is employed a tactel with a greater size then it will be easier to cover large area with less number of tactels. So, in this section it has been compared the resolution from two different sizes of tactel, shown in Figure (6.5).

Tactel$_L$

Tactel$_S$

$A_1 = 91.11$ [mm^2]
$A_2 = 91.11$ [mm^2]
$A_3 = 17.76$ [mm^2]
$A_2/A_1 = 1$

$A_1 = 19.90$ [mm^2]
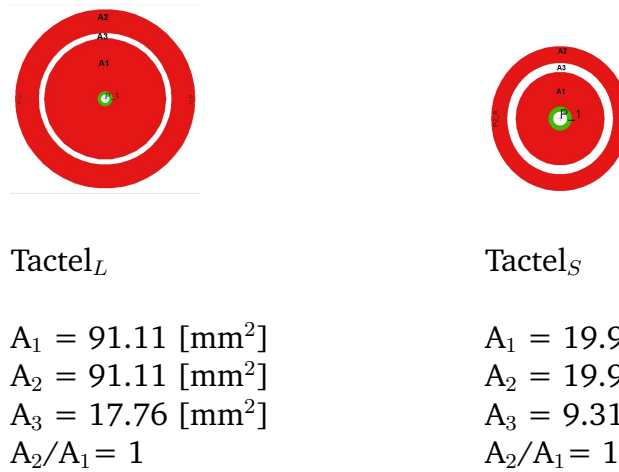$A_2 = 19.90$ [mm^2]
$A_3 = 9.31$ [mm^2]
$A_2/A_1 = 1$

Fig. 6.5: shows the tactels employed to compare the resolution with different size.

There have been performed several experiments with different objects and the output of the sensor has been taken. The employed objects are an object with square shape, object with rectangular shape and a pen, these objects are shown below:

Fig. 6.6: shows the objects measured for each size of tactel.

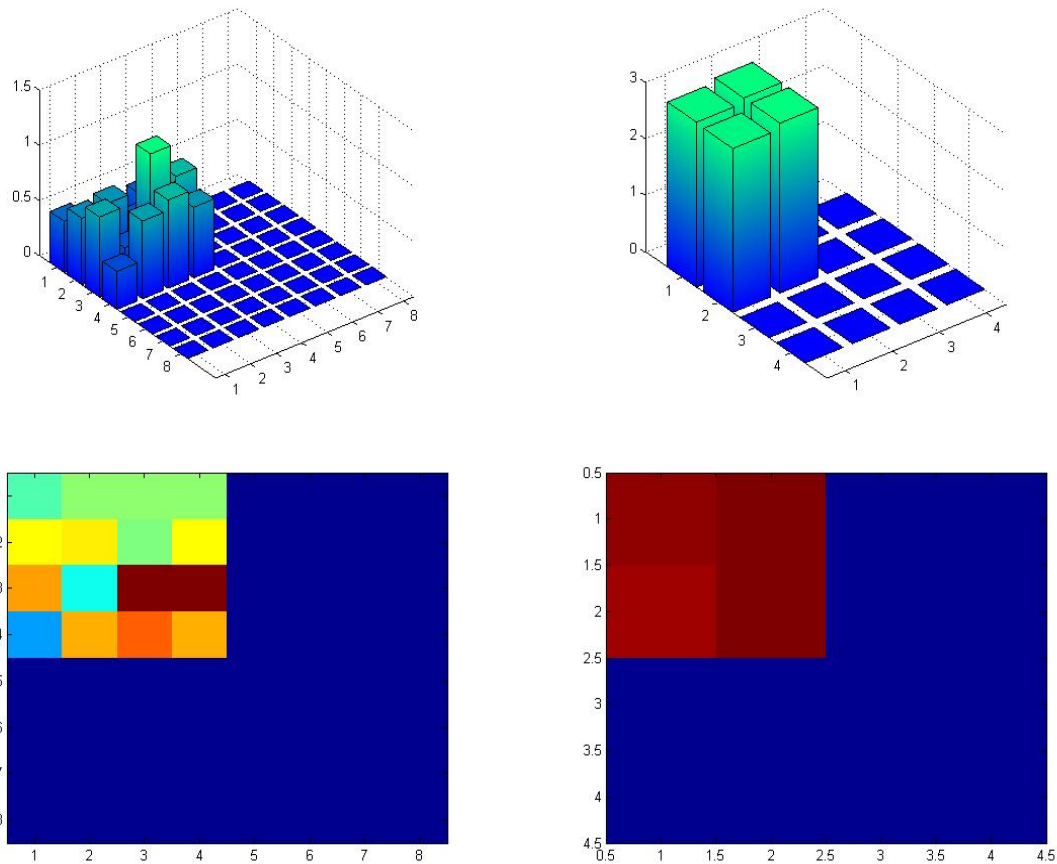In the Figures (6.7), (6.8) and (6.9) are shown the output for each size of tactel.

Fig. 6.7: shows the output for each size of tactel, in this case the output corresponds to square shape. The 3D pictures have been obtained using the function implemented in matlab **dibujar.mat**, the 2-D pictures have been obtained using the Matlab command **imagesc(matrix)**
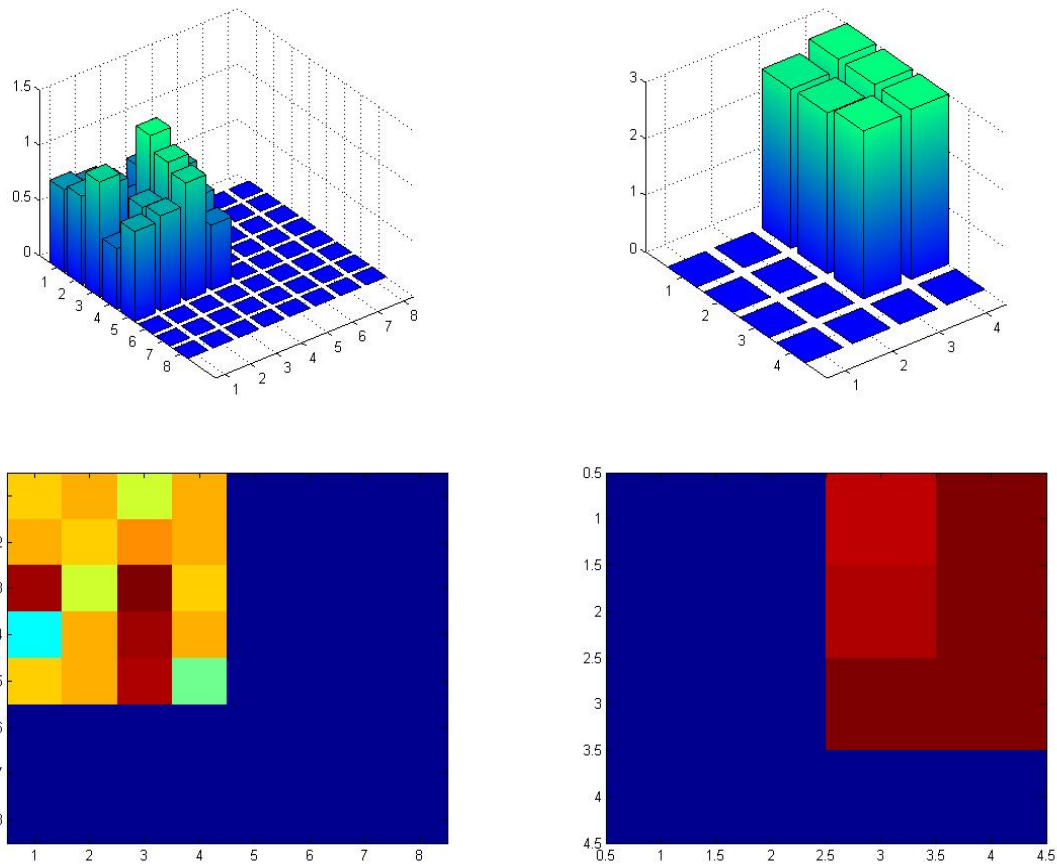
Fig. 6.8: shows the output for each size of tactel, in this case the output corresponds to rectangle shape. The 3D pictures have been obtained using the function implemented in matlab **dibujar.mat**, the 2-D pictures have been obtained using the Matlab command **imagesc(matrix)**.
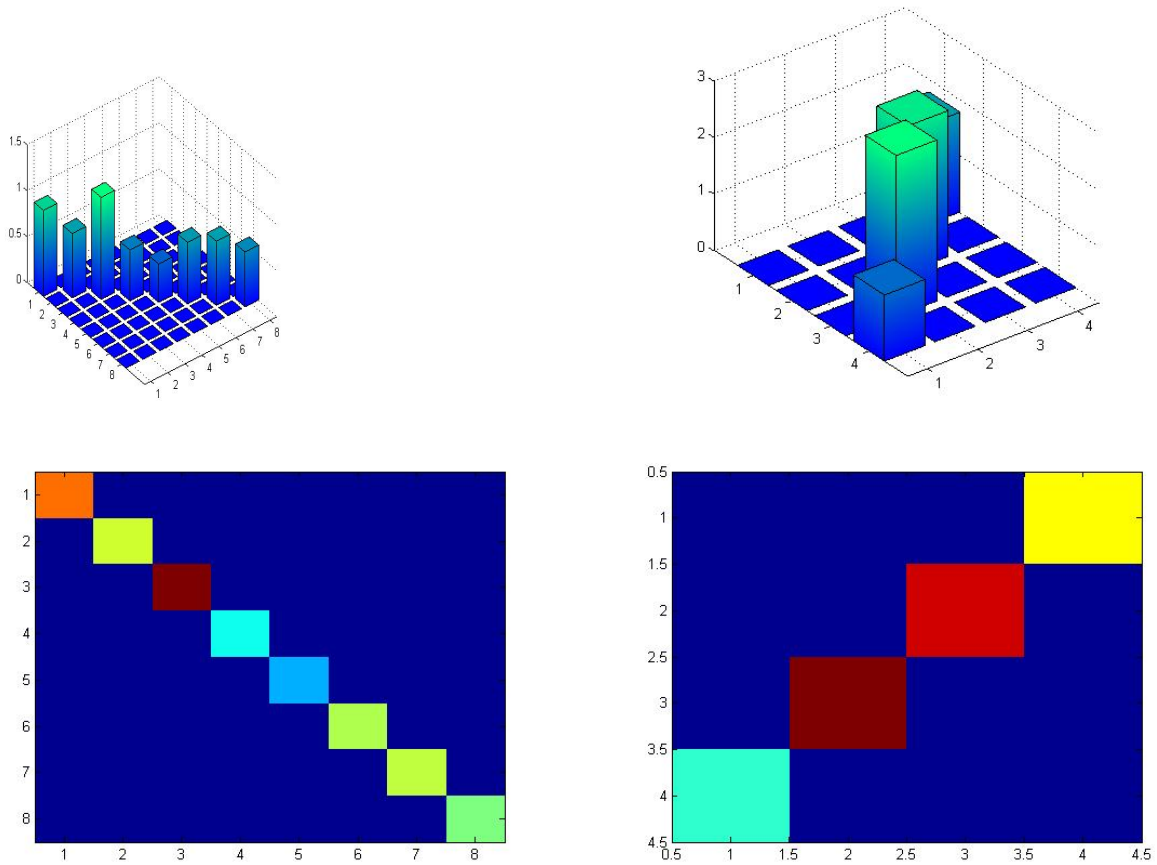
Fig. 6.9: shows the output for each size of tactel, in this case the output corresponds to stick shape. The 3D pictures have been obtained using the function implemented in matlab **dibujar.mat**, the 2-D pictures have been obtained using the Matlab command **imagesc(matrix)**.

6.4 Multi-Scale and Low-Power Sensor for Large Areas

In this report is presented a novel method to achieve a reduction in the consumption while the tactile sensor does not detect which has been touch. Thus, on this way the readout circuit will remain in stand by until the controller detects a changing of pressure, then the controller scans the matrix to get the current pressure. The circuit proposed is shown in the Figure (6.10).

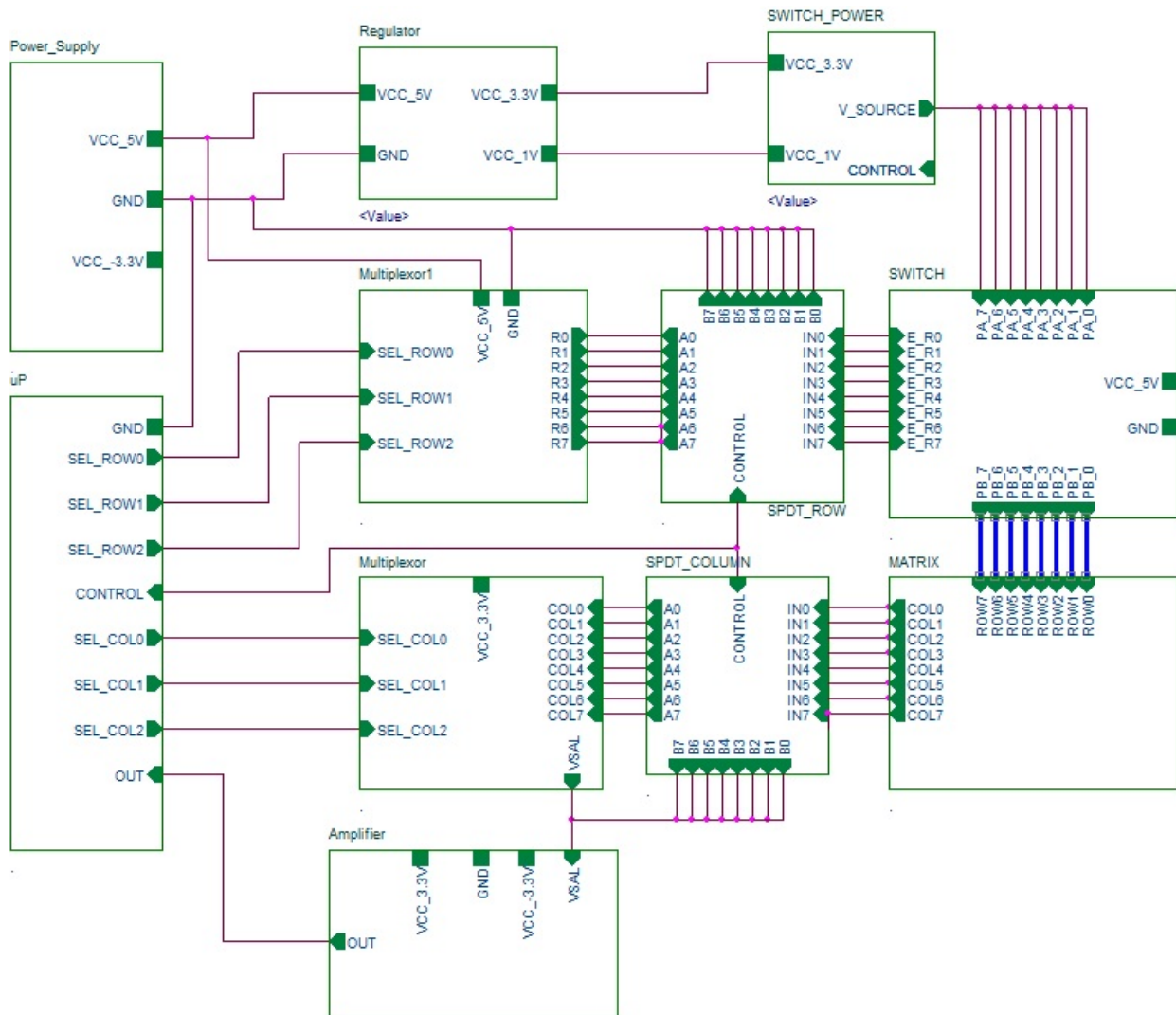Fig. 6.10: Schematic developed to achieve a sleep mode solution.

The principal changes have been to include a SPDT device between the columns of the matrix and the multiplexer, another SPDT between multiplexor and the switch block and the SWITCH POWER. The CONTROL signal controls the system, when the control signal is set as High Level, RUNNING MODE, the system should work with the normal configu-

ration, that is, through the multiplexers can be selected all tactels on the matrix, thus, the SPDT block connects the Port IN with the Port A , and the voltage supplied to the tactels will be 3.3 V. However, when the control signal is set to Low LEVEL, SLEEP MODE, the SPDT blocks connects the Port IN to Port A, that is, all columns are connected to VSAL and the enable pins of the switches are set to LOW LEVEL, that is to say, all switches are enabled, thus all rows are selected. Thus, the matrix is equivalent to one resistance. Furthermore, the voltage supply of the tactels switches also from 3.3 V to 1 V, so it is possible to reduce the consumption of the sensor. The Control signal is configured from the DAQ Board, when the output system is lower than a value fixed, the system should remain in SLEEP MODE, when the output is higher than the value fixed the system should switch to RUNNING MODE, then the matrix should be scanned.

The first point is to obtain the offset of the sensor and the output voltage from that offset. In the Figure (6.11) is shown the offset of the sensor when no pressure is applied over it. For this offset is obtained an output voltage of 0.035 V, obviously the data has been obtained for ambient temperature, that is, around of 20 ^{o}C. If the value detects for the sensor is higher than the offset voltage, the sensor should active and scans the whole matrix. However, if the sensor is lower than offset voltage, so the matrix should remain in the same state.
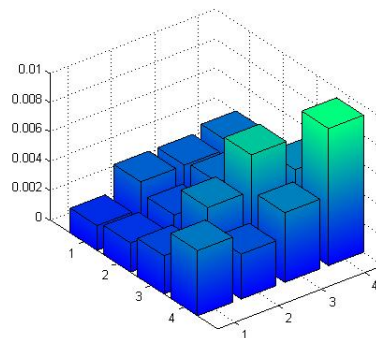
Fig. 6.11: Offset of the sensor for a matrix 4 x 4. For this offset the output is 0.035 V for ambient temperature.

Thus, when one tactel has been touched the output voltage will rise this value and the sensor will be switched to RUNNING MODE. The minimum pressure to activate the sensor is 0.5 [Kg] for each tactel. In the Figure (6.12) is shown the process to achieve the sleep mode.
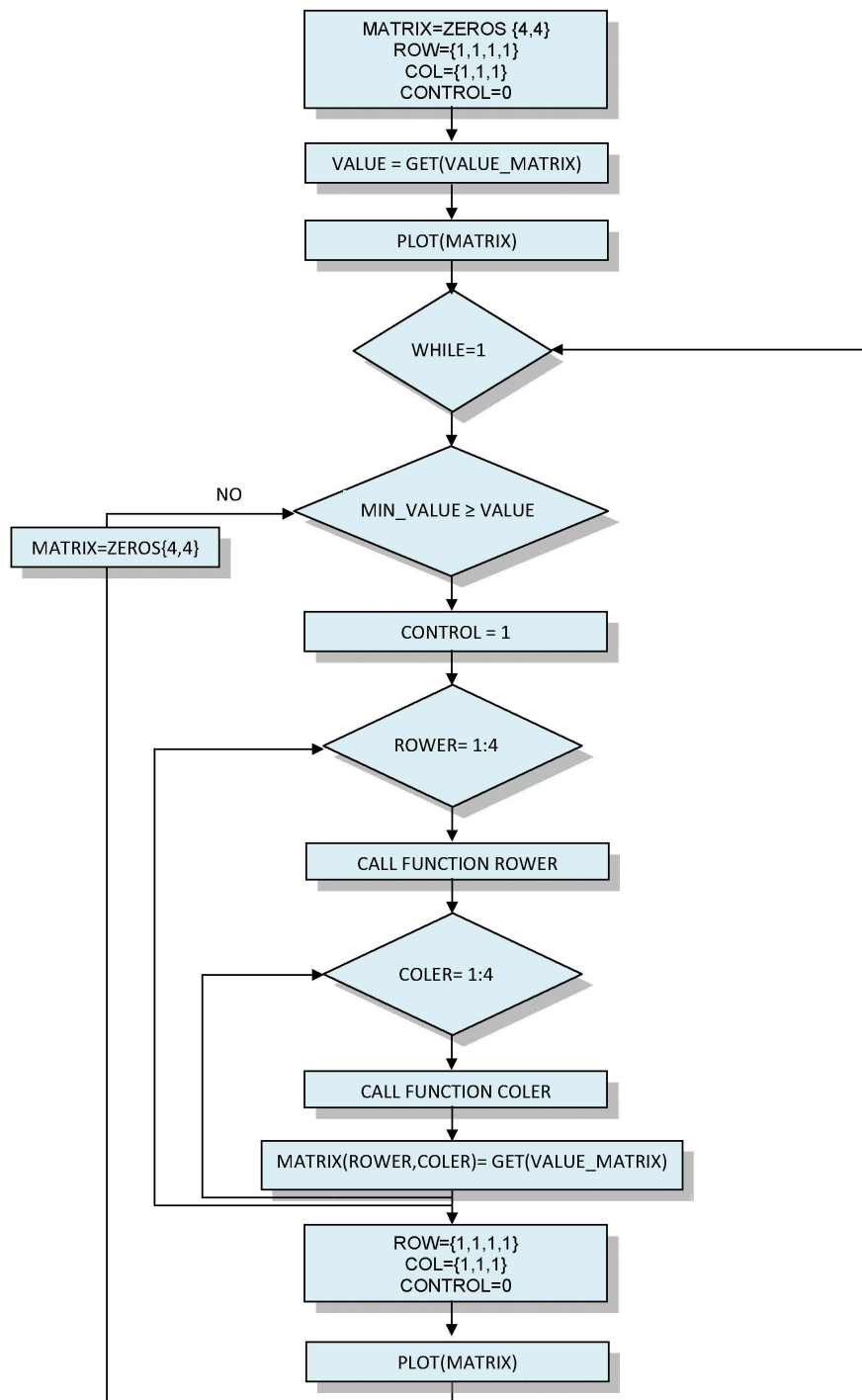
Fig. 6.12: Process to achieve the sleep mode through Matlab.

Smart floor based on tactile sensor

Once the novel method has been explained, the next step is to explain how is possible to cover large areas with this method. The tactile sensor for large area is divided in many modules until the whole area is covered. Each module has a microcontroller which controls the system and then it could communicate with the host computer or central unit. The Figure (6.13) shows the approach where the smart floor is composed of several modules as shown in the figure and they are connected with a central unit. With this approach, each module remains in SLEEP MODE, low power consumption, until that one module is pressured, in this moment, pressured module should read the whole matrix while the other module remains in SLEEP MODE because they have not been touched. So it will be possible to detect what person or object is found pressuring the sensor.

Fig. 6.13: shows the concept proposed where the smart floor is composed from multiple modules as shown.[34]

The principal issue is, what is the minimum sample speed to detect what object or person has touched the matrix. For instance, if the tactile sensor is going to be employed for smart floor as shown in the above figure , it means, it is necessary to identify when one person has stepped on the floor. The average speed when one person walks is about 4 Km/h, that is, 1.1 $m/s \approx 1\ m/s$, if one person travels 0.8 meters per step and the time one person spends in the footprint is 40%, it is obtained that the pressure on the smart floor takes 0.32 s.

$$time\_step = \frac{distance\_one\_step}{average\_velocity}(\%\_footprint) = \frac{0.8[m]}{1[m/s]} * 0.4\% = 320[ms]$$

So, the system should be able to detect that the sensor has been touched and to scan the matrix before the pressure has been removed. So, the sample speed depends on the number of elements the matrix has and the duty cycle is used. The table (6.5) shows the

duty cycle which is necessary depending on the number of elements and the total time to scan the whole matrix.

Nº of elements	Time to scan whole matrix [ms]			
	300	100	50	1
64 (8x8)	4.68	1.56	0.78	0.015
100 (10x10)	3	1	0.5	0.01
254 (16x16)	1.18	0.39	0.19	0.004
400 (20x20)	0.75	0.25	0.125	0.0025
1024 (32X32)	0.029	0.09	0.048	0.001

Table 6.5: shows the duty cycle [ms] for different number of elements and different scanning time to measure the whole matrix.

Once the duty cycle, number of elements and the sample speed have been selected, the next step is distinguish what kind of person or thing is on the smart floor, that is, our smart floor system is able to measure the pressure exerted on a floor tile and should be able to recognize the user based on their footstep force profile as they walk over the tile.

[37]*The floor has good features, such as: the users always walk over it; it is always there (even in the dark); and it can sense information not only about users but also about objects. With the Smart Floor, the user does not need to carry anything (like a badge) or remember anything (like a password); one simply walks over the floor tile and the system utilizes the user's biometric data for recognition. The Smart Floor should also work fine when the room is dark or noisy, and it does not care if a view of the user is occluded. In addition, the floor gives accurate position information. Lastly, the algorithms for identification and tracking are fairly simple and not computationally intensive.*

The purpose of the Smart Floor project should be to create and validate biometric user identification based on user's footsteps.

---

[37]The italized/emphasized text is a verbatim quotation from [31]

7 Optimization of the development of the tactile sensor

The first and most direct optimisation for the tactile sensor should be to remove the pull-up resistance and regulator 5/3.3 V and to change the topology of the operational amplifiers. According to the Table (6.1), these devices have the highest consumption and they are the principal candidates to be changed or removed.

To remove the pull-up resistance, the multiplexer which actives the switch should be changed for a digital multiplexor instead of an analog multiplexer. Thus, the pull-up resistance can be removed. There are some devices which can be candidates, for instance the demultiplexer $74AC138$. It has 8 outputs and the no output selecting are left in High Level, therefore the pull-up resistance can be removed and the maximum quiescent current is 4 μA.
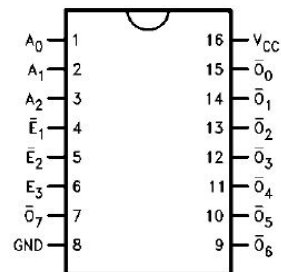

Fig. 7.1: shows the digital multiplexer 74AC138 which replaces the previous analog multiplexer.

To remove the regulator 5/3.3 V, the current switch should be changed for other switches which can be supplied with 3.3 V instead of 5 V as the currents devices. There are not many devices whose behaviour can be adjusted to these requirements, but a possible candidate could be the $IDTQS3VH244$, the quiescent current is practically as the same the current device used and the pin-out is the same exactly.

Once the previously devices have been removed , it is necessary to change the topology of the operational amplifiers and if it is possible only to use one of them. There are many topologies to accomplish these requirements, but a possible solution could be to employ an amplifier instrumentation with the following configuration:
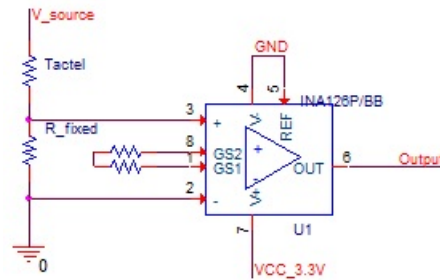
Fig. 7.2: shows the new configuration to measure the drop of voltage in the tactel.

For instance the operational amplifier could be the $INA126$ where its quiescent current is 150 μA. The Figure (6.10) showed the previous design and with the changing described the new system will be:
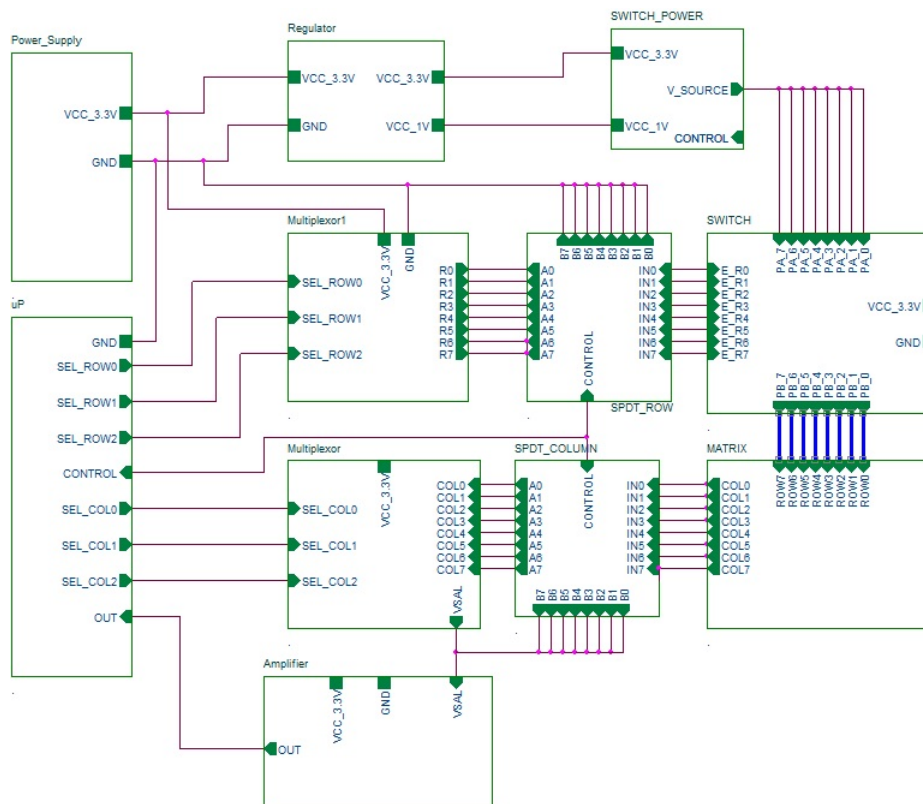

Fig. 7.3: depicts the final design where a 3.3 V voltage supply is necessary.

For the Regulator Block is necessary to use a regulator from 3.3 V to 1 V, there are many regulator to accomplish this, for instance the voltage regulator LP3879 where its quiescent current is about 15 μA. The SWITCH POWER block is the responsible of switching the

V_SOURCE signal depending if the system is on RUNNING MODE or SLEEP MODE. The performance of this block could be:
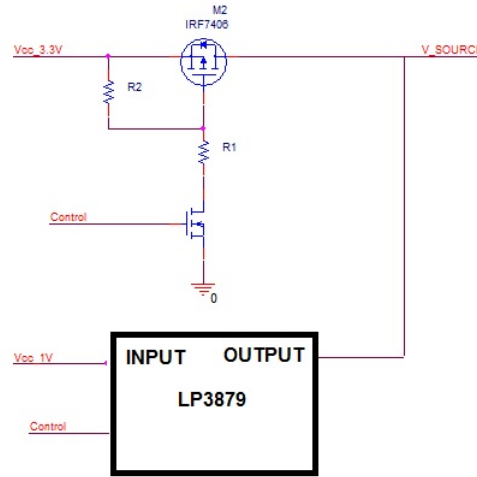

Fig. 7.4: shows a possible approach for the SWITCH POWER Block.

So, when the control signal is set to High Level the V_signal is connected to 3.3 V voltage supply because the system should work the normal way and the regulator has a pin input which when is set to High Level the output is disabled. However, the control signal is set to Low Level, the Mosfet M_2 is opened and the output of the regulator will be enabled. So, for the new system described is possible to achieve a new consumption:

Device	N^o	V.(+)[V]	V.(-)[V]	C.(+)[mA]	C.(-)[mA]	T.C.[mW]
INA126	1	3.3	-	0.15	-	0.495
LP3879	1	3.3	-	0.01	-	0.033
SPDT	4	3.3	-	0.004	-	0.0136
74AC138	1	3.3	-	0.004	-	0.012
Multiplexer	1	3.3	-	0.001	-	0.003
IDTQS3VH244	8	3.3	-	0.008	-	0.024
Total				**0.177**		**0.58**

Table 7.1: depicts the new consumption for the new system proposed.

As can be seen the current decreases drastically as the power consumption, furthermore, with this configuration is not necessary to employ a negative voltage supply.

8 Future works

The first improvement for the tactile sensor should be changing the DAQ (DT9816) by a microcontroller. The DAQ only allows a matrix of 64 tactels and if it is switched by microcontroller is possible to reach a higher size. Furthermore, with a microcontroller can be achieved a higher sampled speed, since the DAQ is limited for the driver between the DAQ with the host computer, limiting the same speed. Another issue to take into account is, the microcontroller cannot be connected with MATLAB via USB directly. So, the connection could be done via RS232 since MATLAB can communicate with this port directly but the data flow will be constraint. So, another possibility would be implementing a driver to communicate the microcontroller with Matlab via USB but this is not easy of accomplishing.

The second improvement should be choose which tactel shape has the best resolution, currently we have implemented two size but the tests in relationship with the resolution should be validated.

The third improvement would be changing the current inflexible PCB by flexible PCB. With a flexible PCB is possible to achieve higher pressure and force over the electrodes.

The fourth improvement could be developed an integrated circuit (IC) which improves the performance and compact-ability of the system. In the Figure (6.10) is shown the current implemented board. The blocks labelled as Multiplexor_1, SPDT_row and Switch could be integrated in one only device. The new device should rise the number of inputs and outputs. Thus, the new device should have at least 32 inputs and 32 outputs, only has a voltage supply, the control signal should connect all enable pin of the SWITCH block in HIGH LEVEL, that is, all rows are activated. However, when the control pin is set in Low Level, the enable pin should be selected independently with the inputs of the multiplexer. A possible configuration is shown in the Figure (8.1).
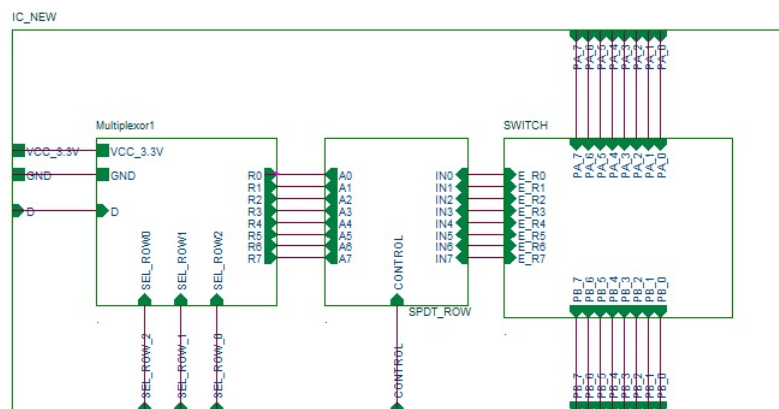

Fig. 8.1: Overview of the new device with the principals pins which should have.

Another device could be developed to select the column. The working principle could be the following: when the CONTROL signal is set as LOW LEVEL, the columns are selected independently. Thus, the output is connected with each tactel. However, when the CONTROL signal is set as HIGH LEVEL, all columns are selected, so when any tactel is pressured the V_output should change. Furthermore, the new device should include an operational amplifier where the gain can be configurable.
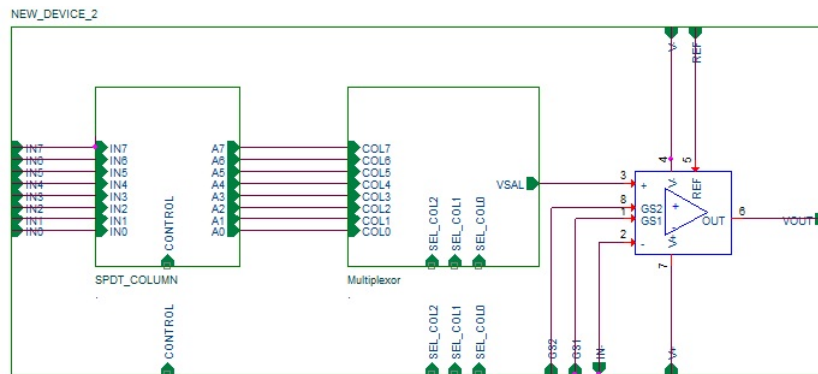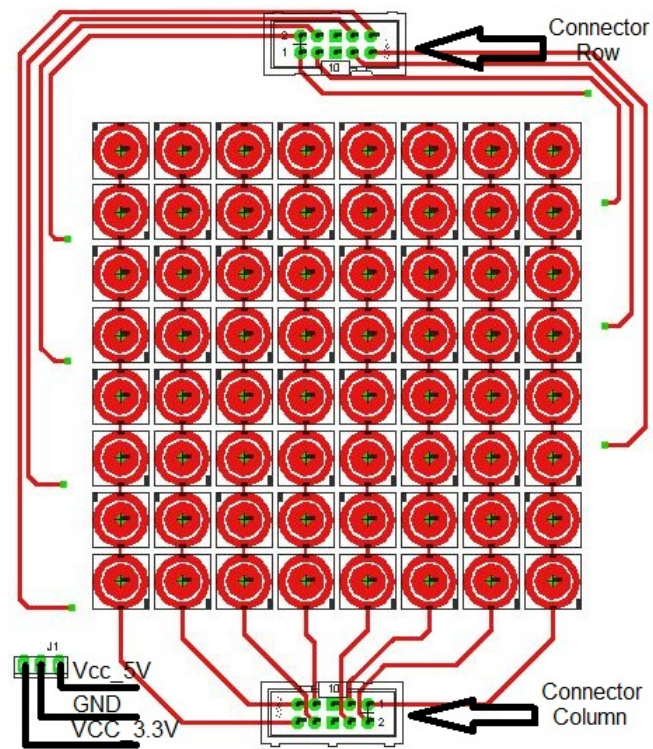

Fig. 8.2: Overview of the new device with the principals pins which should have.
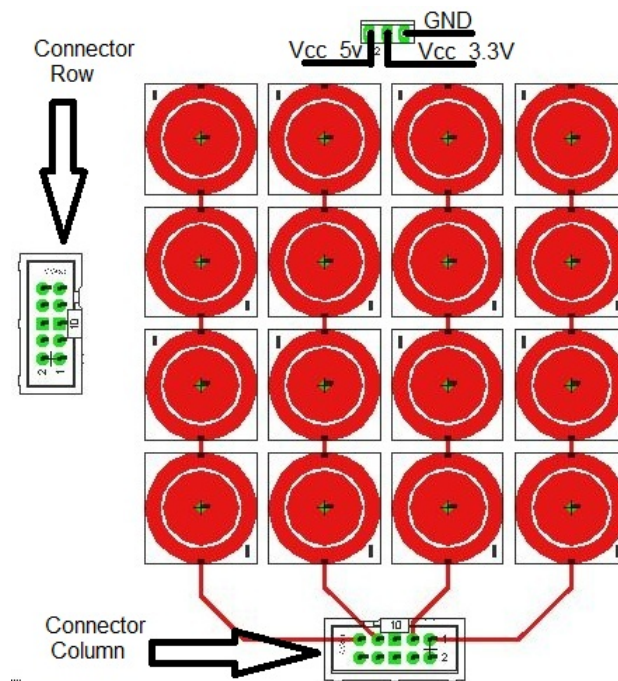
9   Conclusions

- There have been evaluated and defined the requirements to manufacture a tactile sensor. In the report has been explained the most important elements of the tactile sensors.

- The principle of elastoresistance is studied in detail. The fact that only the contact resistance between the foam and the electrodes plays the principal role is confirmed.

- The electrodes with balanced areas and less gap between electrodes have a best performance, less hysteresis, higher sensitivity. Furthermore, the circular shape has a better performance than the square shape. For it, there have been carried out many experiments to get to these assumptions.

- The EMI/Static conductive materials have been used to develop the sensor. Furthermore, there has been clamped the material on the electrodes without losing sensitivity, glueing the conductive material with "commercial" glue.

- A novel method to measure the tactels independently has been developed and the experiments have shown the consumption is lower than the classics methods. This novel method can be used to cover large area with lower consumption.

- To cover large areas is not necessary to employ a small size of tactel. There have been done several tests which show that with large size is possible to get a good resolution and sensitivity.

- There has been developed a new technique to measure the tactels solely when the matrix has been touched. While the tactels are not pressured, the system remains in SLEEP MODE, the consumption decreases and the matrix is not scanned.

A   Manufacturing Boards
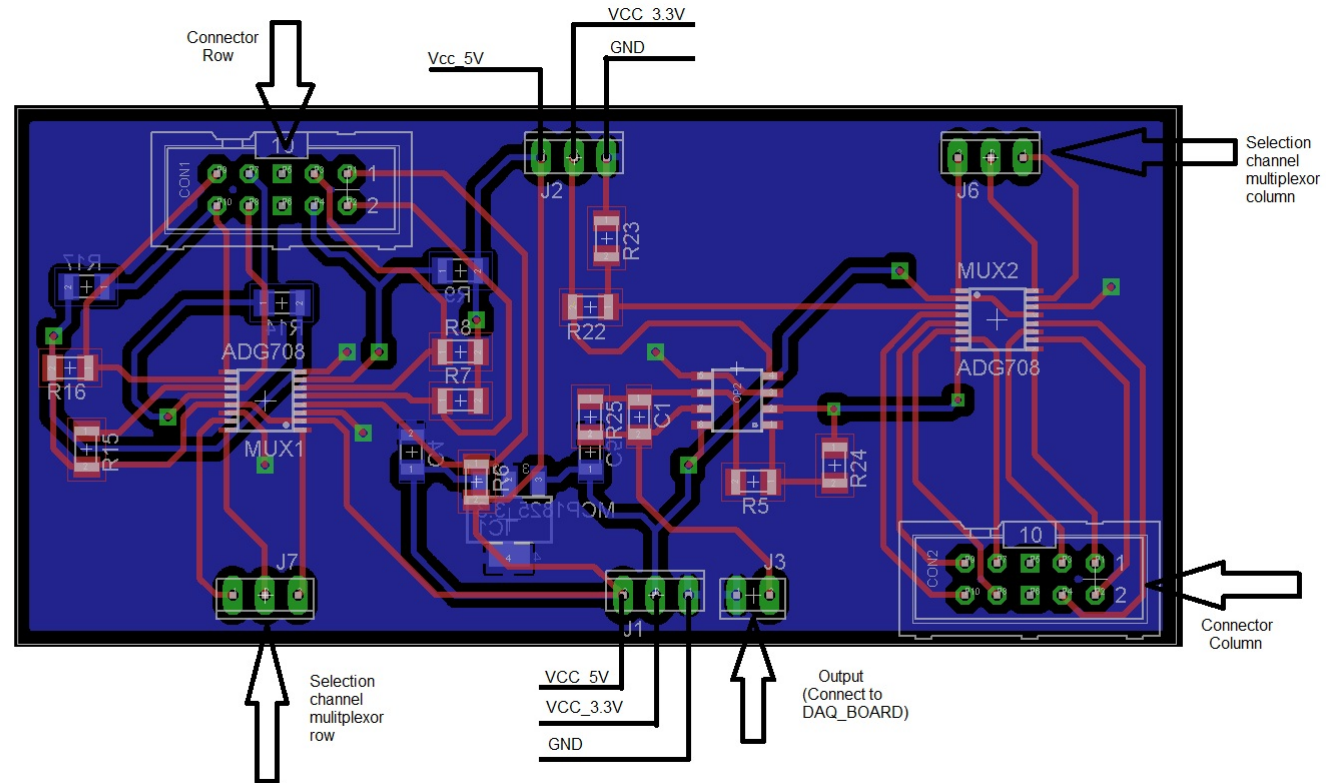
Board Matrix 8x8

Board Matrix 4x4

Board Electronic

Connector Row

VCC_3.3V

Vcc_5V

GND

Selection channel multiplexor column

Selection channel mulitplexor row

VCC_5V

VCC_3.3V

GND

Output (Connect to DAQ_BOARD)

Connector Column

References

[1] R.E.Saad ." Tactile Sensing", Press LLC 2000.

[2] Wen-Yang Chang, Te-Hua Fang, Heng-Ju Lin, Yu-Tang Shen, and Yu-Cheng Lin ." A Large Area Flexible Array Sensors Using Screen Printing Technology", JOURNAL OF DISPLAY TECHNOLOGY, VOL. 5, NO. 6, JUNE 2009.

[3] Automation and Robotic http://www.soton.ac.uk/~rmc1/robotics/artactile.htm. University of Southampton(9-2011).

[4] María José Barquero ,Javier Serón, Alfonso García-Cerezo ." Large Area Smart Tactile Sensor for Rescue Robot", 2009 IEEE.

[5] TSUYOSHI SEKITANI1, MAKOTO TAKAMIYA2, YOSHIAKI NOGUCHI1 ." A large-area wireless power-transmission sheet using printed organic transistors and plastic MEMS switches", Published online: 29 April 2007.

[6] M.Shimojo, M. Ishikawa, K. Makino ." A tactile sensor sheet using pressure conductive rubber with electrical-wire stitched method", IEEE Sensors Journal, Vol.4, NO.5, 2004.

[7] Adel.S.Sedra, Kenneth C.Smith"Microelectronic Circuit", Oxford University Press.

[8] R.A. Russell ." A tactile sensory skin for measuring surface contours", IEEE Conference TENCON, Australia, 1992.

[9] .Pauwel Goethals "Development of a Tactile Feedback System for Robot Assisted Minimally Invasive Surgery",Arenberg Doctoraatsschool Wetenschap and Technologie.

[10] Huang Ying 1, Fu Xiulan ,Wang Min , Huang Panfeng, Ge Yunjian ." Research on Nano-SiO2/Carbon Black Composite for Flexible Tactile Sensing ",Proceedings of the 2007 International Conference on Information Acquisition , 2007, Jeju City, Korea.

[11] .Julian Castellanos-Ramos,Rafael Navas Gonzalez "Tactile sensors based on conductive polymers",Springer-Verlag 2009.

[12] Pauwel Goethals, Mauro M. Sette, Dominiek Reynaerts, and Hendrik Van Brussel "Flexible Elastoresistive Tactile Sensor for Minimally Invasive Surgery." Katholieke Universiteit Leuven. Department of Mechanical Engineering.

[13] Thomas V. Papakostas, Julian Lima, and Mark Lowe ." A Large Area Force Sensor for Smart Skin Applications",Proceedings of the 2007 International Conference on Information Acquisition , Sensors, Proceedings of IEEE, vol.2, pp.1620–1624, June 2002.

[14] Karsten Weiss, Heinz Wärn. " The Working Principle of Resistive Tactile Sensor Cells" Proceedings of the IEEE International Conference on Mechatronics and Automation Niagara Falls, Canada, 2005.

[15] Y.J.Yang, M.-Y. Cheng, S.C. Shih, X.H. Huang." A 32 x 32 temperature and tactile sensing array using PI-copper films", Int Adv Manuf Technol (2010).

[16] Makoto Shimojo, Akio Namiki, Masotoshi Ishikawa." A Large Area Flexible Array Sensors Using Screen Printing Technology ", IEEE SENSORS JOURNAL, VOL. 4, NO. 5, OCTOBER 2004.

[17] Y. Takahashi, K. Nishiwaki, S.Kagami, H. Mizoguchi, H. Inoue." High-speed Pressure Sensor Grid for Humanoid Robot Foot. ", IEEE/IROS 2005.

[18] Hong Liua,Yuan-Fei Zhanga, Yi-Wei Liua, Ming-He Jin." Measurement errors in the scanning of resistive sensor arrays", Sensors and Actuators 163 (2010).

[19] R.S. Saxena, R.K. Bhan, Anita Aggrawal." A new discrete circuit for readout of resistive sensor arrays", Sensors and Actuators A 149 (2009) 9399.

[20] Giorgio Cannata, Marco Maggiali." Processing of an Embedded Tactile Matrix Sensor", International Conference on Robotics and Biomimetics, 2006, Kunming, China.

[21] GYing Huang,Bei Xiang1 Yunjian Ge Xiaohui Ming1." Two Types of Flexible Tactile Sensor Arrays of Robot for Three-dimension Force Based on Piezoresistive Effects. ", International Conference on Robotics and Biomimetics, Bangkok, Thailand, February 21 - 26, 2009.

[22] Wen-Yang Chang, Te-Hua Fang, Heng-Ju Lin." A Large Area Flexible Array Sensors Using Screen Printing Technology ", JOURNAL OF DISPLAY TECHNOLOGY, VOL. 5, NO. 6, JUNE 2009.

[23] Y.-J. Yang, M.-Y. Chenga, W.-Y. Changa, L.-C. Tsao, S.-A. Yang,." An integrated flexible temperature and tactile sensing array using PI-copper films ", Sensors and Actuators A 143 (2008).

[24] Datasheet of pressure-conductive foam CS57-7RSC, PCR Company. http://pcr.lar.jp/pcr/CSAJapanese.html (8-2011).

[25] Datasheet of pressure-conductive foam PE, Pro-pack Technical Inc.www.propack.com.sg/conductive_pu_foam.html (8-2011).

[26] Datasheet of Conductive PE Foam, Pro-pack Technical Inc.hwww.pro-pack.com.sg/conductive_pe_foam.html (8-2011).

[27] Datasheet of Conductive Rubber Foam, Pro-pack Technical Inc.www.pro-pack.com.sg/conductive_rubber_foam.html (8-2011).

[28] Weiss K, Worn H "Tactile sensor system for an anthropomorphic robotic hand". IEEE International conference on manipulation and grasping IMG 2004,Italy.

[29] Datasheet of electrically conductive adhesive film, 3M Electronics Inc., http://www.mpsupplies.com/3MElectricallyCondutiveTape9703.pdf (8-2011).

[30] Datasheet of DT9816, www.datatranslation.com/products/dataacquisition/usb/dt9816.asp (9-2011).

[31] Robert J. Orr and Gregory D. Abowd "The Smart Floor: A Mechanism for Natural User Identification and Trackin".Georgia Institute of Technology 2000.

[32] PCR Technical,"How to use Analog Pressure-Conductive Rubber CSA". Shinomiya, Hiratsuka-city, Kanagawa, 254-0014, Japan.

[33] Tommaso DAlessio, " Measurement errors in the scanning of piezoresistive sensors arrays", Sensors and Actuators 72(1999)71_76.

[34] Smart Kitchen Ltd. www.smartkitchens.co.uk (09-2011)